

CORRELATION OF URANYL NITRATE DIFFUSION
COEFFICIENTS DERIVED FROM DIAPHRAGM
CELL, INTERFEROMETER, AND
CAPILLARY CELL METHODS

By

JAMES LeROY SNYDER

Bachelor of Science
University of Illinois
Urbana, Illinois
February, 1958

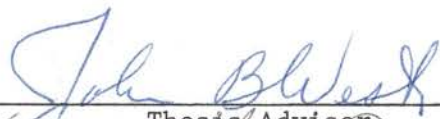
Master of Science
Oklahoma State University
Stillwater, Oklahoma
May, 1965

Submitted to the Faculty of the Graduate College
of the Oklahoma State University
in partial fulfillment of the requirements
for the Degree of
DOCTOR OF PHILOSOPHY
May, 1972

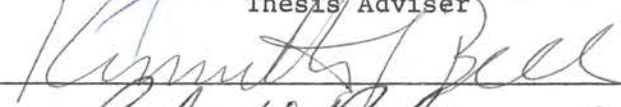
AUG 16 1973

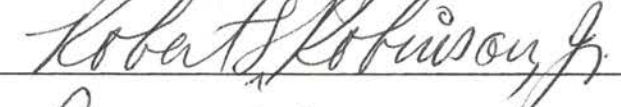
CORRELATION OF URANYL NITRATE DIFFUSION
COEFFICIENTS DERIVED FROM DIAPHRAGM
CELL, INTERFEROMETER, AND
CAPILLARY CELL METHODS

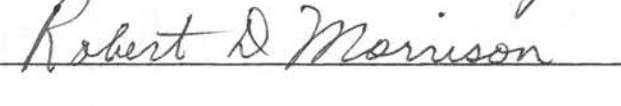
Thesis Approved:

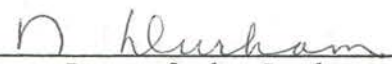


Thesis Adviser









Dean of the Graduate College

PREFACE

A number of experimental methods have been and are used to measure electrolyte solution diffusion coefficients. However, results for a common electrolyte, uranyl nitrate, have varied widely. Although efforts to refine experimental methods to improve the accuracy of measured data are extensive, correlation of data from different methods has been unsuccessful due to insufficient data and data inaccuracy.

A review of the experimental results on the measurement of the diffusion coefficient for uranyl nitrate solutions reveals serious discrepancies between different experimental methods. Therefore, the objective of this study was to obtain additional data on this system, pursue the correlation of the diffusion coefficient results, and attempt to resolve these discrepancies.

My most particular expression of gratefulness goes to Dr. J. B. West for his patience, guidance, encouragement, and humanity throughout this study. I am also thankful to Dr. R. N. Maddox, Dr. K. J. Bell, and Dr. R. L. Robinson for their help during my stay at the University.

Appreciation is expressed to Dr. J. B. Finley and Dr. R. D. Skinner for the use of their diffusion coefficient data for the correlation work.

I cannot find words to express my feelings for the encouragement given by my parents in Illinois.

I wish to express my appreciation to the United States Atomic Energy Commission, under Contract AT(11-1)-846, for financial support during my graduate study.

TABLE OF CONTENTS

Chapter	Page
I. INTRODUCTION	1
II. THEORY	3
A. Determination of Uranyl Nitrate Diffusion Coefficients	5
B. Experimental Variables	6
C. Calculation of Diffusion Coefficients	7
D. Correlation of Diffusion Coefficients	9
E. Multiple Linear Regression	13
F. Selective Curve-Fitting	13
III. EXPERIMENTAL APPARATUS	15
A. The Magnetically-Stirred Diaphragm Cell	15
B. Analytical Equipment	21
C. Materials	21
D. Capillary Cell Apparatus	21
E. Interferometer Apparatus	22
IV. EXPERIMENTAL PROCEDURE	23
A. Magnetically-Stirred Diaphragm Cell	23
B. Capillary Cell	34
C. Interferometer	34
V. RESULTS AND DISCUSSION	36
A. Diaphragm Cell Experimental Data	36
B. Comparison With Other Diaphragm Cell Data	39
C. Comparison With Capillary Cell Integral Diffusion Coefficients	42
D. Diaphragm Cell Differential Diffusion Coefficients	44
E. Interferometer Differential Diffusion Coefficients	55
F. Capillary Cell Diffusion Coefficients	59
G. Effect of Calculated Limiting Values	65
H. Comparison of Differential Diffusion Coefficients	69
I. Selective Curve-Fit Analysis	71

Chapter	Page
VI. CONCLUSIONS AND RECOMMENDATIONS	73
A SELECTED BIBLIOGRAPHY	77
APPENDIX A - CALCULATION OF INTEGRAL DIFFUSION COEFFICIENTS FROM DIAPHRAGM CELL DATA	79
APPENDIX B - DERIVATION OF DIFFERENTIAL DIFFUSION COEFFICIENTS FROM DIAPHRAGM CELL INTEGRAL DIFFUSION COEFFICIENTS	82
APPENDIX C - SELECTIVE CURVE-FIT REGRESSION EQUATIONS	84
APPENDIX D - DIAPHRAGM CELL COMPARTMENT VOLUME BUOYANCY CORRECTION	86
APPENDIX E - DIAPHRAGM CELL COMPARTMENT VOLUME CALIBRATION DATA	91
APPENDIX F - DIAPHRAGM CELL DIAPHRAGM VOLUME BUOYANCY CORRECTION	95
APPENDIX G - DIAPHRAGM CELL DIAPHRAGM VOLUME CALIBRATION DATA	97
APPENDIX H - CELL CONSTANT COMPUTER PROGRAM	99
APPENDIX I - CELL CONSTANT CALIBRATION DATA	101
APPENDIX J - REFRACTOMETER CALIBRATION DATA	103
APPENDIX K - DIAPHRAGM CELL EXPERIMENTAL DATA	106
APPENDIX L - ERROR ANALYSIS OF DIAPHRAGM CELL DATA	109
APPENDIX M - SELECTION OF DIAPHRAGM CELL DIFFUSION COEFFICIENT REGRESSION MODEL	113
APPENDIX N - INTERFEROMETER DATA	127
APPENDIX O - CAPILLARY CELL DATA	129
APPENDIX P - SELECTIVE CURVE-FIT ANALYSIS	131
APPENDIX Q - NOMENCLATURE	149

LIST OF TABLES

Table	Page
I. Diaphragm Cell Integral Diffusion Coefficients	37
II. Diaphragm Cell Average Integral Diffusion Coefficients	40
III. Coefficient of Variation for Diaphragm Cell Integral Diffusion Coefficients	43
IV. Calculated Values for D_{Cm} , Derived from Diaphragm Cell Data	49
V. Calculated Differential Diffusion Coefficients Derived from Diaphragm Cell Data	52
VI. Numerical Solution of Fick's Second Law for Capillary Cell Data Utilizing Finley's Equation	53
VII. Numerical Solution of Fick's Second Law for Capillary Cell Data Utilizing Equation (36)	62
VIII. Comparison of Diffusion Coefficient Curve-Fitting Results with Calculated Limiting Values	66
IX. Diaphragm Cell Compartment Volume Calibration Data	92
X. Diaphragm Cell Diaphragm Volume Calibration Data	98
XI. Cell Constant Calibration Data	102
XII. Refractometer Calibration Data	105
XIII. Diaphragm Cell Experimental Data	107
XIV. Limiting Diffusion Coefficients and Slopes Generated in Multiple Linear Regression of Integral Diffusion Coefficients	125
XV. Interferometer Data	128
XVI. Capillary Cell Data	130

Table	Page
XVII. Statistical Analysis of D vs \bar{c} Correlation for Diaphragm Cell Data, Data Set Includes $D_0 = 10.226$. . .	133
XVIII. Statistical Analysis of D vs \sqrt{c} Correlation for Diaphragm Cell Data, Data Set Includes $D_0 = 10.226$	134
XIX. Statistical Analysis of D vs \bar{c} Correlation for Diaphragm Cell Data, Data Set Includes $D_0 = 8.722$	135
XX. Statistical Analysis of D vs \sqrt{c} Correlation for Diaphragm Cell Data, Data Set Includes $D_0 = 8.722$	136
XXI. Statistical Analysis of D vs \bar{c} Correlation for Interferometer Data, Data Set Includes $D_0 = 10.226$	137
XXII. Statistical Analysis of D vs \sqrt{c} Correlation for Interferometer Data, Data Set Includes $D_0 = 10.226$	138
XXIII. Statistical Analysis of D vs \bar{c} Correlation for Interferometer Data, Data Set Includes $D_0 = 8.722$	139
XXIV. Statistical Analysis of D vs \sqrt{c} Correlation for Interferometer Data, Data Set Includes $D_0 = 8.722$	140
XXV. Statistical Analysis of D vs \bar{c} Correlation for Interferometer Data, Data Set Excludes D_0	141
XXVI. Statistical Analysis of D vs \sqrt{c} Correlation for Interferometer Data, Data Set Excludes D_0	142
XXVII. Statistical Analysis of D vs \bar{c} for Capillary Cell Data, Data Set Includes $D_0 = 10.226$	143
XXVIII. Statistical Analysis of D vs \sqrt{c} for Capillary Cell Data, Data Set Includes $D_0 = 10.226$	144
XXIX. Statistical Analysis of D vs \bar{c} for Capillary Cell Data, Data Set Includes $D_0 = 8.722$	145
XXX. Statistical Analysis of D vs \sqrt{c} for Capillary Cell Data, Data Set Includes $D_0 = 8.722$	146
XXXI. Statistical Analysis of D vs \bar{c} for Capillary Cell Data, Data Set Excludes D_0	147
XXXII. Statistical Analysis of D vs \sqrt{c} for Capillary Cell Data, Data Set Excludes D_0	148

LIST OF FIGURES

Figure	Page
1. Magnetically-Stirred Diaphragm Cell	16
2. Diaphragm Diffusion Cell	17
3. Lower Compartment Volume Calibration	25
4. Comparison of Diaphragm Cell Integral Diffusion Coefficients	41
5. Comparison of Integral Diffusion Coefficients	45
6. Multiple Linear Regression of \bar{D}_{c_m} , as a Function of c_m for Diaphragm Cell Data - Trial 1	48
7. Multiple Linear Regression of \bar{D}_{c_m} , as a Function of c_m for Diaphragm Cell Data - Trial 2	50
8. Multiple Linear Regression of Diaphragm Cell Dif- ferential Diffusion Coefficients According to the Model: $D = D_0 + P\bar{c}^{0.5} + Q\bar{c}^{1.0} + R\bar{c}^{2.0} + S\bar{c}^{3.0}$	54
9. Multiple Linear Regression of Interferometer Dif- ferential Diffusion Coefficients According to the Model: $D = D_0 + P\bar{c}^{0.5} + Q\bar{c}^{1.0} + R\bar{c}^{2.0} + S\bar{c}^{3.0}$	57
10. Multiple Linear Regression of Interferometer Dif- ferential Diffusion Coefficients According to the Model: $D = D_0 + P\bar{c}^{0.5} + Q\bar{c}^{1.0} + R\bar{c}^{2.0}$	58
11. Comparison of Calculated Final Concentration for Capillary Cells With Experimental Data	63
12. Multiple Linear Regression of Capillary Cell Integral Diffusion Coefficients According to the Model: $D = D_0 + P\bar{c}^{0.5} + Q\bar{c}^{1.0} + R\bar{c}^{2.0} + S\bar{c}^{3.0}$	64
13. Effect of Calculated Limiting Slope on Curve-Fitting of Diaphragm Cell Differential Diffusion Coefficients	68
14. Comparison of Differential Diffusion Coefficients From All Experimental Methods	70

15. Multiple Linear Regression of Diaphragm Cell Integral Diffusion Coefficients According to the Model:
 $\bar{D} = D_0 + Pc_{B_0}^{0.5} + Qc_{B_0}^{1.0} + Rc_{B_0}^{2.0} + Sc_{B_0}^{3.0} \dots \dots \dots 115$
16. Multiple Linear Regression of Diaphragm Cell Integral Diffusion Coefficients According to the Model:
 $\bar{D} = D_0 + Pc_{B_0}^{0.5} + Qc_{B_0}^{1.0} + Rc_{B_0}^{2.0} \dots \dots \dots 116$
17. Multiple Linear Regression of Diaphragm Cell Integral Diffusion Coefficients According to the Model:
 $\bar{D} = D_0 + Pc_{B_0}^{1.0} + Qc_{B_0}^{2.0} + Rc_{B_0}^{3.0} \dots \dots \dots 117$
18. Multiple Linear Regression of Diaphragm Cell Integral Diffusion Coefficients According to the Model:
 $\bar{D} = D_0 + Pc_{B_0}^{1.0} + Qc_{B_0}^{2.0} \dots \dots \dots 118$
19. Multiple Linear Regression of Diaphragm Cell Average Integral Diffusion Coefficients According to the Model:
 $\bar{D} = D_0 + Pc_{B_0}^{0.5} + Qc_{B_0}^{1.0} + Rc_{B_0}^{2.0} + Sc_{B_0}^{3.0} \dots \dots \dots 120$
20. Multiple Linear Regression of Diaphragm Cell Average Integral Diffusion Coefficients According to the Model:
 $\bar{D} = D_0 + P\bar{c}_{B_0}^{0.5} + Q\bar{c}_{B_0}^{1.0} + R\bar{c}_{B_0}^{2.0} \dots \dots \dots 121$
21. Multiple Linear Regression of Diaphragm Cell Average Integral Diffusion Coefficients According to the Model:
 $\bar{D} = D_0 + P\bar{c}_{B_0}^{1.0} + Q\bar{c}_{B_0}^{2.0} + R\bar{c}_{B_0}^{3.0} \dots \dots \dots 122$
22. Multiple Linear Regression of Diaphragm Cell Average Integral Diffusion Coefficients According to the Model:
 $\bar{D} = D_0 + P\bar{c}_{B_0}^{1.0} + Q\bar{c}_{B_0}^{2.0} \dots \dots \dots 123$

CHAPTER I

INTRODUCTION

This study was initiated to investigate the sources of discrepancies in diffusion coefficient data for the uranyl nitrate-water binary system as obtained from several experimental methods.

Since Fick (6) introduced his first law of diffusion in 1855, relating the flux of a component by molecular diffusion to the observed concentration gradient necessary for diffusion to occur, extensive research efforts have been devoted to determining the nature of the proportionality coefficient relating these two quantities. The proportionality coefficient has been called the "true" or differential diffusion coefficient.

The state of liquid theory is very complex and remains relatively undeveloped. The complexity increases when study is centered on electrolyte solutions due to the additional effect of the ionic charges on diffusion. The complexity further increases when the study advances from the more simple symmetric monovalent molecules to unsymmetrical polyvalent molecules. In addition, experimental methods of a quite varied nature present varied limitations in the measurement of diffusion coefficients (18, 26). The difference among laboratory techniques necessitates a corresponding difference in the mathematical treatment of the experimental data to obtain the differential diffusion coefficients.

This study encompasses the analysis of data of diffusion of an unsymmetrical polyvalent uranium salt, uranyl nitrate, by three experimental methods: the magnetically-stirred diaphragm cell, the birefringent interferometer, and the capillary cell. Diffusion coefficients obtained from these methods have shown wide discrepancies. Capillary cell results (7) show a distinct minimum in the lower concentration range (0.04-0.40 molar uranyl nitrate) whereas preliminary diaphragm cell and interferometer results did not substantiate this minimum. Preliminary interferometer results indicated that a diffusion coefficient minimum may exist at low concentrations, but it is not as pronounced as that indicated by the capillary cell data.

A research program was established with an objective of obtaining a broader insight into the effect of mathematical techniques on resulting diffusion coefficients. This program included the following:

- a) the experimental determination of uranyl nitrate diffusion coefficients in the concentration range 0.1-1.0 molar uranyl nitrate using the diaphragm cell,
- b) a review and analysis of experimental factors affecting the diffusion coefficient results for all three experimental methods,
- c) a study of the curve-fitting of the diffusion coefficients derived from the three experimental methods,
- d) a statistical consistency analysis of the methods for curve-fitting the data obtained from all three experimental methods.

CHAPTER II

THEORY

If the state of a mixture of two miscible liquids is such that local concentration gradients are present, a driving force exists which tends to eliminate these differences. The resultant liquid particle movement has been termed diffusion and was first described by Fick (6) in 1885 according to the following equation:

$$J = -D \frac{\partial c}{\partial x} \quad (1)$$

for unidirectional diffusion. Equation (1) is known as Fick's First Law of Diffusion and relates the mass flux J with the concentration gradient $(\frac{\partial c}{\partial x})$ via the proportionality coefficient D . The term D is known as the differential diffusion coefficient. Although D is often referred to as the diffusion "constant," it is not defined as such and will vary with the concentration changes. Equation (1) is applicable to experimental studies on steady-state systems. The use of equation (1) leads to the following equation to describe unsteady-state systems:

$$\frac{\partial c}{\partial t} = \frac{\partial}{\partial x} (D \frac{\partial c}{\partial x}) \quad (2)$$

Equation (2) is known as Fick's Second Law of Diffusion. Since Fick's Laws were first presented, experimental work has shown that the assumption of the concentration gradient as the diffusion driving force is

incorrect (8). The chemical potential gradient is accepted today as the true driving force (10, 13, 19). However, Fick's Laws are still utilized today due to their simplicity and applicability to the analysis of experimental data.

As stated above, Fick's Laws as shown in Equations (1) and (2) are for unidirectional flow. The direction of flow, x , is usually measured from some arbitrary plane fixed with respect to the experimental apparatus containing the diffusion system. When working with liquids, this approach is the simplest experimental means of fixing the reference plane. However, Equations (1) and (2) are valid provided there is no volume change on mixing (17, 20). In the derivation of Equations (1) and (2), an elemental volume across which diffusion occurs was assumed to be constant. Therefore, the dimensions of the volume could be referred to the experimental apparatus. If a volume change occurs upon mixing of the solute and solvent, the elemental volume changes with respect to concentration and thus the dimensions of the volume are concentration dependent. In this case, the reference frame for the dimensions must be changed. If Equations (1) and (2) are regarded only as definitions of D , a change in the reference frame is quite legitimate. However, it must be remembered that the value of D will depend upon the selection of the reference frame. Hartley and Crank (14) have detailed the relations between diffusion coefficients defined with respect to various reference planes. Bird, Stewart, and Lightfoot (1) show the derivations of various reference frames when there is a volume change on mixing. Olander (17) presents an additional method to be used in such cases. He concludes that for most binary liquids, the effect of volume changes on mixing are too small to alter appreciably the

diffusion coefficients measured in diaphragm cells or capillary cells. However, exceptions do occur, and each system should be evaluated for possible volume changes on mixing before the diffusion study is undertaken.

A. Determination of Uranyl Nitrate Diffusion

Coefficients

The experimental methods used to obtain diffusion coefficients for uranyl nitrate include the magnetically-stirred diaphragm cell, the birefringent interferometer, and the capillary cell. Measurement of diffusion coefficients using the diaphragm cell and the capillary cell usually involve relatively large concentration differences. The diffusion coefficient is initially assumed to be constant in order to calculate an integral diffusion coefficient from the experimental data. The derivation of differential diffusion coefficients recognizes a concentration dependency of the diffusion coefficient and normally assumes some concentration-dependent function for the diffusion coefficient. The concentration-dependent function can be estimated initially utilizing the calculated integral diffusion coefficients. The initial function is then adjusted until the experimental data can be reproduced.

When the birefringent interferometer is used, concentration differences are normally sufficiently small that the assumption of a constant diffusion coefficient is valid. Differential diffusion coefficients can be derived directly from the experimental data.

Discrepancies have been observed between values of the diffusion coefficient for uranyl nitrate when they are obtained by these different experimental methods (29). The diffusion coefficient as obtained

by the capillary cell shows a distinct minimum with concentration, whereas the values obtained by the diaphragm cell and the interferometer do not appear to support the depth of this minimum.

Three major factors are considered to contribute to the ultimate determination of the diffusion coefficient, namely experimental variables, calculation methods with inherent assumptions, and correlation of the diffusion coefficients derived from the experimental data.

B. Experimental Variables

Each experimental method is concerned with a number of experimental variables, some specific to the particular method and some due to the general nature of diffusion experiments. These general effects include temperature control, vibration, sampling and associated analytical techniques.

In addition, for the uranyl nitrate-water system, composition changes may be possible due to polymerization or complex formation of the diffusing species or hydrolysis of uranyl nitrate from different hydration states. Several complex forms for uranyl nitrate are discussed by Cordfunke (3).

Some of the specific variables inherent to each method are listed below. For the magnetically-stirred diaphragm cell, the major sources of error include:

- (a) cell calibration,
- (b) cell stirring,
- (c) potential bulk streaming of solute,
- (d) concentration limitations,
- (e) surface diffusion,

- (f) length of diffusion time.

For the birefringent interferometer, the major sources of error include:

- (a) correct focusing of the optical system,
- (b) exact measurement of system magnification,
- (c) initial boundary formation,
- (d) light wavelength used,
- (e) consistency of boundary conditions during experimental runs.

For the capillary cell, the major sources of error include:

- (a) initial immersion of capillary cell,
- (b) stirring of solution into which solute diffuses,
- (c) consistency of boundary conditions during experimental runs,
- (d) length of diffusion time.

For the most part, however, these variables can be compensated for so that they no longer have any significant effect on the final results. For example, sufficient work has been completed to indicate what rate of stirring in the diaphragm cell will insure uniformity in the diaphragm cell compartments and prevent formation of stagnant layers on the diaphragm (16, 17, 18, 26).

On the basis of improvements made on each of these variables, it is not felt that a detailed study of any specific variable would reveal the nature of the above mentioned discrepancies in the diffusion coefficient of uranyl nitrate.

C. Calculation of Diffusion Coefficients

The major theoretical sources of error inherent in the calculation of diffusion coefficients from diaphragm cell measurements are listed

below:

- (a) quasi-steady state assumption,
- (b) integral diffusion coefficient is a double average over time and concentration,
- (c) concentration-averaged diffusion coefficient, $\bar{D}(t)$, is assumed constant in order to relate to differential diffusion coefficient.

Integral diffusion coefficients are calculated according to the following equation:

$$\bar{D} = \frac{1}{\beta t} \ln\left(\frac{c_{B_0} - c_{B_0}}{c_B - c_T}\right) \quad (3)$$

The derivation of Equation (3) is shown in Appendix A. The method of Stokes (27) was used to derive differential diffusion coefficients.

This method is outlined in Appendix B.

The major theoretical sources of error inherent in the calculation of diffusion coefficients from interferometer data are listed below:

- (a) measurement of fringe spacing,
- (b) magnification,
- (c) determination of fractional portion of light retardation,
- (d) determination of point where the lowest bright band has its maximum intensity.

The calculation of interferometer diffusion coefficients used in this study is outlined in detail by Skinner (24).

The major theoretical sources of error inherent in the calculation of diffusion coefficients from capillary cell data are listed below:

- (a) assumption of constant D or a concentration-dependent D,
- (b) number of terms considered in expression for D (normally dictated by length of diffusion run),
- (c) method for calculating differential diffusion coefficient:

- (1) plot of series expression versus Dt/a^2 with interpolation at \bar{c}/c_0 ,
- (2) slope of plot of $\ln(\bar{c}/c)$ versus t .

The calculation of capillary cell diffusion coefficients used in this study is outlined in detail by Finley (7).

D. Correlation of Diffusion Coefficients

Relatively minimal work has been pursued to correlate the diffusion coefficients derived from the different experimental methods. Finley (7) used multiple linear regression of the capillary cell integral diffusion coefficients to obtain an initial definition of the differential diffusion coefficient. The following model was used:

$$D = D_0 + Pc^{0.5} + Qc^{1.0} + Rc^{2.0} + Sc^{3.0} \quad (4)$$

The coefficients in Equation (4) were then adjusted until use of Equation (4) in a numerical solution of Fick's Second Law could reproduce the experimental concentrations.

In correlating diffusion coefficients, use can be made of the behavior of diffusion coefficients at low concentrations. Finley used the limiting equation of Harned and Owen (12) as shown below

$$D = D_0 - \delta_{(D)}\sqrt{c} \quad (5)$$

The limiting diffusion coefficient D_0 is calculated according to the following equation:

$$D_0 = 8.936 \times 10^{-10} T \frac{(V_1 + V_2) \lambda_1^0 \lambda_2^0}{V_1 |z_1|} \left[\frac{\lambda_1^0 \lambda_2^0}{\Lambda^0} \right] \quad (6)$$

The limiting slope $\delta_{(D)}$ is calculated according to the following equation:

$$\delta_{(D)} = \frac{1.3273 \times 10^{-3} (\sum V_i Z_i)^{3/2}}{D_*^{3/2} T^{1/2} V_1 |Z_1|} \left[\frac{\lambda_1^0 \lambda_2^0}{\Lambda^0} \right] + \frac{2.604 \times 10^8 (\sum V_i Z_i)^{1/2}}{\eta_0 D_*^{1/2} T^{-1/2} |Z_1 Z_2|} \left[\frac{|Z_2| \lambda_1^0 - |Z_1| \lambda_2^0}{\Lambda^0} \right]^2 \quad (7)$$

The Nernst-Hartley limiting equation as presented in Robinson and Stokes (20) also includes a thermodynamic correction term:

$$D = D_0 \left(1 + \frac{d \ln \gamma}{d \ln c} \right) \quad (8)$$

The activity correction term relates the calculated limiting diffusivity to the chemical potential driving force. The limiting diffusion coefficient D_0 in Equation (8) is also calculated by Equation (6).

The complete derivation of the above equations is not shown here but can be found in the above references. The limiting equation is derived from a force balance on the diffusing ionic species. The forces considered include the following:

- (a) forces due to the chemical potential gradient,
- (b) forces due to the electrical field established by the unequal mobilities of the diffusing ions.

The final form of the limiting equation shows the absolute ionic mobilities represented in terms of limiting equivalent conductivities, λ^0 .

Limiting equivalent conductivities of high accuracy are required to calculate accurate limiting diffusion coefficients and limiting slopes. Finley (7) used an average limiting equivalent conductivity of

31.45 for the uranyl ion to calculate limiting values. This value is an average of the values reported by Ewell and Eyring (5)-- $\lambda_1^0 = 30.9$ -- and Goldenberg and Amis (9)-- $\lambda_1^0 = 32.0$. The limiting equivalent conductivity for the nitrate ion is that of Shedlovsky (22)-- $\lambda_2^0 = 71.46$. These values yield a limiting diffusion coefficient of 8.722×10^{-6} cm²-sec and a limiting slope of 17.968×10^{-6} .

Hale (11) obtained and reported limiting ionic conductivities for uranyl ion, $\lambda^0(\text{UO}_2^{+2}, \text{Ag}) = 39.9 \pm 1.0$ at 25°C. Hale's conductance investigations indicated increased hydrolysis of the uranyl ion at concentrations below about 0.09. He also attributed the low value of conductance, i.e., $\lambda^0 = 39.9$ compared to $\lambda^0 = 50$ to 60 for most bivalent cations, to the highly hydrated character of the uranyl ion in aqueous solution. Shedlovsky (22) did not report the precision of the values for nitrate ions. He did indicate equipment design consistency of from 0.01 to 0.02% for the relative conductance values. A high degree of confidence can be placed in the Nernst limiting values relative to the reproducibility of the experimental data.

This new limiting diffusion coefficient, $D_0 = 10.226 \times 10^{-6}$ cm²-sec⁻¹, is used as a regression point in the curve-fitting of diffusion coefficient data from all three experimental methods. Various equation models in addition to that shown in Equation (4) are also tested, including models without the square-root term. Results are compared with those derived with use of $D_0 = 8.722 \times 10^{-6}$ cm²-sec⁻¹ as used in Finley's work. In addition, diffusion coefficient results are curve-fitted without use of a limiting diffusion coefficient as a regression point. Differential diffusion coefficients derived from the diaphragm cell are also curve-fitted using both sets of limiting diffusion

coefficients and limiting slopes. Results of the above discussed work are compared as appropriate and discussed.

When a salt diffuses as a result of a concentration gradient, both the cation and the anion must move at the same velocity to maintain solution neutrality. The ions are sufficiently far apart in dilute solutions that they exert little influence on one another. However, as the concentration of these ions increases certain effects occur as a result of the interaction between the electrical fields of these ions.

The electrophoretic effect occurs as an ion moves through a viscous medium. The diffusing ion will tend to drag along the solution in the vicinity of the diffusing ion. Therefore, adjacent ions do not move relative to a stationary medium, but with or against the moving stream. The magnitude of this effect will be dependent upon the concentration.

Another effect is called the relaxation effect. External forces will influence the motion of ions which in turn will cause the symmetrical distribution of the ions to be disturbed. In a solution which is in equilibrium the ions surrounding a central ion are distributed symmetrically over a time average and do not exert a resultant force on the central ion. As the ion considered central moves away from its central position, a restoring force is exerted on this ion. This restoring force, known as the relaxation effect, dissipates as the surrounding ions are rearranged by their thermal motions.

Onsager and Fuoss (19) studied the electrophoretic effects in terms of the velocity and the absolute mobility of the ions: The two electrophoretic terms are complex functions of the viscosity of the solvent, temperature chemical potential gradient, and an electrical force due to the electrical attraction of the faster moving ions for the

slower ones.

The study of electrolyte diffusion becomes more complex when concentrated solutions are considered. Additional ionic effects, negligible at dilute concentrations, become more significant. Some of the ions will carry an attached layer of solvent molecules as part of the diffusing solute ion. In addition, viscosity forces will be quite different due to the presence of a higher population density of ions. Present theoretical corrections for electrophoretic effects are less satisfactory for concentrated solutions.

At dilute concentrations, it has been noted previously that the equivalent conductivity will increase due to the increased hydrolysis of the uranyl ion (11). This effect in turn could result in a minimum for the uranyl ion at intermediate concentrations.

E. Multiple Linear Regression

Multiple linear regression was used for all curve-fitting contained in this study. A treatment of multiple linear regression can be found in any standard statistics text, such as Steel and Torrie (25).

F. Selective Curve-Fitting

A selective curve-fit analysis is also used to determine the statistical consistency of a regression model used to curve-fit diffusion coefficients as a function of concentration. The selective curve-fit analysis performs a multiple linear regression of the diffusion coefficients according to specified regression equations. The regression equations used are listed in Appendix C. Statistical variables calculated for each curve-fit include minimum standard deviation, maximum

deviation from the diffusion coefficient and value of concentration variable at which deviation occurs, residual squared, and F-ratio. This analysis is used to analyze the curve-fit of D as a function of both c and \sqrt{c} . An attempt was made to obtain an indication of what regression equation form expressing the differential diffusion coefficient as a function of concentration would consistently produce the most favorable statistical indicators. This analysis is applied to the diffusion coefficients derived from all three experimental methods.

CHAPTER III

EXPERIMENTAL APPARATUS

A discussion of the experimental apparatus used for the diaphragm cell, capillary cell and shearing interferometric methods follows. Emphasis is placed on the diaphragm cell apparatus as work on this equipment constituted a major portion of the project work. This equipment was originally used by Robinson (21). However, some changes were made for improved operation. A description of the capillary cell apparatus used by Finley (7) and the interferometer developed by Skinner (23, 24) is limited to essential information for explanatory purposes. The reader should consult the above references for detailed equipment descriptions.

A. The Magnetically-Stirred Diaphragm Cell

A.1. The Diffusion Cells

The major portion of the experimental work performed in this study was accomplished in six magnetically-stirred diaphragm cells. The diaphragm cell is illustrated in Figures 1 and 2. The design is a modification of that used by Dullien (4) and similar to that used by Burchard and Toor (2), and Robinson (21). The cell is a cylindrical vessel separated into two compartments, an upper compartment, A, and a lower compartment, B (letters refer to Figure 1). The two compartments are separated by a porous diaphragm, C. Capillary extensions connect

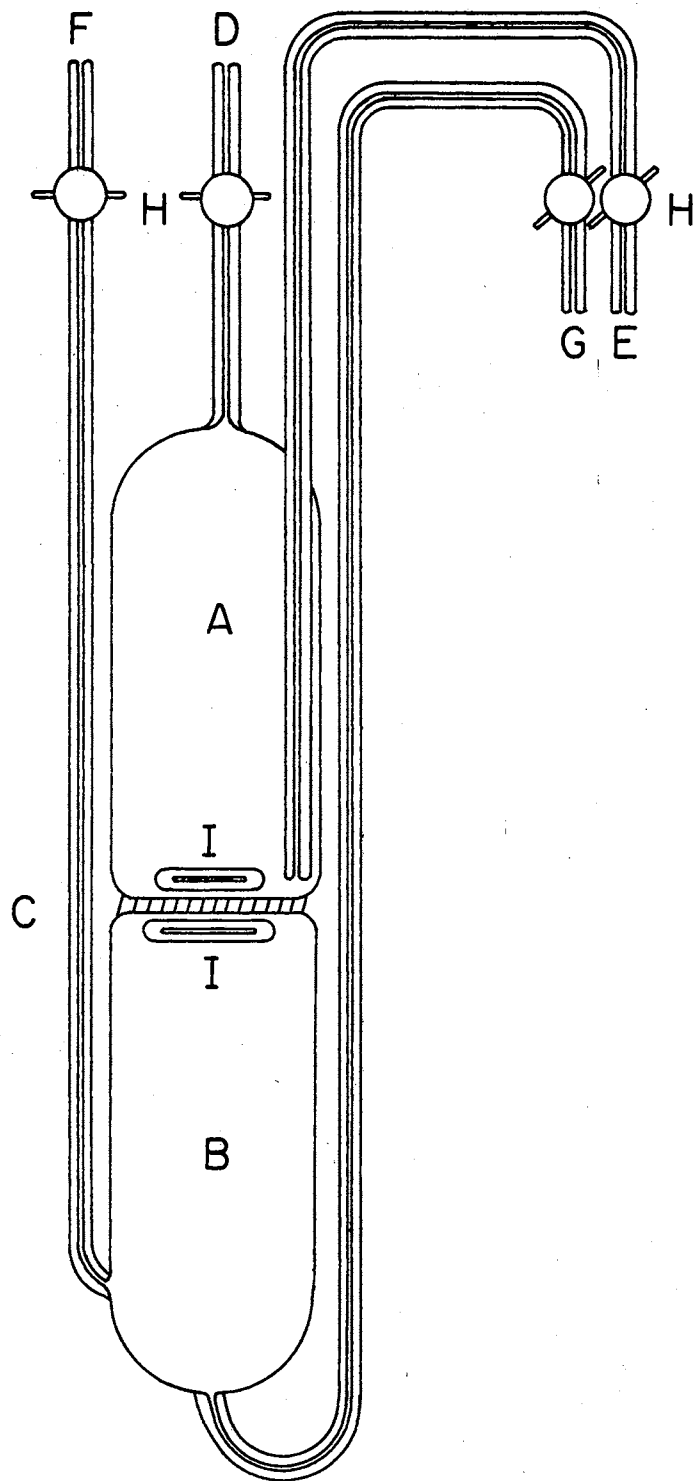


Figure 1. Magnetically-Stirred Diaphragm Cell

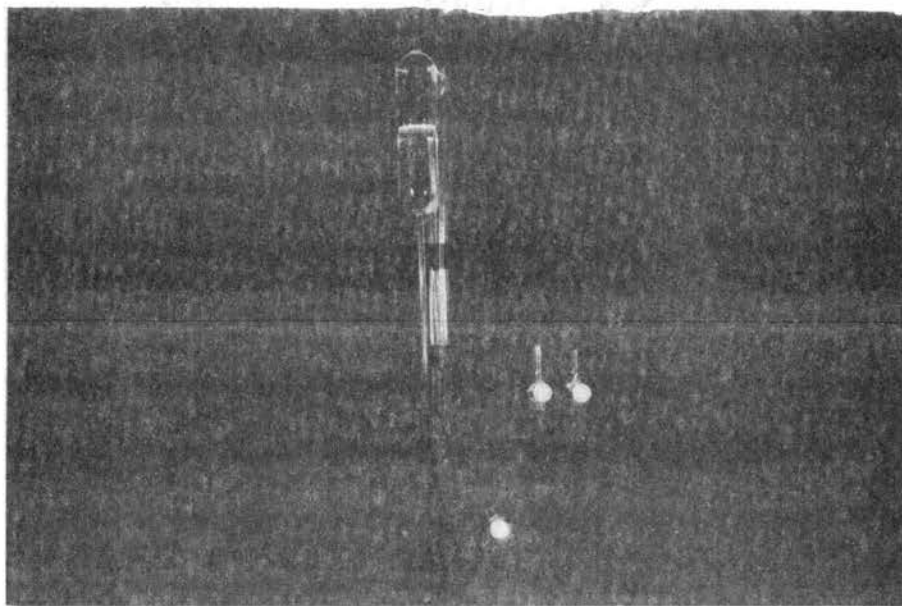


Figure 2. Diaphragm Diffusion Cell

the internal portion of the cell to the surroundings and are used for filling and emptying the cell. Capillary extensions D and E are connected to the upper compartment while F and G are connected to the lower compartment. The capillary extensions are fitted with Teflon-plug stopcocks, H. Two different types of stopcocks were used as discussed below. Each compartment contains a stirrer, I. The body of the cell, the diaphragm and the capillary extensions are made of pyrex glass. The stirrers are iron wire sealed in soft glass. The dimensions of the diaphragm cell are the same as those used by Robinson (21) except that the overall height of the cell and capillary extensions was approximately 60 cm.

The diaphragms were constructed from blanks containing an F (fine) grade diaphragm (Fisher Catalog, Item 11-136). F grade corresponds to a pore size of 2-5 microns, which is well below the recommended upper limit of approximately 15 microns (20). Diaphragms with pores larger than 15 microns are reported to allow bulk streaming of the fluid through the diaphragm.

The stirrers were constructed by sealing a small piece of iron wire in a glass casing. Stirrer volume and subsequent air inclusion were varied so that upper compartment stirrers would sink in pure water and lower compartment stirrers would float in pure water. The optimum stirrer design was found to be the minimum stirrer diameter which would contain the iron wire and a maximum stirrer length which would fit inside the diaphragm cell. These specifications still have to be compatible with density requirements for sinking or floating. Any appreciable variation in stirrer size, particularly with respect to stirrer length, would allow the stirrer to become offset from the

diaphragm cell centerline when under the influence of the cell support rotating magnetic field and to come to rest in a "dead spot" within the cell. Several stirrers were tested until each cell contained two stirrers which operated satisfactorily.

Teflon-plug stopcocks were used on the diaphragm cells in lieu of the "polyethylene screw clips" used by Robinson. The Teflon-plug stopcocks provided easier operation when filling and sampling, precluded stopcock grease contamination and held an aspirator vacuum. Two different designs of the Teflon-plug stopcocks were used. The first type was a spring-loaded stopcock (Pyrex Catalog, Item 7281) with a constant tension on the stopcock handle. The second contained an adjustable nut which allowed variation of the tension on the stopcock handle (Pyrex Catalog, Item 7282) and facilitated operation.

Six diaphragm cells were constructed as the cell support allows simultaneous operation of six cells. The capillary extensions were taped together with electrical tape (See Figure 2.) to provide additional sturdiness to the cell.

A.2. Cell Support and Stirring

The cell support for the six diaphragm cells was the same as used by Robinson (21). No modifications were made in this equipment area.

A.3. The Constant Temperature Bath

The constant temperature bath was the same as used by Robinson (21) except for the modifications discussed below.

The bath oil used by Robinson was an absorber oil petroleum fraction. This oil was replaced with Conoco GP-7 spindle oil. The

spindle oil displayed the same heat transfer characteristics as the absorber oil petroleum fraction and also demonstrated a much better thermal stability, maintained a clear appearance and allowed visual observation of the cells during operation.

The bath oil was cooled by pumping cooling water through a coil in the bath. Two coils were available for operation, but operation of only one coil was sufficient to provide the necessary cooling. The cooling water temperature was maintained at 7-13°C. below the bath temperature by a portable cooling unit (Blue M Electric Co., Model PCC-1A). The cooling water temperature was adjusted as necessary to provide approximately equal heating and cooling cycle times for stable temperature control of the bath. The vertical immersion pump initially used for cooling water circulation displayed extremely poor reliability for continuous service due to motor burnout and was replaced by a centrifugal pump (Eastern Model D-11).

The bath oil was initially stirred with a friction-drive, variable speed mixer. The mixer displayed poor reliability due to the wearing of the rubber drive wheels. The wearing also led to mixer vibration and subsequent vibration in the constant temperature bath. The mixer was replaced with a direct-drive, constant speed mixer (Lightning Model L) which exhibited smoother operation in continuous service and minimized vibration.

The bath temperature was measured with a NBS calibrated thermometer (Princo, No. 580362). Control on the bath temperature varied from ± 0.03 to $\pm 0.05^\circ\text{C}$. However, temperature control inside the diaphragm cells was much finer. Temperature control was tested by inserting the thermometer into a test tube filled with distilled water and immersing

the test tube in the constant temperature bath to simulate the diaphragm cell conditions. Temperature variation of the water inside the test tube was less than $\pm 0.005^{\circ}\text{C}$.

B. Analytical Equipment

Uranyl nitrate solutions were analyzed by refractive index on a Bausch and Lomb, Precision Refractometer (Model No. 33-45-03) with sodium light.

Weights for the diaphragm cell volumetric calibrations were made on a Volland and Sons Balance (Model No. 18559) with a 200 gram capacity and a sensitivity of 0.1 mg.

C. Materials

Uranyl nitrate solutions were prepared from A.C.S. reagent grade uranyl nitrate purchased from the General Chemical Division of Allied Chemical Company.

Potassium chloride used was "Baker Analyzed" Reagent, J. T. Baker Chemical Company and had a stated purity of 99.9 weight per cent.

D. Capillary Cell Apparatus

A brief description of the capillary cell apparatus used by Finley (7) is given below. This equipment consisted of four major components: diffusion cell, capillaries, constant temperature bath and analytical equipment. The diffusion cell was a rectangular polyethylene vessel divided into four compartments by Lucite baffles. A stirrer circulated solvent through the compartments. Capillary holders immersed in the diffusion cell contained capillaries made from 0.5 mm and 0.75 mm

precision bore capillary tubing. Capillaries were two cm long, closed at one end and outside-tapered and fire-polished at the open end. The constant temperature bath was a water bath controlled by a mercury differential-type thermoregulator to within $\pm 0.01^{\circ}\text{C}$. Analysis of uranyl nitrate solutions was made by liquid scintillation counting. Details of construction and manufacturers' specifications are given by Finley (7).

E. Interferometer Apparatus

A brief description of the shearing interferometer developed by Skinner (23, 24) is given below. This equipment consisted of five major components: an optical bench, an optical system, a diffusion cell, a constant temperature bath and analytical equipment. The optical bench consisted of two channel irons twelve feet long bolted together by five iron straps. The optical system consisted of a mercury vapor lamp light source, two polarizers, two cell lens, a focusing lens, a Savart plate and a camera. The diffusion cell was the flowing junction type constructed of stainless steel with optically flat glass windows for passage of light through the diffusing solution. The constant temperature bath was a water bath controlled by a Fisher controller using a thermistor probe as the sensing element. Uranyl nitrate analyses were made on the refractometer used in the diaphragm cell work. A David W. Mann Precision Instruments microscope was used to measure concentration gradient fringes. Details of construction and manufacturers' specifications are given by Skinner (23).

CHAPTER IV

EXPERIMENTAL PROCEDURE

Experimental procedures for operation of the magnetically stirred diaphragm cell are given below. Brief summaries of experimental procedures for the capillary cell and the interferometer are included. Detailed descriptions are available in the literature.

A. Magnetically-Stirred Diaphragm Cell

A.1. Diaphragm Cell Volume Calibration

The cell compartments and the diaphragm were calibrated for volume using distilled water. The calibration procedure for the cell upper compartment is the same as used by Robinson (21) but is included here for completeness. The calibration procedure for the lower compartment was modified as discussed below.

To calibrate each compartment, the entire cell was filled with water. The lower compartment was filled first by applying aspirator vacuum at capillary leg D (refer to Figure 1, Chapter III, for cell orientation) and drawing water into the lower compartment through leg G. Sufficient water was drawn into the cell to fill the lower compartment and diaphragm, and have approximately one-half inch of water on the top of the diaphragm. Aspirator vacuum was applied to leg F to completely fill this leg. The cell was then degassed (See degassing procedure below.) to remove all air from the lower compartment. Liquid

for the upper compartment was degassed, and aspirator vacuum was again applied to leg D to fill the upper compartment through leg E. The diaphragm cell with both compartments, the diaphragm and all capillary extensions filled with water was ready for sampling.

Compartment volume calibrations excluded the volumes of the capillary legs leading into the compartments. To sample the upper compartment, the cell was clamped in an inverted position. A slight air pressure was applied to leg E to initiate water flow from leg D. The initial portion of the water flowing from leg D was discarded. Sample collection in a tared weighing bottle was initiated when the first air bubble entered the upper compartment from leg E. Once air enters the top compartment, water will flow from leg D by gravity. Sample collection was terminated when the first air bubble entered leg D from the upper compartment. The weighing bottle was then reweighed.

Ambient temperatures were measured during the tare and gross weighings for purposes of buoyancy corrections. Ambient temperature was measured during sampling to convert the compartment calibration from a weight basis to a volume basis. A sample calculation of the buoyancy correction for cell compartment calibrations is shown in Appendix D.

The sampling procedure for the lower compartment is similar to that for the upper compartment although some modifications are necessary to insure accurate sampling. The diaphragm cell is filled with water as described above. Air pressure is applied at leg F and sample collection made from leg G. However, some precaution was necessary to prevent the air pressure applied to the lower compartment from forcing water in the diaphragm and upper compartment from the diaphragm cell through leg D. The laboratory arrangement for this procedure is shown in Figure 3.

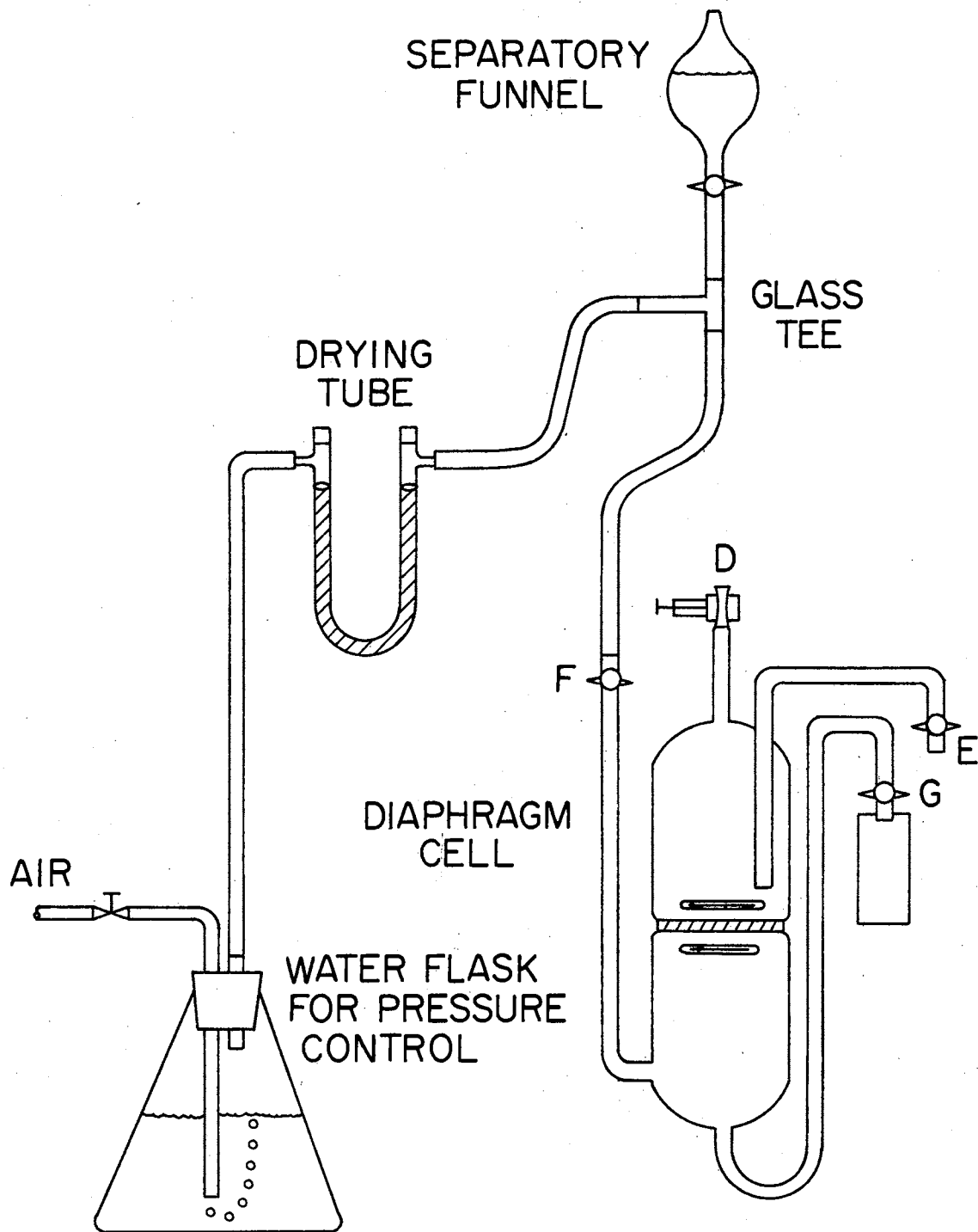


Figure 3. Lower Compartment Volume Calibration

Connections between the diaphragm cell, water flask, separatory funnel and glass tee are Tygon tubing. After the diaphragm cell is filled with water, a one-inch piece of rubber tubing with a pinchclamp was inserted over the end of leg D. With the air pressure shut off, sufficient water head was applied to leg F from the separatory funnel to force water out of the diaphragm cell through leg D. When water started flowing from leg D, the pinchclamp on the rubber tubing was shut off.

The stopcock on leg G was then opened and the water level above leg F allowed to fall below the glass tee. The separatory funnel was then shut off and air pressure applied to leg F. The water level in the flask was used to control the air pressure and sampling rate. The initial portion of the sample flowing from leg G was discarded. Sample collection in a tared weighing bottle was initiated when the first air bubble entered the lower compartment from leg F. Sample collection was terminated when the first air bubble entered leg G from the lower compartment. The weighing bottle was reweighed. Buoyancy corrections were made in an identical manner to those of the upper compartment. Cell compartments were calibrated to an accuracy of 0.1%. Cell compartment volume calibrations are shown in Appendix E.

The calibration procedure for the cell diaphragm was similar to that used by Robinson (21). The diaphragm was prepared for calibration by flushing with distilled water, acetone, and ether, and oven-drying at 220°F. for twelve hours. Ambient temperature was measured during syringe weighing and during water addition to the diaphragm for buoyancy corrections. The buoyancy correction for diaphragm calibration is similar to that used for compartment volume calibration. A brief description of the diaphragm buoyancy correction, delineating differences

from the method used for diaphragm compartments, is given in Appendix F. Cell diaphragm volumes were calibrated to within ± 0.01 ml. The calibrations are shown in Appendix G.

A.2. Leveling the Diaphragm

A leveling procedure was used to insure that the diaphragms were level when the cells were in operation. The cell support was removed from the oil bath and placed on a laboratory table. The cell support was leveled using a carpenter's level and the leveling screws through each corner. The six diaphragm cells were placed in the individual cell holders. The free set screw in the cell holder was then tightened against the diaphragm cell wall to hold the cell in place. A cathetometer was used to check the level of both the upper and lower surfaces through all three windows in the cell holder. If any deviation from a level diaphragm surface was observed, the positions of the permanent set screws were adjusted until the diaphragm was level when the free set screw was tightened. The cell support was replaced in the oil bath and again leveled using the carpenter's level and the tightening screws. When a diaphragm cell was placed in its respective cell holder and the free set screw tightened, a level diaphragm surface was assumed.

A.3. Stirring Rate

The stirring rate in the diaphragm cell was controlled by varying the speed of the motor controller connected to the control gear motor drive. The speed of the central gear was measured by timing with a stopwatch the speed of the locking nut on the bushing connecting the drive shaft to the variable-speed motor. The speed of the individual

ring gears and the corresponding speed of the diaphragm stirrers was determined from the gear ratio between the central gear and the ring gears. Operation of the diaphragm stirrers was observed to insure that one revolution of the stirrer was obtained for each revolution of the ring gear. The stirring rate of the diaphragm stirrers was set at 85 rpm and maintained at this value for all experimental runs in this study.

A.4. Preparation of Solutions

A 0.1N potassium chloride solution was prepared by accurately weighing 14.9110 grams of KCl on the Volland and Sons balance. This material was then dissolved in distilled water in a 2000-ml Erlenmeyer flask and distilled water added to make 2000 ml of solution. This solution was used for the cell constant calibration runs.

Twenty-one 1-ml samples of uranyl nitrate solution ranging from 0.02M to 2.00M were prepared by accurately weighing the required amounts of uranyl nitrate hexahydrate on the Volland and Sons balance and dissolving the weighed material in sufficient distilled water to make 1 ml of solution. These samples were used to calibrate the refractometer.

Uranyl nitrate solutions used for the experimental runs were prepared by weighing sufficient uranyl nitrate hexahydrate to make 200 ml of solution with an approximate concentration of 3.0M. Lower concentrations were then obtained by dilution. Concentrations were then measured at the beginning and end of an experimental run using the refractometer.

A.5. Filling and Sampling the Diaphragm Cells

To fill the diaphragm cell, the stopcocks on legs E and F were closed (Figure 1). Aspirator vacuum was applied at leg D and the lower compartment solution (more concentrated solution) was drawn into the lower compartment through leg G. Enough solution was drawn into the cell in this manner to fill the lower compartment and diaphragm and leave approximately one-half inch of solution above the diaphragm. Aspirator vacuum was applied to leg F to draw solution from the lower compartment into this leg. Leg F was completely filled with solution.

The diaphragm cell was then degassed (See degassing procedure below.). Prior to filling the upper compartment, the diaphragm cell was brought to the oil bath temperature in a constant-temperature water bath. The solvent for the upper compartment was degassed on a hot-plate and cooled as rapidly as possible to the oil bath temperature. The diaphragm cell was removed from the water bath and all liquid removed from the upper compartment. The upper compartment was filled with about 20 cc of the degassed solvent by applying aspirator vacuum at leg D and drawing liquid into the cell through leg E. This solvent was used to rinse the upper compartment and was then removed and discarded.

The upper compartment was then completely filled with solvent as described above, and the cell was placed into the oil bath to start the experimental run. Temperature effects during filling were minimal. The room temperature-oil bath temperature difference was approximately 2°C., and filling of the upper compartment was completed in approximately 30 seconds.

Upon removal of the diaphragm cell from the oil bath, the upper

compartment was sampled first. Aspirator vacuum was applied to leg E and sufficient liquid removed to insure complete removal of all stagnant liquid in leg E. The diaphragm cell was then inverted. Air pressure was applied at leg E, and upper compartment solution removed through leg D and collected. The diaphragm cell was placed upright. Aspirator vacuum was applied to leg F and sufficient liquid removed to insure complete removal of all stagnant liquid in leg F. Air pressure was then applied to leg F and lower compartment solution removed through leg G. Sufficient liquid from leg G was discarded to insure complete removal of all stagnant liquid from leg G. The remainder of the lower compartment solution was then discarded.

A.6. Degassing the Diaphragm Cell

When the diaphragm cell lower compartment was filled with solution as described previously, a small bubble of air remained trapped on the under side of the diaphragm. This air bubble was removed by degassing. The diaphragm cell was clamped into a beaker of silicone oil which was placed upon a hot plate. The diaphragm cell was immersed to approximately the diaphragm level. The lower compartment solution was then brought to boiling. The boiling was continued until approximately half the lower compartment solution was forced into the upper compartment. A Kimwipe was placed across the top of leg D to retain any liquid forced out through this capillary leg and to prevent contamination of the silicone oil with uranyl nitrate. The diaphragm cell was removed from the silicone oil bath and allowed to cool to room temperature, creating a vacuum in the vapor space above the solution in the lower compartment.

The vapor space was then filled completely with solution drawn through the diaphragm.

A.7. Cell Constant Calibration

The diaphragm cells were calibrated for the cell constant using 0.1N potassium chloride solution. The potassium chloride was used as the lower compartment solution and distilled water as solvent in the upper compartment. Each cell was filled as described previously. The cell was inserted into the oil bath as soon as the upper compartment was filled with solvent. The timing of the experimental run is described in the next section.

For making calibration weighings, 100-ml weighing bottles and caps were carefully cleaned with cleaning solution (concentrated sulfuric acid with dissolved sodium dichromate), distilled water, and acetone and dried in an oven at approximately 105°C. The oven temperature was then increased to approximately 260°C. After cooling, the weighing bottles and caps were then weighed on the Mettler balance in a prescribed manner. Four weighing bottles and caps were wiped clean with a moist chamois cloth, placed inside the balance and allowed to reach equilibrium with the ambient temperature for approximately one-half hour. Three of the four bottles would be used for receiving one of three triplicate samples from one cell compartment. The fourth weighing bottle was used as a standard bottle whose weight permitted convenient correction of the weights for buoyancy effects. A weighing bottle was placed on the balance pan. A second bottle was moved to the position of the first bottle. Rotation was continued until all weighing bottles had been moved one position. The first bottle was then weighed

and moved to the position of the fourth bottle. This rotation procedure was followed until all weighing bottles had been weighed three times. Both tare and gross weighings were made in this manner.

At the end of the diffusion run, the diaphragm cells were removed from the constant-temperature bath and sampled as described above into 100-ml sample bottles as rapidly as possible. A 10-ml calibrated sampling pipette was used to sample the solution and deliver the sample to the tared weighing bottle. Triplicate samples of each solution were taken. The samples were then placed in an oven to evaporate all liquid at 60°C. The oven temperature was then increased to 260°C. to remove any residual moisture. The weighing bottles with potassium chloride residue were reweighed in the same manner as the empty weighing bottles. Cell constants were calculated by the integral diaphragm diffusion coefficient equation. The calculations were made on an IBM 1620 computer. A program listing of this program is shown in Appendix H.

Cell constant reproducibility was 0.8%. Lower compartment stirrers became damaged in two of the cells during operation and were replaced. Upper compartment volumes and cell constants were recalibrated for these two cells. For the remaining four cells, cell constants were checked at the end of the experimental work with potassium chloride to determine any attrition effects. The average deviation in cell constant values was less than 0.3%. The cell constant calibration data are shown in Appendix I.

A.8. Experimental Run Procedure

Filling and sampling procedures are described above. The run time for each cell was measured with an electric wall clock. Run initiation

was taken as that time following rinsing of the upper compartment when sufficient solvent had been drawn into the upper compartment to completely cover the diaphragm. This time was selected as a concentration gradient and established at this time. Elapsed time between this run initiation time and insertion of the diaphragm cell into the constant-temperature bath was approximately 30 seconds. Run termination was taken as that time when the diaphragm cell was inverted and sufficient sample was removed from the upper compartment to remove all liquid in contact with the upper surface of the diaphragm. Elapsed time between removal of the diaphragm cell from the constant-temperature bath and this run termination time was approximately 30 seconds. The temperature of the constant-temperature bath was measured approximately every 8 hours during the experimental runs.

A.9. Refractometer Calibration

Twenty one 1-ml samples of uranyl nitrate solution were prepared as described above for calibration of the Bausch and Lomb refractometer. The refractive index of each calibration sample was measured in triplicate. The refractometer scale reading can be estimated to one part in 14,600 or the refractive index to 0.00003 units. Uranyl nitrate concentration was then correlated against refractive index using least-mean-squares regression. The standard error of estimate for the correlation is 0.00468M. Calibration data and the concentration correlation are shown in Appendix J.

Refractive index measurements on the compartment solutions from the experimental runs were measured in duplicate. The prism faces of the refractometer were cleaned with xylene between each reading.

B. Capillary Cell

The experimental procedure used to determine diffusion coefficients by the capillary cell method is outlined below. For a detailed explanation of experimental procedures used with the capillary cell, reference is made to Finley (7).

1. The constant temperature bath was brought to temperature equilibrium.
2. The capillary cells were cleaned with chromic acid solution, distilled water, and acetone.
3. The capillary cells were charged with solute using a micro-syringe.
4. The capillary cells were carefully lowered into the diffusion cells to initiate the diffusion runs.
5. At the end of the diffusion runs, the samples were removed and prepared for scintillation counting by adding the scintillation solvent.
6. The samples were then stored for 24 hours to allow light decay.
7. The samples were then analyzed on the scintillation counter.

C. Interferometer

The experimental procedure used to determine diffusion coefficients with the interferometer is outlined below. For a detailed explanation of experimental procedures used with the interferometer, reference is made to Skinner (22).

1. The diffusion cell, feed separatory funnels, and feed lines were thoroughly cleaned.

2. The diffusion cell was placed in the constant-temperature bath and the bath was brought to temperature equilibrium.

3. The diffusion cell compartments were filled with the solutions being studied.

4. The interface was sharpened.

5. The drain lines were closed to initiate the diffusion run.

6. The data were obtained by photographing the diffusion gradients at timed intervals.

7. The photographs were developed and analyzed.

CHAPTER V

RESULTS AND DISCUSSION

A. Diaphragm Cell Experimental Data

The raw experimental data consisting of refractive index measurements of concentration and experimental run times for all 42 experimental runs are shown in Appendix K. The diaphragm cell concentrations--to include c_T , c_B , c_{B_0} , \bar{c} , and \sqrt{c} --and calculated integral diffusion coefficients for all 42 experimental runs are shown in Table I. An error analysis of the calculated integral diffusion coefficients by error propagation was made according to the following equation:

$$d\bar{D} = \left(-\frac{d\beta}{\beta^2 t} - \frac{dt}{\beta t^2}\right) \ln\left(\frac{c_{B_0}}{c_B - c_T}\right) + \frac{1}{\beta t} \frac{dc_{B_0}}{c_{B_0}} + \frac{dc_T - dc_B}{\beta t (c_B - c_T)} \quad (9)$$

where:

$$\begin{aligned} dc_{B_0} = & \left(\frac{V_T + \frac{1}{2}V_D}{V_B + V_D}\right) dc_T + \left(\frac{V_B + \frac{1}{2}V_D}{V_B + V_D}\right) dc_B + \left(\frac{c_T}{V_B + V_D}\right) dV_T \\ & + \left(\frac{c_B}{V_B + V_D} - \frac{V_T c_T + V_B c_B + \frac{1}{2}V_D c_T + \frac{1}{2}V_D c_B}{(V_B + V_D)^2}\right) dV_B \\ & + \left(\frac{\frac{1}{2}(c_T + c_B)}{V_B + V_D} - \frac{V_T c_T + V_B c_B + \frac{1}{2}V_D c_T + \frac{1}{2}V_D c_B}{(V_B + V_D)^2}\right) dV_D \quad (10) \end{aligned}$$

The derivation of Equations (9) and (10) is shown in Appendix L.

Error analysis of all 42 experimental runs yielded an error in the

TABLE I
DIAPHRAGM CELL INTEGRAL DIFFUSION COEFFICIENTS

Run No.	Run Set 1					
	c_T	c_B	c_{B_0}	\bar{c}	$\sqrt{\bar{c}}$	$D \times 10^6$
111	0.5870	0.9395	1.5748	0.7553	0.8691	8.414
112	0.0052	0.0327	0.0381	0.0133	0.1353	4.316
113	0.3344	0.7107	1.0719	0.5141	0.7170	9.009
114	0.0750	0.1290	0.2101	0.1008	0.3175	8.902
115	0.2326	0.5227	0.7739	0.3712	0.6093	8.692
121	0.0522	0.1413	0.1952	0.0958	0.3096	8.245
122	0.1495	0.3453	0.4997	0.2453	0.4953	8.618
123	0.0321	0.0627	0.0958	0.0470	0.2169	8.000
124	0.7016	1.8014	2.5254	1.2398	1.1135	7.873
131	0.6164	0.9493	1.5696	0.7816	0.8841	8.717
132	0.0047	0.0321	0.0367	0.0183	0.1353	3.890
133	0.3452	0.7563	1.1028	0.5491	0.7410	8.492
134	0.0821	0.1512	0.2337	0.1164	0.3412	7.973
135	0.2590	0.5548	0.8148	0.4057	0.6370	8.975
141	0.0434	0.1474	0.1877	0.0969	0.3113	7.703
142	0.1653	0.3614	0.5156	0.2662	0.5160	8.329
143	0.0403	0.0677	0.1054	0.0544	0.2333	8.823
144	0.7721	1.7826	2.5022	1.2921	1.1367	8.041
151	0.7486	1.4236	2.1382	1.0920	1.0450	9.215
152	0.1047	0.2224	0.3223	0.1646	0.4057	9.087
153	0.0037	0.0108	0.0143	0.0073	0.0855	4.821

TABLE I (CONTINUED)

Run No.	c_T	c_B	c_{B_0}	\bar{c}	$\sqrt{\bar{c}}$	$D \times 10^6$
161	0.7090	1.3558	2.0986	1.0228	1.0113	5.744
162	0.1012	0.2262	0.3321	0.1619	0.4023	8.185
163	0.0037	0.0104	0.0142	0.0069	0.0833	4.839
Run Set 2						
211	0.0686	0.1274	0.2012	0.0968	0.3111	8.720
212	0.1178	0.2977	0.4241	0.2040	0.4516	9.460
213	0.15601	0.3044	0.4722	0.2271	0.4766	8.951
221	0.1807	0.4598	0.6463	0.3173	0.5633	9.008
222	0.1759	0.4541	0.6356	0.3120	0.5586	8.862
223	0.2255	0.6447	0.8772	0.4306	0.6562	8.934
231	0.2635	0.7959	1.0596	0.5276	0.7264	8.988
232	0.2651	0.7877	1.0531	0.5244	0.7241	9.150
233	0.3333	1.0242	1.3578	0.6761	0.8223	8.803
241	0.3430	1.1359	1.4544	0.7510	0.8666	9.189
242	0.3304	1.1650	1.4715	0.7599	0.3717	8.590
243	0.3963	1.3399	1.7079	0.8819	0.9391	8.883
251	0.4849	1.3295	1.7920	0.9141	0.9561	8.682
252	0.6472	1.2908	1.9100	0.9743	0.9870	8.618
253	0.3999	1.6740	2.0533	1.0470	1.0234	8.530
261	0.3985	2.2296	2.6399	1.2866	1.1343	7.577
262	0.4183	2.2456	2.6771	1.3047	1.1422	7.907
263	0.4401	2.2920	2.7464	1.3384	1.1569	8.129

integral diffusion coefficient, $d\bar{D}$, of $0.501 \times 10^{-6} \text{ cm}^2\text{-sec}^{-1}$, or an average error of 9.80% of the calculated integral diffusion coefficients. This error analysis was biased by four experimental runs--112/132/153/163--as these runs were conducted at concentrations below 0.05 molar. These four runs were excluded from subsequent evaluations because Stokes (18) has proved that diaphragm cell measurements yield erroneous results at concentrations below 0.05 molar with the error increasing at more dilute concentrations. Error analysis of the remaining 38 experimental runs yielded an error, $d\bar{D}$, of $0.147 \times 10^{-6} \text{ cm}^2\text{-sec}^{-1}$, or an average error of 1.74% of the calculated integral diffusion coefficients.

The diaphragm cell data were then averaged according to average concentration as shown in Table II. The average deviation in the integral diffusion coefficients ranged from 0.073×10^{-6} to $0.451 \times 10^{-6} \text{ cm}^2\text{-sec}^{-1}$. These deviations averaged $0.238 \times 10^{-6} \text{ cm}^2\text{-sec}^{-1}$ for all experimental values obtained from averaging two or more experimental runs (excludes experimental runs 134, 233, 252 and 124).

B. Comparison With Other Diaphragm Cell Data

The integral diffusion coefficients shown in Table II are compared with those of Ondrejcin (18) in Figure 4. These values are plotted as a function of $\sqrt{c_{B_0}}$. (The integral diffusion coefficients are not compared as a function of \sqrt{c} since Ondrejcin presents only initial concentration data.) Limiting diffusion coefficients and slopes calculated from both limiting equivalent conductivities discussed in Chapter II are also shown in Figure 4.

Ondrejcin states that the average coefficient of variation of

TABLE II
DIAPHRAGM CELL AVERAGE INTEGRAL DIFFUSION COEFFICIENTS

Runs Averaged	c_T	c_B	c_{B_0}	\bar{c}	$\sqrt{\bar{c}}$	$D \times 10^6$	Average Deviation in D
123/143	0.0362	0.0652	0.1006	0.0507	0.2253	8.412	0.412
121/211/ 141/114	0.0598	0.1360	0.1985	0.0976	0.3124	8.410	0.436
134	0.0821	0.1512	0.2337	0.1164	0.3412	7.973	---
162/152	0.1025	0.2243	0.3272	0.1632	0.4040	8.636	0.451
212/213	0.1369	0.3010	0.4481	0.2155	0.4643	9.205	0.255
122/142	0.1574	0.3534	0.5076	0.2558	0.5057	8.474	0.144
222/221	0.1783	0.4569	0.6410	0.3147	0.5610	8.935	0.073
115/135/ 223	0.2390	0.5741	0.8220	0.4025	0.6344	8.867	0.117
113/232/ 231/133	0.3020	0.7626	1.0719	0.5288	0.7273	8.909	0.209
233	0.3333	1.0242	1.3578	0.6761	0.8225	8.803	---
241/111/ 242/131	0.4692	1.0474	1.5176	0.7620	0.8729	8.728	0.231
243/251	0.4406	1.3347	1.7499	0.8980	0.9476	8.782	0.101
252	0.6472	1.2908	1.9100	0.9743	0.9870	8.618	---
161/253/ 151	0.6192	1.4845	2.0967	1.0540	1.0267	8.830	0.254
124	0.7016	1.8014	2.5254	1.2398	1.1165	7.873	---
261/144/ 262/263	0.5072	2.1374	2.6414	1.3055	1.1426	7.914	0.172
Average Reproducibility = 2.59%							

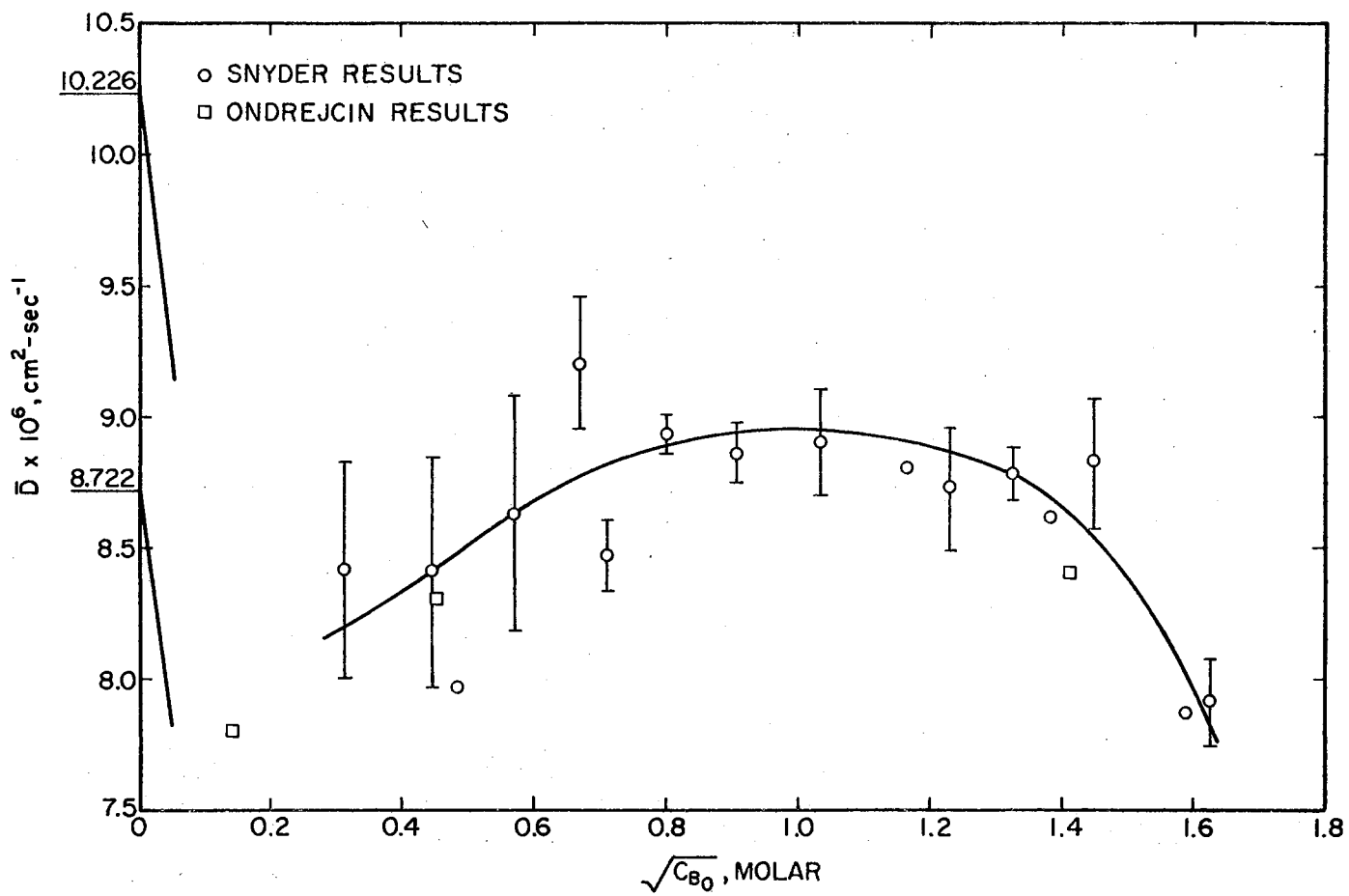


Figure 4. Comparison of Diaphragm Cell Integral Diffusion Coefficients

uranium diffusion coefficients in his work is 4.8%. For comparison, the coefficient of variation was calculated for the integral diffusion coefficients shown in Table III. (The coefficient of variation is calculated only for those integral diffusion coefficients obtained from averaging two or more experimental runs. Experimental runs 134, 233, 252 and 124 are not included in these calculations.) The calculated coefficients of variation are shown in Table III. The average coefficient of variation is 3.8%. This value indicates improved experimental reproducibility when compared to Ondrejcin's coefficient of variation of 4.8%.

No attempt is made here to establish the presence or value of a minimum diffusion coefficient at low concentration. However, for the integral diffusion coefficients obtained in this study, a minimum may exist in the concentration range $c_{B_0} = 0.10-0.30$. An increase in the integral diffusion coefficient toward the limiting diffusion coefficient $D_0 = 10.226 \times 10^{-6}$ could possibly occur at concentrations lower than $c_{B_0} = 0.10$. Inclusion of Ondrejcin's value of $\bar{D} = 7.8 \times 10^{-6}$ at $c_{B_0} = 0.20$ indicates a minimum may exist at even lower concentrations with possible increase toward the limiting diffusion coefficient $D_0 = 8.722 \times 10^{-6}$. However, it is noted that \bar{c} for Ondrejcin's experimental point at $c_{B_0} = 0.20$ is probably near the recommended concentration lower limit for diaphragm cell operation.

C. Comparison With Capillary Cell Integral

Diffusion Coefficients

The diaphragm cell integral diffusion coefficients are compared with the capillary cell integral diffusion coefficients obtained by

TABLE III
 COEFFICIENT OF VARIATION FOR DIAPHRAGM CELL
 INTEGRAL DIFFUSION COEFFICIENTS

Runs Averaged	$\bar{D} \times 10^6$	Coefficient of Variation, %
123/143	8.412	6.9
121/211/141/114	8.410	6.4
134	7.973	---
162/152	8.636	7.4
212/213	9.205	3.9
122/142	8.474	2.4
222/221	8.935	1.2
115/135/223	8.867	1.7
113/232/231/133	8.909	3.2
233	8.803	---
241/111/242/131	8.728	3.8
243/251	8.782	1.6
252	8.618	---
161/253/151	8.830	4.0
124	7.873	---
261/144/262/263	7.914	3.1
Average Coefficient of Variation = 3.8%		

Finley (7) in Figure 5. Finley's results show a distinct minimum in the range $\sqrt{c} = 0.30-0.50$. As shown in Figure 5, this minimum does not appear to be supported by the diaphragm cell results. Further comment on this discrepancy is here deferred until subsequent results on the derivation of differential diffusion coefficients are discussed.

D. Diaphragm Cell Differential Diffusion Coefficients

The method of Stokes (27) for deriving differential diffusion coefficients from integral diffusion coefficients is shown in Appendix B. A definition basic to Stokes' method is the relationship between the two diffusion coefficients. The exact dependency of \bar{D} with time is given by the following equation:

$$\bar{D} = \frac{1}{t} \int_0^t \bar{D}(t) dt \quad (11)$$

In Stokes' method, however, the integrand in Equation (11) is treated as having a constant value equal to its value when the upper and lower compartment concentrations are halfway between their initial and final values. The relationship between the differential diffusion coefficient D and the integral diffusion coefficient \bar{D} is then given by the following equation:

$$\bar{D} = \frac{1}{c_{m'} - c_{m''}} \int_{c_{m''}}^{c_{m'}} D dc \quad (12)$$

where:

$$c_{m'} = \frac{c_{B_0} + c_B}{2} \quad \text{and:} \quad c_{m''} = \frac{c_{T_0} + c_T}{2} \quad (13)$$

$$(14)$$

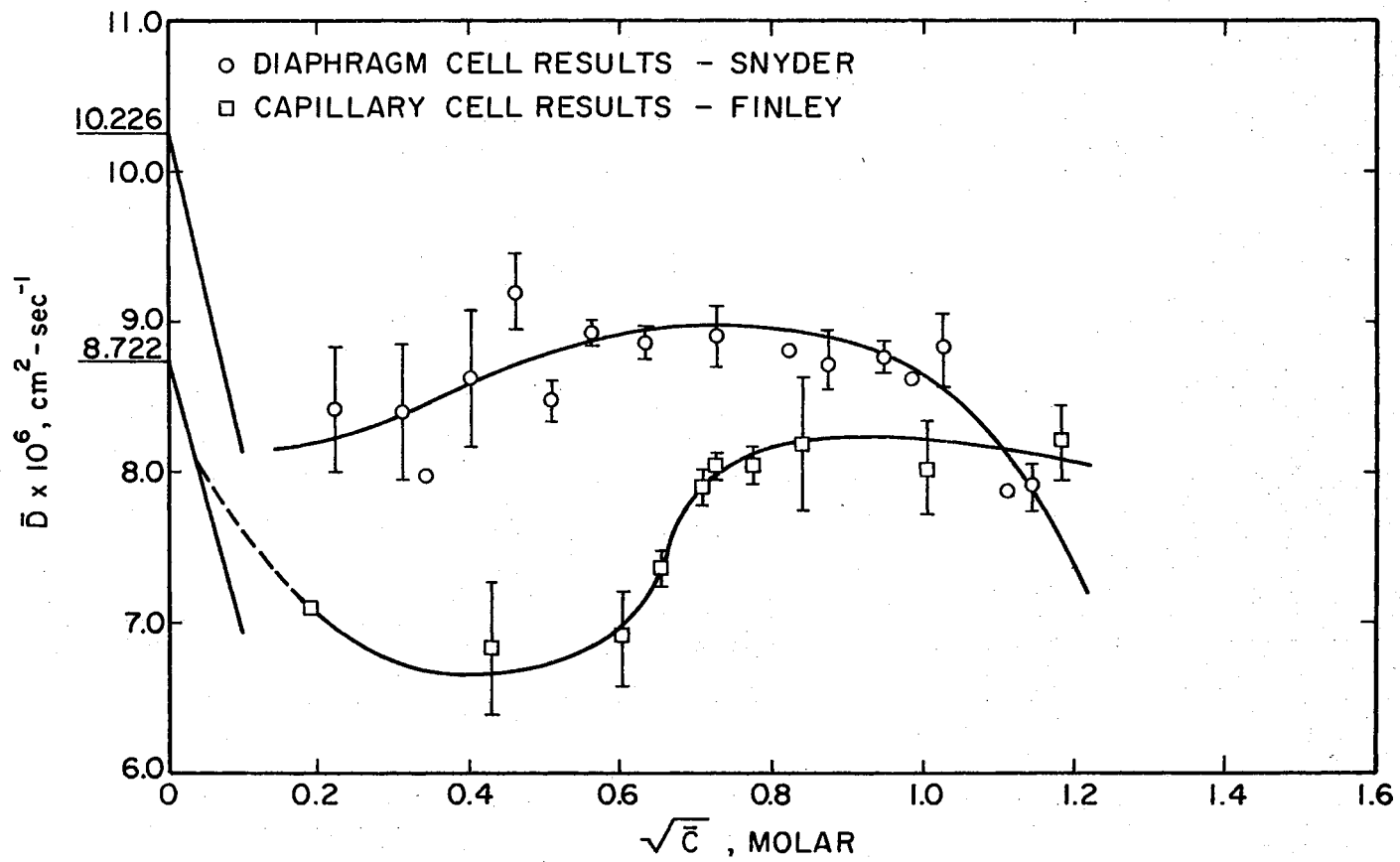


Figure 5. Comparison of Integral Diffusion Coefficients

Stokes (27) has shown that use of Equation (12) is not in error by more than 0.02%.

The initial step in deriving differential diffusion coefficients by the method of Stokes (27)--curve-fitting of \bar{D} as a function of c_{B_0} --was used to find the best multiple linear regression model for further work. Several multiple linear regression models were tested. A cubic equation including a square-root term was selected as shown below:

$$\bar{D} = D_0 + P c_{B_0}^{0.5} + Q c_{B_0}^{1.0} + R c_{B_0}^{2.0} + S c_{B_0}^{3.0} \quad (15)$$

Details of model testing are discussed in Appendix M.

The regression equations of \bar{D} as a function of c_{B_0} which are used to derive differential diffusion coefficients appear below. Using $D_0 = 10.226 \times 10^{-6}$:

$$\begin{aligned} \bar{D} = & 10.143 \times 10^{-6} - 8.001 \times 10^{-6} c_{B_0}^{0.5} + 9.947 \times 10^{-6} c_{B_0}^{1.0} \\ & - 3.590 \times 10^{-6} c_{B_0}^{2.0} + 0.519 \times 10^{-6} c_{B_0}^{3.0} \end{aligned} \quad (16)$$

Using $D_0 = 8.722 \times 10^{-6}$:

$$\begin{aligned} \bar{D} = & 8.687 \times 10^{-6} - 2.081 \times 10^{-6} c_{B_0}^{0.5} + 3.597 \times 10^{-6} c_{B_0}^{1.0} \\ & - 1.407 \times 10^{-6} c_{B_0}^{2.0} + 0.158 \times 10^{-6} c_{B_0}^{3.0} \end{aligned} \quad (17)$$

The next step in the method of Stokes (27) was to use Equations (16) and (17) to estimate values for $\bar{D}_{c_m''}$ at c_m'' . These values were then used to calculate $\bar{D}_{c_m'}$ according to the following equation:

$$\bar{D}_{c_m'} = \bar{D} - \left(\frac{c_m''}{c_m'} \right) (\bar{D} - \bar{D}_{c_m''}) \quad (18)$$

The values for \bar{D}_{c_m} were curve-fitted as a function of c_m using regression model (15). The resulting regression equations are shown in

Figure 6 and are as follows:

$$\begin{aligned} \bar{D}_{c_m} = & 10.076 \times 10^{-6} - 7.391 \times 10^{-6} c_m^{0.5} + 9.508 \times 10^{-6} c_m^{1.0} \\ & - 3.908 \times 10^{-6} c_m^{2.0} + 0.653 \times 10^{-6} c_m^{3.0} \end{aligned} \quad (19)$$

$$\begin{aligned} \bar{D}_{c_m} = & 8.662 \times 10^{-6} - 1.965 \times 10^{-6} c_m^{0.5} + 3.641 \times 10^{-6} c_m^{1.0} \\ & - 1.710 \times 10^{-6} c_m^{2.0} + 0.247 \times 10^{-6} c_m^{3.0} \end{aligned} \quad (20)$$

The data values for \bar{D}_{c_m} , obtained through use of Equations (16) and (17) and used in the multiple linear regression are also shown in Figure 6.

Equations (19) and (20) were then used to re-estimate \bar{D}_{c_m} , and \bar{D}_{c_m} was recalculated using Equation (18). The values for \bar{D}_{c_m} , derived from this second trial remained essentially constant. The values for \bar{D}_{c_m} , for both trials are shown in Table IV. The values for \bar{D}_{c_m} , from this second trial were then curve-fitted as a function of c_m . The resulting regression equations, with the values for \bar{D}_{c_m} obtained with Equations (19) and (20) are shown in Figure 7 and are as follows:

$$\begin{aligned} \bar{D}_{c_m} = & 10.012 \times 10^{-6} - 7.102 \times 10^{-6} c_m^{0.5} + 9.193 \times 10^{-6} c_m^{1.0} \\ & - 3.779 \times 10^{-6} c_m^{2.0} + 0.628 \times 10^{-6} c_m^{3.0} \end{aligned} \quad (21)$$

$$\begin{aligned} \bar{D}_{c_m} = & 8.638 \times 10^{-6} - 1.868 \times 10^{-6} c_m^{0.5} + 3.541 \times 10^{-6} c_m^{1.0} \\ & - 1.671 \times 10^{-6} c_m^{2.0} + 0.240 \times 10^{-6} c_m^{3.0} \end{aligned} \quad (22)$$

Equations (25) and (26) were then used to calculate the differential diffusion coefficients according to the following equation:

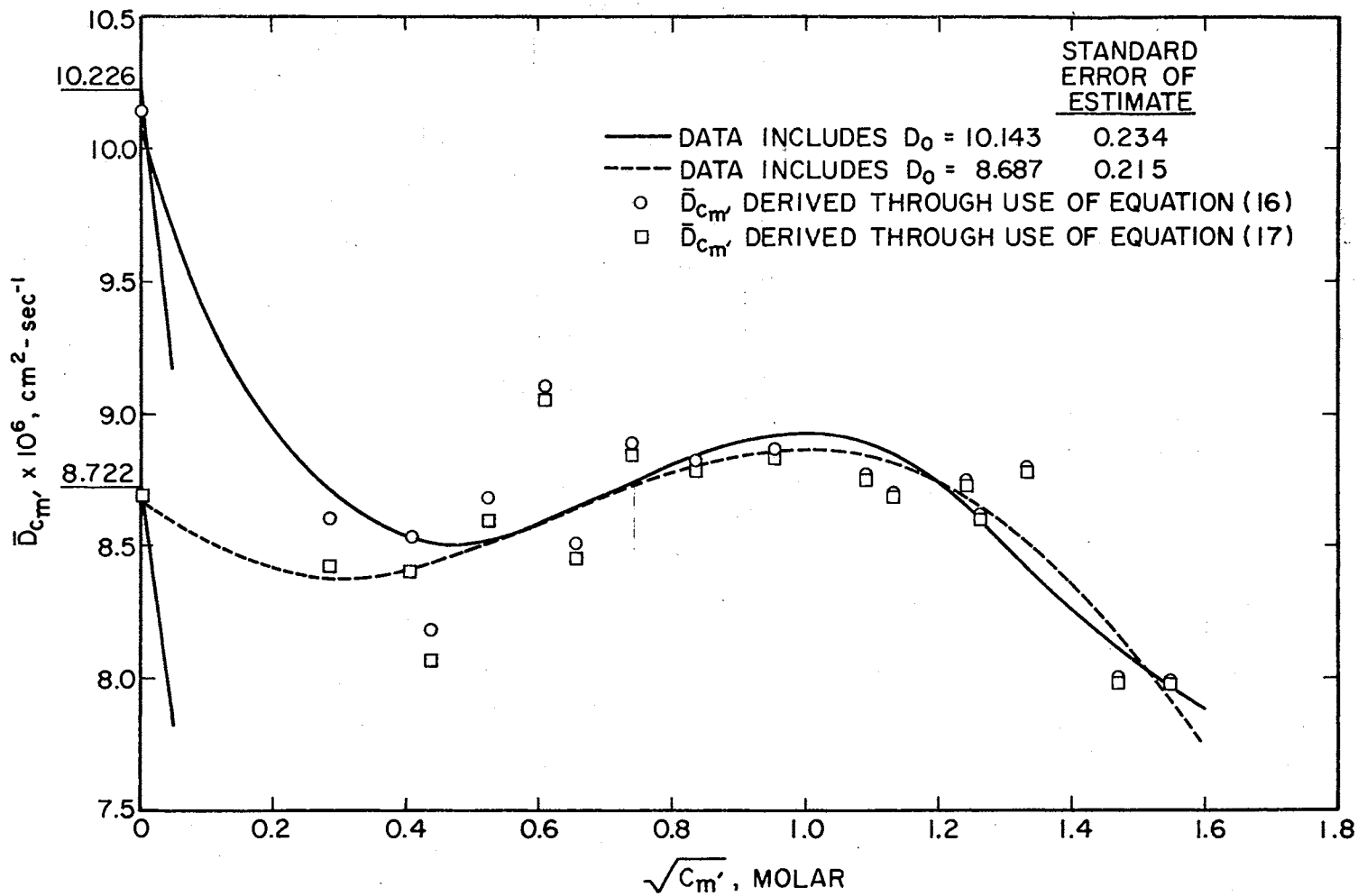


Figure 6. Multiple Linear Regression of $\bar{D}_{c_m'}$, as a Function of c_m' for Diaphragm Cell Data - Trial 1

TABLE IV
 CALCULATED VALUES FOR D_{c_m} , DERIVED FROM DIAPHRAGM CELL DATA

c_m'	D_{c_m} , Derived Using $D_o = 10.226 \times 10^{-6}$		D_{c_m} , Derived Using $D_o = 8.722 \times 10^{-6}$	
	Trial 1	Trial 2	Trial 1	Trial 2
0.0829	8.594	8.596	8.425	8.423
0.1673	8.524	8.529	8.414	8.413
0.1925	8.176	8.184	8.067	8.067
0.2757	8.672	8.681	8.591	8.592
0.3746	9.115	9.108	9.055	9.056
0.4305	8.508	8.520	8.456	8.458
0.5489	8.882	8.894	8.844	8.846
0.6980	8.807	8.822	8.783	8.786
0.9172	8.834	8.850	8.824	8.827
1.1910	8.752	8.766	8.746	8.750
1.2825	8.670	8.690	8.677	8.682
1.5423	8.729	8.744	8.733	8.736
1.6004	8.584	8.606	8.599	8.605
1.7906	8.763	8.782	8.775	8.780
2.1634	7.972	7.989	7.983	7.987
2.3894	7.967	7.980	7.972	7.975

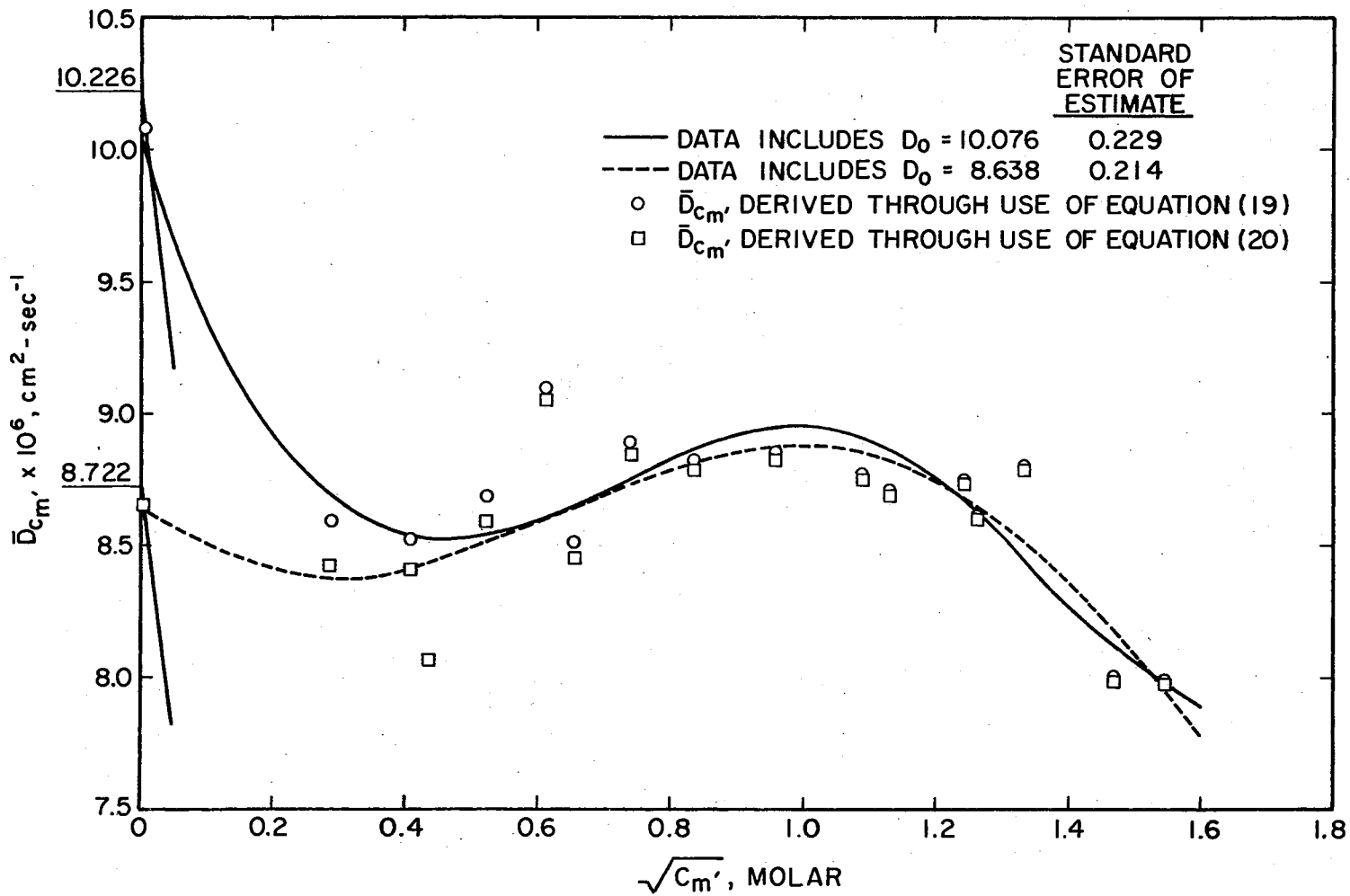


Figure 7. Multiple Linear Regression of $\bar{D}_{cm'}$, as a Function of $c_{m'}$ for Diaphragm Cell Data - Trial 2

$$D = \bar{D}_{c_m} + c \frac{d\bar{D}_{c_m}}{dc} \quad (23)$$

The term $\frac{d\bar{D}_{c_m}}{dc}$ is easily calculated by differentiation of Equations (21) and (22). The calculated values for the differential diffusion coefficients are shown in Table V.

The differential diffusion coefficients shown in Table VI were then curve-fitted as a function of \bar{c} according to the following regression model:

$$D = D_0 + P\bar{c}^{0.5} + Q\bar{c}^{1.0} + R\bar{c}^{2.0} + S\bar{c}^{3.0} \quad (24)$$

The calculated limiting diffusion coefficients were also used as input data in the multiple linear regression. The resulting regression equations, along with the differential diffusion coefficients as shown in Table VI, are shown in Figure 8 and are as follows:

$$D = 10.222 \times 10^{-6} - 11.914 \times 10^{-6}\bar{c}^{0.5} + 20.410 \times 10^{-6}\bar{c}^{1.0} \\ - 12.941 \times 10^{-6}\bar{c}^{2.0} + 3.108 \times 10^{-6}\bar{c}^{3.0} \quad (25)$$

$$D = 8.719 \times 10^{-6} - 3.362 \times 10^{-6}\bar{c}^{0.5} + 8.109 \times 10^{-6}\bar{c}^{1.0} \\ - 5.948 \times 10^{-6}\bar{c}^{2.0} + 1.327 \times 10^{-6}\bar{c}^{3.0} \quad (26)$$

Standard errors of estimate for Equations (25) and (26) are comparable-- 0.026 for Equation (25) and 0.025 for Equation (26). Differential diffusion coefficients calculated from equations (25) and (26) are comparable except at values of $\sqrt{\bar{c}}$ less than approximately 0.3 where the effect of the limiting diffusion coefficient used in the multiple linear regression is realized. Both Equations (25) and (26) show a

TABLE V
 CALCULATED DIFFERENTIAL DIFFUSION COEFFICIENTS DERIVED FROM
 DIAPHRAGM CELL DATA

\bar{c}	D Derived Using $D_0=10.226 \times 10^{-6}$	D Derived Using $D_0=9.722 \times 10^{-6}$
0.0507	8.524	8.350
0.0976	8.373	8.407
0.1164	8.367	8.439
0.1632	8.412	8.529
0.2155	8.527	8.640
0.2558	8.627	8.720
0.3147	8.777	8.828
0.4025	8.981	9.028
0.5288	9.188	9.085
0.6761	9.275	9.126
0.7620	9.250	9.040
0.8980	9.002	8.993
0.9743	8.968	8.899
1.0540	8.797	8.778
1.2398	8.289	8.415
1.3055	8.106	8.270

TABLE VI

NUMERICAL SOLUTION OF FICK'S SECOND LAW FOR CAPILLARY CELL DATA
UTILIZING FINLEY'S EQUATION

$$D = 8.7379 \times 10^{-6} - 24.463 \times 10^{-6}c^{0.5} + 39.566 \times 10^{-6}c^{1.0} \\ - 17.857 \times 10^{-6}c^{2.0} + 3.355 \times 10^{-6}c^{3.0}$$

c_0	Experimental Final Concentration	Calculated Final Concentration	% Error	Experimental \bar{c}	Calculated \bar{c}	% Error
0.05	0.022	0.022	0.0	0.036	0.036	00.0
0.25	0.114	0.120	+5.3	0.182	0.185	+1.6
0.50	0.228	0.239	+4.8	0.364	0.3695	+1.5
0.60	0.260	0.283	+8.8	0.430	0.4415	+2.7
0.71	0.292	0.329	+12.7	0.501	0.5195	+3.7
0.75	0.307	0.346	+12.7	0.5285	0.548	+3.7
0.86	0.346	0.390	+12.7	0.603	0.625	+3.7
1.00	0.409	0.444	+8.6	0.7045	0.722	+2.5
1.50	0.620	0.623	+0.5	1.060	1.0615	+0.1

Average Deviation in Calculated Final Concentration = 0.0217

Average Deviation in Calculated Average Concentration = 0.0108

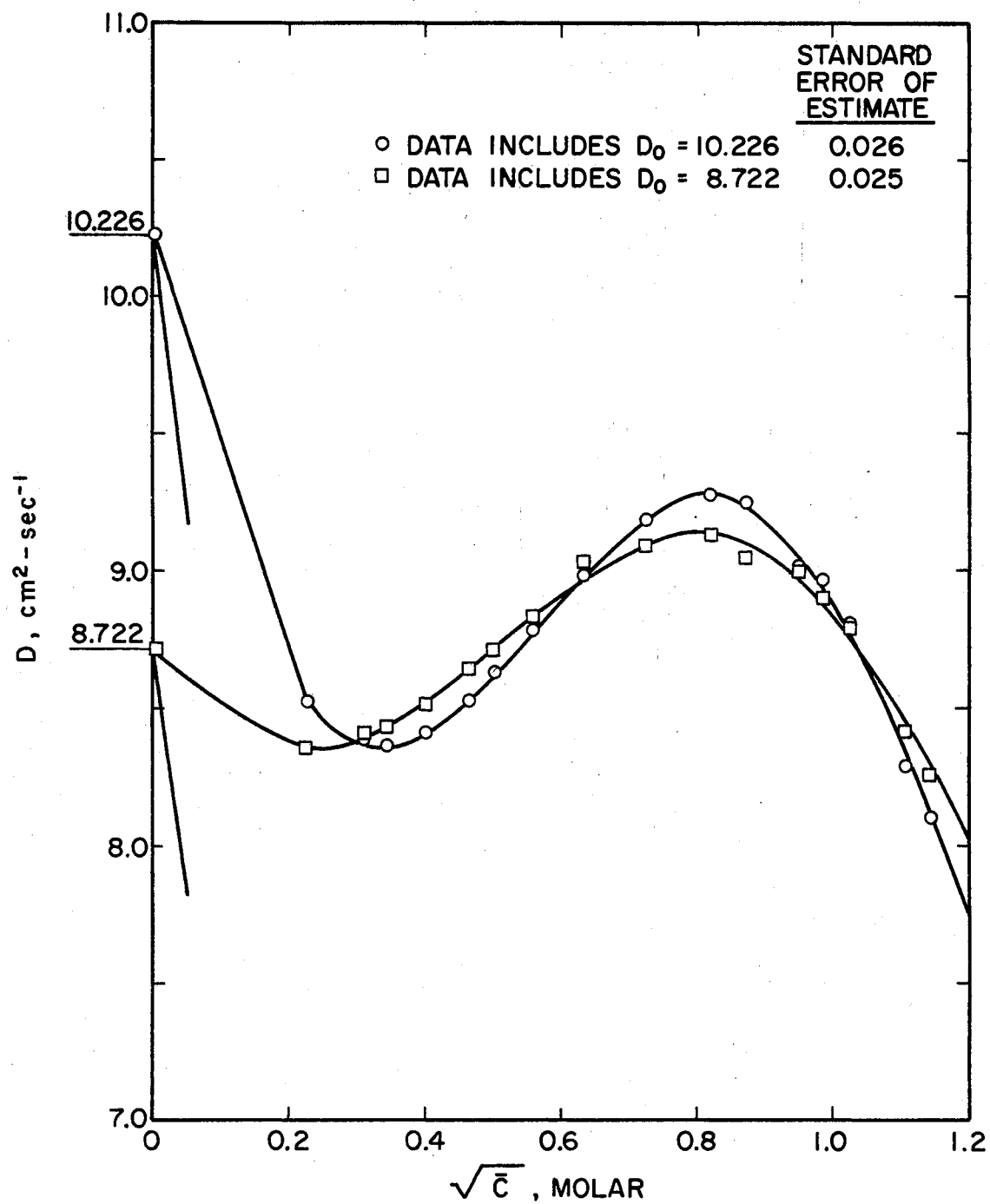


Figure 8. Multiple Linear Regression of Diaphragm Cell Differential Diffusion Coefficients According to the Model:
 $D = D_0 + P\bar{c}^{0.5} + Q\bar{c}^{1.0} + R\bar{c}^{2.0} + S\bar{c}^{3.0}$

minimum at low concentrations. However, the values of these minimums are in the range $8.3-8.4 \times 10^{-6}$, do not differ widely from diaphragm cell integral diffusion coefficients in this concentration range $\sqrt{c} = 0.2-0.4$, but still differ significantly from the minimum exhibited by the capillary cell integral diffusion coefficients (see Figure 5).

A decision as to which of the above two equations more accurately describes the diaphragm cell differential diffusion coefficients is deferred until other diffusion coefficient data are examined.

Both equations curve upward at low concentration following the theory of dilute solutions. However, neither equation has a limiting slope as sharp as that predicted by the Harned and Owen equation (12). Diffusion coefficients in the concentration range $\sqrt{c} = 0.4-0.8$ increase with concentration increase. This effect may be the result of ionic interactions--the electrophoretic effect and relaxation effect--discussed in Chapter II.

E. Interferometer Differential Diffusion

Coefficients

Interferometer differential diffusion coefficients previously obtained (29) were examined by curve-fitting. These differential diffusion coefficients are shown in Appendix N. On the basis of the results obtained with the diaphragm cell data, multiple linear regression models used included the square-root term. Since the interferometer data were obtained at low concentrations, a quadratic regression model was also examined. The regression models utilized include regression model (24) and the quadratic regression model as shown below:

$$D = D_0 + P\bar{c}^{0.5} + Q\bar{c}^{1.0} + R\bar{c}^{2.0} \quad (27)$$

The differential diffusion coefficients were curve-fitted with the calculated limiting diffusion coefficients, $D_0 = 10.226 \times 10^{-6}$ and $D_0 = 8.722 \times 10^{-6}$, included as input data. Because of the value of the differential diffusion coefficient $D = 10.40$ at very low concentration, the interferometer data were also curve-fitted without use of a limiting diffusion coefficient. The resulting multiple linear regression equations are shown in Figures 9 and 10. The differential diffusion coefficients used in the regressions are also shown.

As anticipated because of the high value of $D = 10.40$ at very low concentration, the regression equation derived using regression model (24) with $D_0 = 8.722 \times 10^{-6}$ as an input data value contains a positive limiting slope. In addition, a distinct discontinuity exists at $\sqrt{c} = 0.01$. This particular regression equation is excluded from further consideration.

All remaining regression equations show very erratic movement. As shown in Figure 9, the two remaining regression equations derived with the cubic regression model (24) show an inflection point in the concentration $\sqrt{c} = 0.03-0.06$, a minimum in the range $\sqrt{c} = 0.20-0.25$, and a maximum in the range $\sqrt{c} = 0.29-0.32$. All these variations in the shape of the regression equations occur within a narrow concentration band. The values of the minima exhibited with these two regression equations are intermediate between the minima obtained with the diaphragm cell differential diffusion coefficients and the capillary cell integral diffusion coefficients. This result in itself may not be unusual, but the minima shown in Figure 9 occur at concentrations much lower than observed with the diaphragm cell and capillary cell data. One conclusion may be that too many terms were used in the cubic regression model (24).

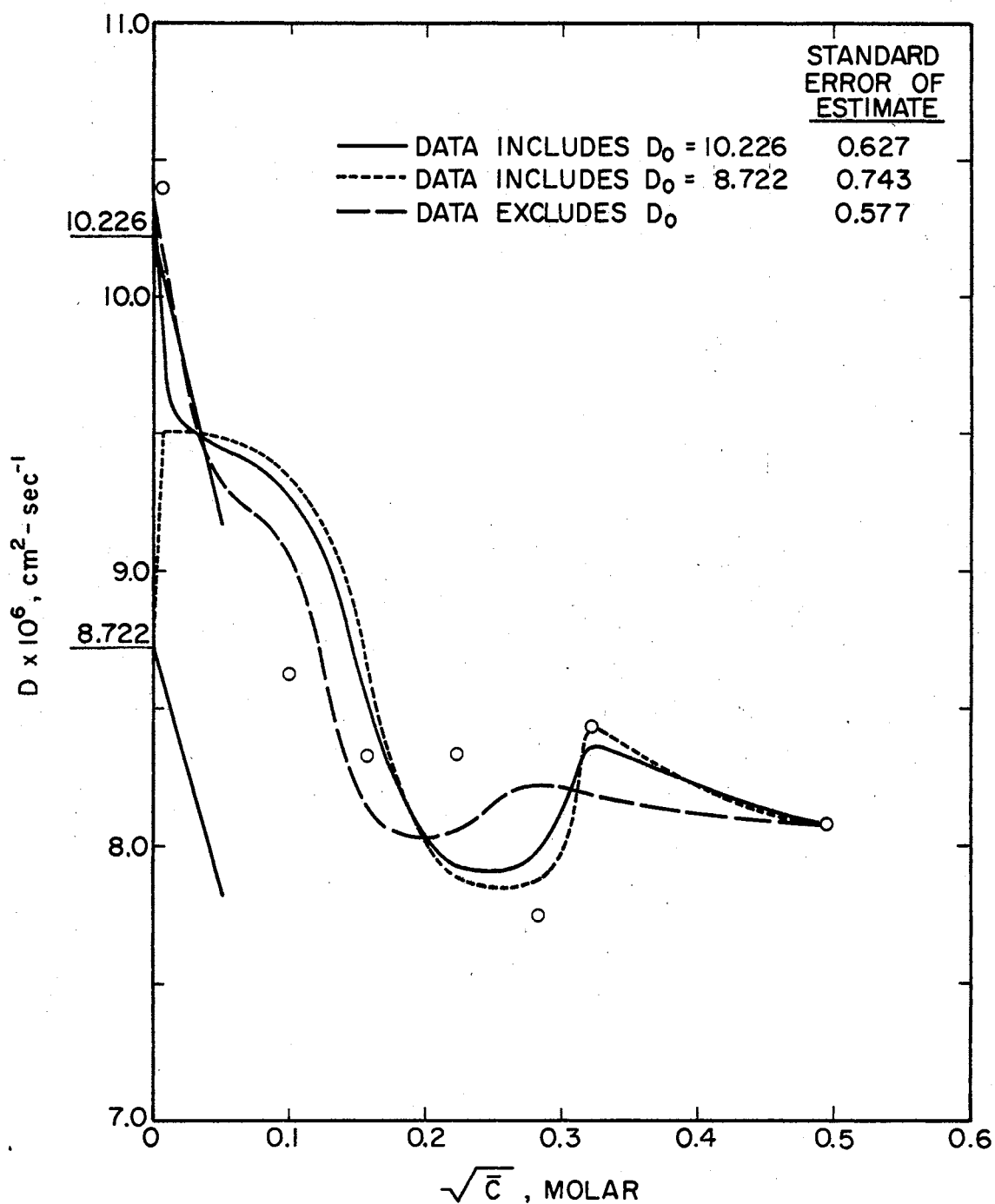


Figure 9. Multiple Linear Regression of Interferometer Differential Diffusion Coefficients According to the Model:
 $D = D_0 + P\bar{C}^{0.5} + Q\bar{C}^{1.0} + R\bar{C}^{2.0} + S\bar{C}^{3.0}$

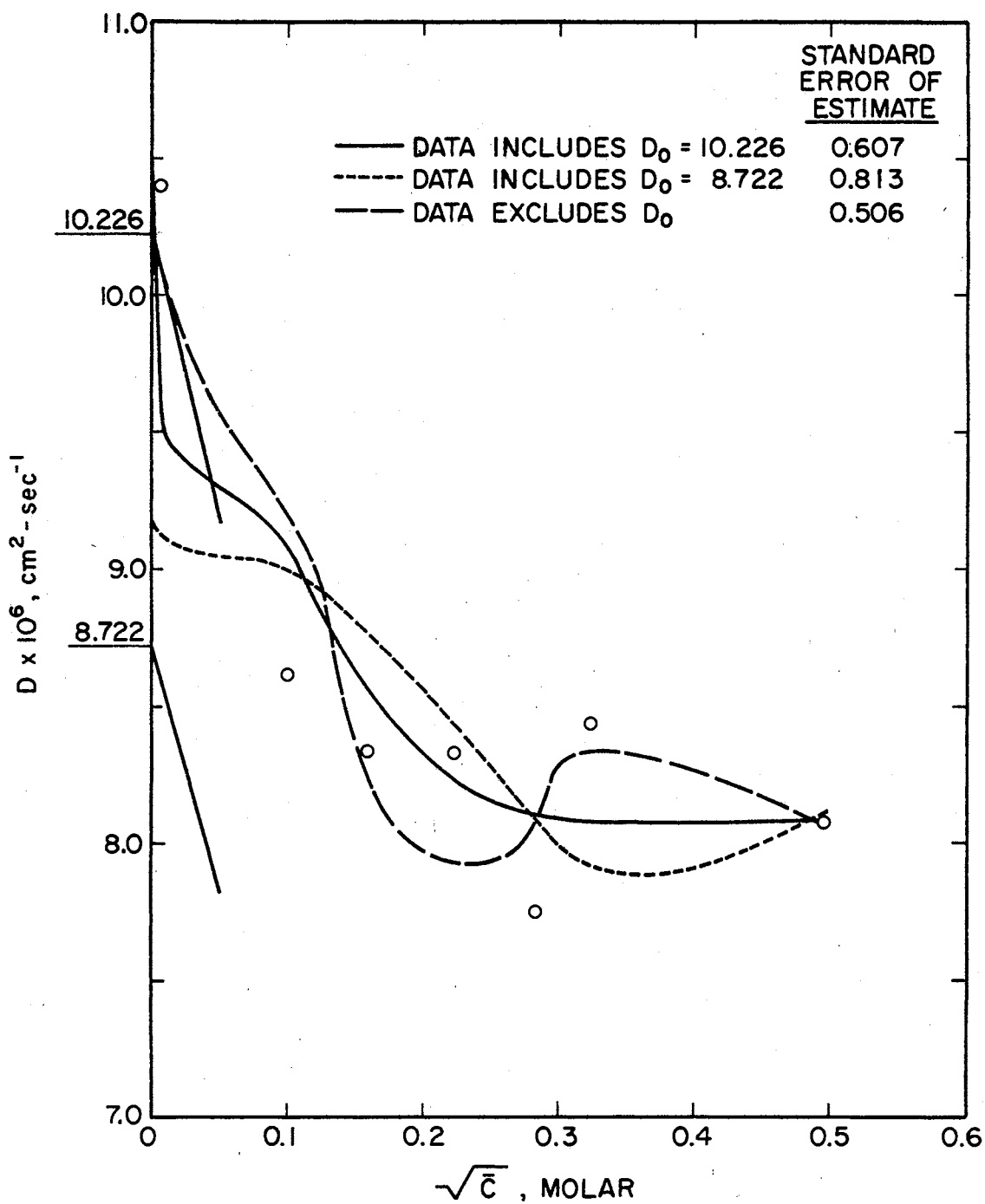


Figure 10. Multiple Linear Regression of Interferometer Differential Diffusion Coefficients According to the Model:
 $D = D_0 + P\bar{c}^{0.5} + Q\bar{c}^{1.0} + R\bar{c}^{2.0}$

This possibility was the basis for additionally examining the quadratic regression model (27).

As shown in Figure 10, little if any improvement is obtained with regression model (27). The regression equation which includes the calculated limiting diffusion coefficient $D_0 = 8.722 \times 10^{-6}$ as input data in the regression shows wide variations from calculated limiting values. The derived limiting diffusion coefficient is 9.203×10^{-6} . The derived limiting slope is -0.194×10^{-6} as compared to the calculated limiting value of -17.968×10^{-6} . The regression equation which includes the limiting diffusion coefficient $D_0 = 10.226 \times 10^{-6}$ as input data again shows the inflection at very low concentration but does not exhibit a maximum as obtained with regression model (24). The regression equation which does not include a value for the limiting diffusion coefficient as input data in the regression is very similar to that obtained with regression model (24) as shown in Figure 9.

Since the regression model containing fewer terms still yielded regression equations which exhibited erratic behavior, it was concluded that insufficient interferometer differential diffusion coefficient data are available to apply multiple linear regression. The interferometer data are hereafter used only for comparison purposes.

F. Capillary Cell Diffusion Coefficients

Capillary cell diffusion coefficients obtained by Finley (7) were examined. The capillary cell integral diffusion coefficients are shown in Appendix O.

Finley's derived equation for the capillary cell differential diffusion coefficient is shown as follows:

$$D = 8.7379 \times 10^{-6} - 24.463 \times 10^{-6} \bar{c}^{0.5} + 39.566 \times 10^{-6} \bar{c}^{1.0} \\ - 17.857 \times 10^{-6} \bar{c}^{2.0} + 3.355 \times 10^{-6} \bar{c}^{3.0} \quad (28)$$

Finley obtained Equation (28) by first applying multiple linear regression to the capillary cell integral diffusion coefficient data using the following regression model:

$$\bar{D} = D_0 - P\bar{c}^{0.5} + Q\bar{c}^{1.0} - R\bar{c}^{2.0} + S\bar{c}^{3.0} \quad (29)$$

The resulting regression equation was then adjusted until use of the adjusted equation in a numerical solution of Fick's Second Law reproduced the experimental concentrations.

The capillary cell integral diffusion coefficients were first curve-fitted using regression model (29) without use of a limiting diffusion coefficient. The resulting regression equation is shown below:

$$\bar{D} = 9.7586 \times 10^{-6} - 19.905 \times 10^{-6} \bar{c}^{0.5} + 32.850 \times 10^{-6} \bar{c}^{1.0} \\ - 20.259 \times 10^{-6} \bar{c}^{2.0} + 5.717 \times 10^{-6} \bar{c}^{3.0} \quad (30)$$

To modify Equation (30) to Finley's equation, the value for D_0 in Equation (30) requires an adjustment of 10.5%. The adjustment of the remaining coefficients in Equation (30) varies from 12-24%.

The integral diffusion coefficients were then curve-fitted using regression model (29) and the calculated limiting diffusion coefficient $D_0 = 8.722 \times 10^{-6}$. The resulting regression equation is shown below:

$$\bar{D} = 8.7701 \times 10^{-6} - 13.594 \times 10^{-6} \bar{c}^{0.5} + 23.087 \times 10^{-6} \bar{c}^{1.0} \\ - 13.685 \times 10^{-6} \bar{c}^{2.0} + 3.636 \times 10^{-6} \bar{c}^{3.0} \quad (31)$$

To modify Equation (31) to Finley's equation, the value for D_0 in Equation (31) requires an adjustment of 0.4%. The adjustment of the remaining coefficients in Equation (31) varies from 8-80%. Equation (31) requires a smaller adjustment in the value of D_0 than does Equation (30) to obtain Finley's equation but a greater adjustment in the value of the limiting slope.

The integral diffusion coefficients were then curve-fitted using regression model (29) and the calculated limiting diffusion coefficient $D_0 = 10.226 \times 10^{-6}$. The resulting regression equation is shown below:

$$D = 10.2068 \times 10^{-6} - 22.764 \times 10^{-6} \bar{c}^{0.5} + 37.271 \times 10^{-6} \bar{c}^{1.0} - 23.234 \times 10^{-6} \bar{c}^{2.0} + 6.658 \times 10^{-6} \bar{c}^{3.0} \quad (32)$$

Equation (32) was used in the numerical solution of Fick's Second Law according to Finley. No adjustment of Equation (32) was required to accurately predict the experimental concentrations. The solution of Fick's Second Law via Finley's equation and Equation (32) is shown in Tables VI and VII, respectively. Use of Equation (32) improved the solution of Fick's Second Law approximately 50%. A comparison of the derived results is shown in Figure 11.

The derived regression equations--Equations (30), (31) and (32)--and Finley's equation are shown in Figure 12. Finley's integral diffusion coefficient data are also shown. All three diffusion coefficient equations obtained in this study are comparable except at concentrations less than $\sqrt{c} = 0.20$. These three equations all exhibit a minimum but less pronounced than that shown by Finley's equation.

Equations (30) and (31) required significant adjustment in either

TABLE VII
 NUMERICAL SOLUTION OF FICK'S SECOND LAW FOR CAPILLARY CELL DATA
 USING EQUATION (32)

c_0	Experimental Final Concentration	Calculated Final Concentration	% Error	Experimental \bar{c}	Calculated \bar{c}	% Error
0.5	0.022	0.019	-13.6	0.036	0.0345	-4.2
0.25	0.114	0.103	-9.6	0.182	0.1765	-3.0
0.50	0.228	0.208	-8.8	0.364	0.354	-2.8
0.60	0.260	0.248	-4.6	0.430	0.424	-1.4
0.71	0.292	0.291	-0.3	0.501	0.5005	-0.1
0.75	0.307	0.307	0.0	0.5285	0.5285	0.0
0.86	0.346	0.350	+1.2	0.603	0.605	+0.3
1.00	0.409	0.404	-1.2	0.7045	0.702	-0.4
1.50	0.620	0.594	-4.2	1.060	1.047	-1.2
2.00	0.813	0.778	-4.3	1.4065	1.389	-1.2

Average Deviation in Calculated Final Concentration = 0.0117

Average Deviation in Calculated Average Concentration = 0.0058

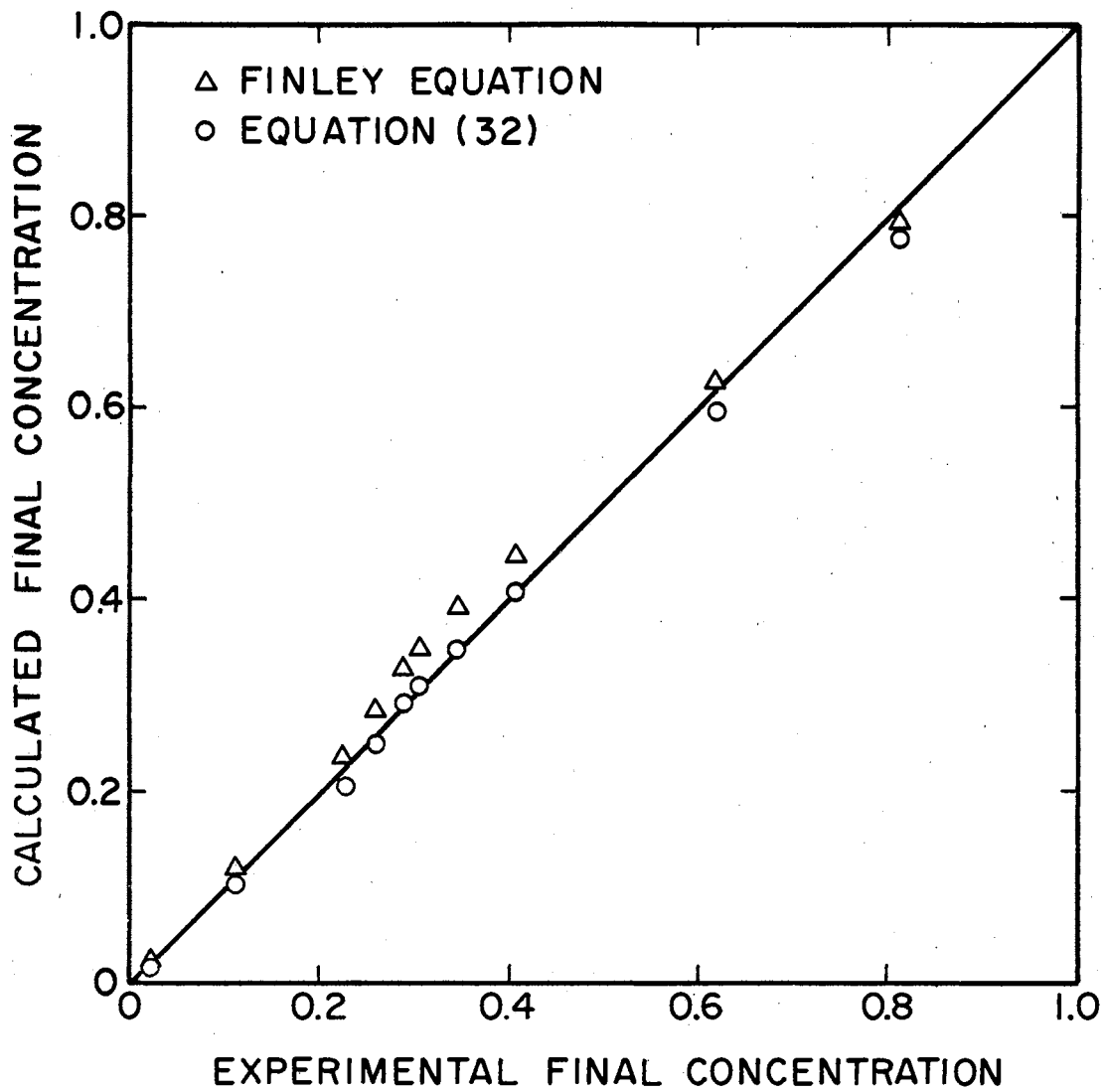


Figure 11. Comparison of Calculated Final Concentration for Capillary Cells With Experimental Data.

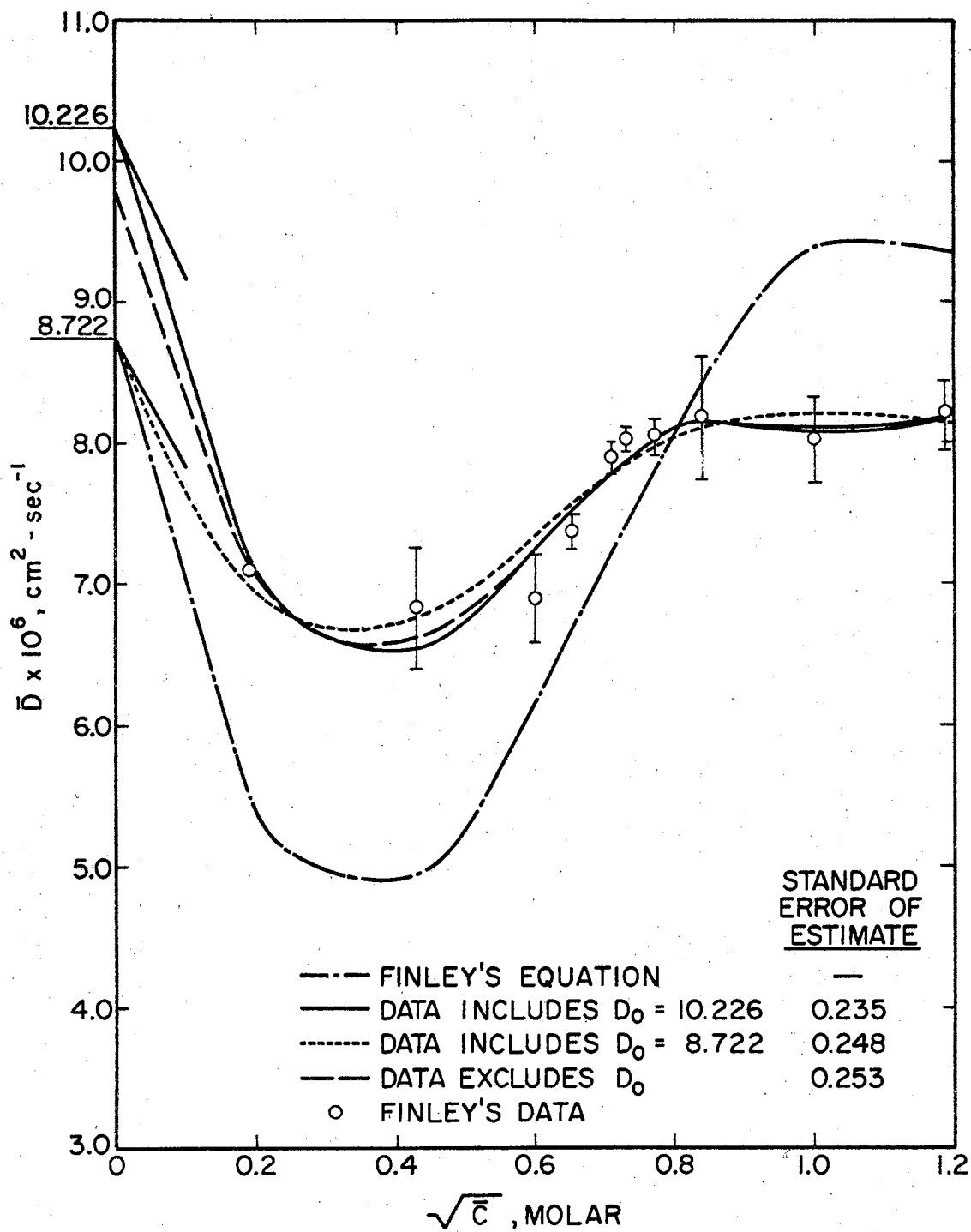


Figure 12. Multiple Linear Regression of Capillary Cell Integral Diffusion Coefficients According to the Model:
 $D = D_0 + P\bar{c}^{0.5} + Q\bar{c}^{1.0} + R\bar{c}^{2.0} + S\bar{c}^{3.0}$

the limiting diffusion coefficient value or limiting slope to obtain Finley's equation and hence a solution of Fick's Second Law. Equation (32), which used the calculated limiting diffusion coefficient $D_0 = 10.226 \times 10^{-6}$ as an input data value in the curve-fitting, required no adjustment to yield a solution of Fick's Second Law with greater accuracy than with use of Finley's equation. Therefore, Equation (32) is presented as representing the capillary cell differential diffusion coefficients. Apparently, use of the newer equivalent limiting conductivities yields limiting diffusion coefficients and limiting slopes of greater accuracy.

On the basis of the above results, Equation (25), which used the calculated limiting diffusion coefficient $D_0 = 10.226 \times 10^{-6}$ in the multiple linear regression of the diaphragm cell data, is now presented as representing the diaphragm cell differential diffusion coefficients.

G. Effect of Calculated Limiting Values

The variation in derived limiting diffusion coefficients from calculated values is shown in Table VIII. Derived values are shown as obtained with the cubic regression model and with use of both calculated limiting diffusion coefficients-- $D_0 = 10.226 \times 10^{-6}$ and $D_0 = 8.722 \times 10^{-6}$. Finley's equation is also shown. The objective in this table is to show which calculated limiting diffusion coefficient, when used in the curve-fitting of diffusion coefficient data, generated limiting values in the regression equation which more nearly reproduced the calculated values.

Variations in the derived limiting diffusion coefficient from calculated values are insignificant regardless of the value of the

TABLE VIII

COMPARISON OF DIFFUSION COEFFICIENT CURVE-FITTING RESULTS WITH CALCULATED LIMITING VALUES

Type of Data	$D_0 \times 10^6$	$\Delta(2)$	% Variation From Calculated Value	$\delta(D)$	$\Delta(2)$	% Variation From Calculated Value
<u>Diaphragm Cell Data</u>						
Use of $D_0 = 8.722 \times 10^{-6}$ -- Equation (26)	8.719	0.003	0.03	3.362	14.606	81.2
Use of $D_0 = 10.226 \times 10^{-6}$ -- Equation (25)	10.222	0.004	0.04	11.914	9.145	43.4
<u>Interferometer Data</u>						
Use of $D_0 = 8.722 \times 10^{-6}$	---	---	---	---	---	---
Use of $D_0 = 10.226 \times 10^{-6}$	10.360	0.134	1.3	7.071	13.988	66.4
<u>Capillary Cell Data</u>						
Use of $D_0 = 8.722 \times 10^{-6}$ -- Equation (31)	8.770	0.048	0.55	13.594	4.374	24.3
Use of $D_0 = 10.226 \times 10^{-6}$ -- Equation (32)	10.207	0.019	0.19	22.764	1.705	8.1
Finley's Correlation -- $D_0 = 8.722$	8.738	0.016	0.18	24.643	6.495	36.1

(1) Calculated limiting values are as follows:

$$\text{with } \lambda_1^0 = 31.45 \text{ -- } D_0 = 8.722 / \delta(D) = 17.968$$

$$\text{with } \lambda_1^0 = 39.9 \text{ -- } D_0 = 10.226 / \delta(D) = 21.059$$

(2) $\Delta = |\text{calculated value} - \text{derived value}|$

calculated limiting diffusion coefficient used for curve-fitting. Use of $D_o = 10.226 \times 10^{-6}$ for curve-fitting shows considerable improvement in the derived limiting slope for the diaphragm cell and capillary cell data. The interferometer data are not comparable as use of $D_o = 8.722 \times 10^{-6}$ yielded a positive limiting slope.

An attempt was made to utilize the calculated limiting slope in curve-fitting the diaphragm cell differential diffusion coefficients as shown in Table VI. Regression model (24) was modified as follows:

$$D - D_o + \delta_{(D)} \bar{c}^{0.5} = Q\bar{c}^{1.0} + R\bar{c}^{2.0} + S\bar{c}^{3.0} \quad (33)$$

Using multiple linear regression, Equation (37) was used to curve-fit the diaphragm cell data. The following calculated limiting values were used in the regression:

$$D_o = 10.226 \times 10^{-6} / \delta_{(D)} = 21.059 \times 10^{-6}$$

$$D_o = 8.722 \times 10^{-6} / \delta_{(D)} = 17.968 \times 10^{-6}$$

The derived regression equations were then used to calculate D over the concentration range. The resulting differential diffusion coefficient curves are shown in Figure 13, along with Equations (25) and (26) which used only the calculated limiting diffusion coefficient and not the limiting slope in the multiple linear regression.

The values of $\delta_{(D)}$ derived using the calculated limiting slopes show a closer approximation to the calculated limiting slopes than do Equations (25) and (26). However, a minimum much lower than that obtained with Equations (25) and (26) exists at low concentration. In addition, a second minimum is exhibited at high concentration-- $\sqrt{\bar{c}} = 1.05-1.10$. The use of too many terms in regression model (33) may

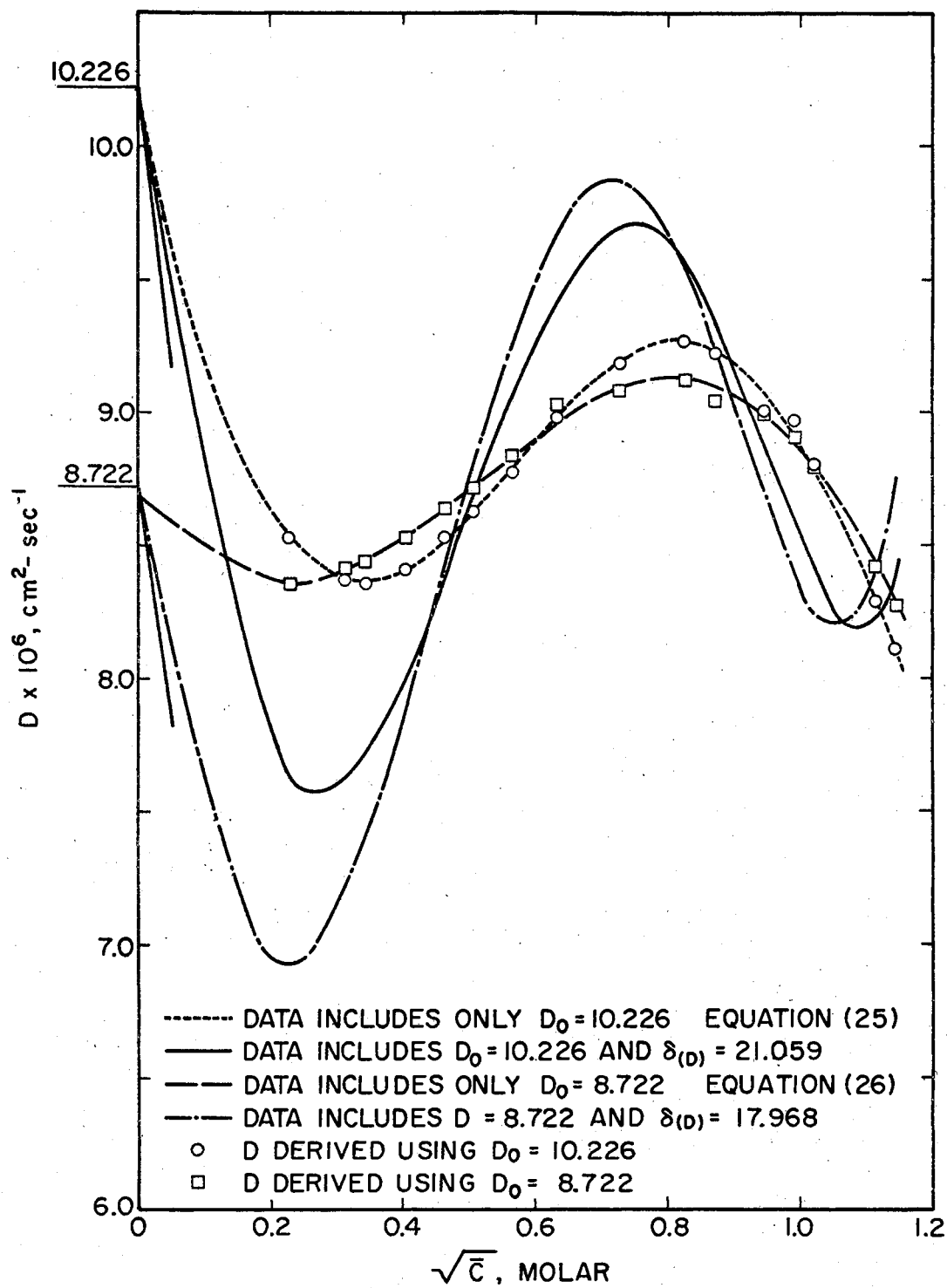


Figure 13. Effect of Calculated Limiting Slope on Curve-Fitting of Diaphragm Cell Differential Diffusion Coefficients

have resulted in the second minimum. However, deletion of the cubic term would result in a simple quadratic model which was previously excluded from consideration. Those results agree with Finley's (7) work in that use of both a limiting diffusion coefficient and limiting slope in correlation of the capillary cell data forces a deep minimum in the differential diffusion coefficient. The above analysis was determined to be inconclusive but may provide a basis for future study.

H. Comparison of Differential Diffusion

Coefficients

A comparison of the results obtained in this study are shown in Figure 14. Shown are Equation (25) describing the diaphragm cell differential diffusion coefficients, Equation (32) describing the capillary cell differential diffusion coefficients, Finley's equation and the interferometer differential diffusion coefficient data. Equation (25) describing the diaphragm cell diffusion coefficients shows the increase in the diffusion coefficient at dilute concentrations as predicted by dilute solution theory. It is noted that the limiting slope is not as pronounced as calculated by the Harned and Owen equation (12). Also, the diffusion coefficient increases with increasing concentration as solution theory might predict. A minimum is shown by both Equations (25) and (32) but not nearly as pronounced as shown by Finley's equation. Finley's equation shows a minimum of $D = 4.9 \times 10^{-6}$ at $\sqrt{c} = 0.40$. Equation (32), which uses $D_0 = 10.226 \times 10^{-6}$ in the multiple linear regression, shows a minimum at $\sqrt{c} = 0.40$, but the minimum value has increased to $D = 6.5 \times 10^{-6}$. Equation (25) shows a minimum value of 8.3×10^{-6} at $\sqrt{c} = 0.32$.

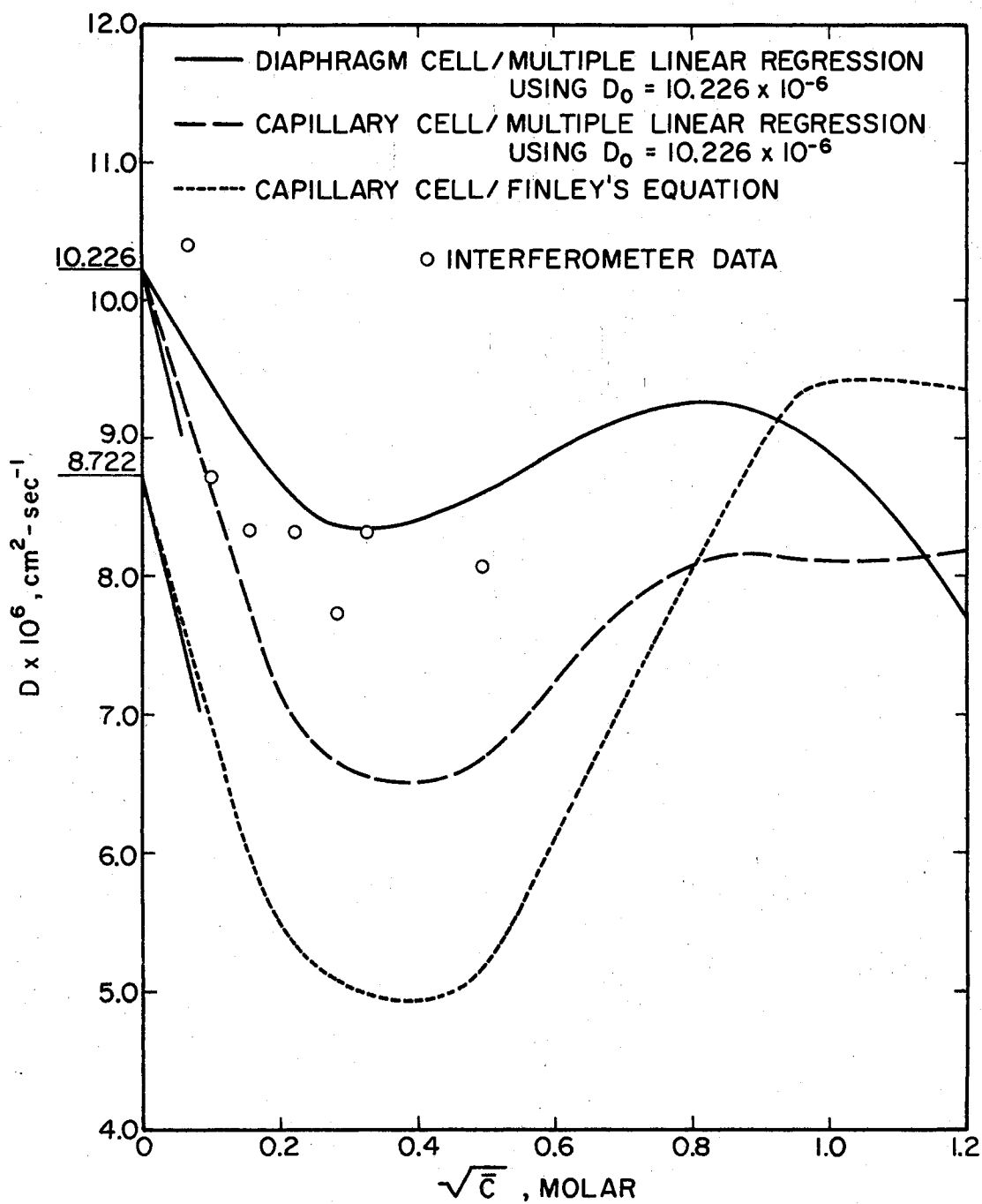


Figure 14. Comparison of Differential Diffusion Coefficients From All Experimental Methods

Two main considerations are shown in Figure 14. First, Equation (25) describing the diaphragm cell differential diffusion coefficients does contain a minimum, but this minimum differs significantly from the minimum in Finley's equation. Secondly, use of the calculated limiting diffusion coefficient $D_0 = 10.226 \times 10^{-6}$ yields Equation (32) containing the minimum, but the value of the minimum has increased toward that shown in Equation (25).

It is also noted that the interferometer differential diffusion coefficients lie somewhat intermediate between the diaphragm cell and capillary cell equations. If the interferometer diffusion coefficient $D = 7.74 \times 10^{-6}$ at $\sqrt{c} = 0.2818$ is neglected, the agreement between the interferometer results and the diaphragm cell equation is very close. Apparently, use of the improved calculated limiting diffusion coefficient $D_0 = 10.226 \times 10^{-6}$ has resulted in improved agreement between results from all three experimental methods.

I. Selective Curve-Fit Analysis

A selective curve-fit of the diaphragm cell differential diffusion coefficients, interferometer differential diffusion coefficients, and the capillary cell integral diffusion coefficients was performed according to the regression models shown in Appendix C. Results were too varied and inconclusive to discuss here and are covered in Appendix P.

However, a minimum standard deviation and a minimum deviation from the experimental diffusion coefficient were obtained with the data from all three experimental methods when the inverse of the diffusion coefficient, $1/D$, was curve-fitted as a function of concentration. Some

additional investigation into the mathematical dependency of the diffusion coefficient upon concentration appears warranted.

CHAPTER VI

CONCLUSIONS AND RECOMMENDATIONS

To describe uranyl nitrate diffusion coefficients as a function of concentration, the cubic multiple linear regression model including the square-root term was confirmed. More recent data for the uranyl ion limiting equivalent conductivity were used to calculate the limiting diffusion coefficient. Use of this calculated diffusion coefficient resulted in an improved diffusion coefficient equation describing results from capillary cell experiments and a new diffusion coefficient equation describing results from diaphragm cell studies. The diaphragm cell results confirm the existence of a diffusion coefficient minimum at low concentration. However, results of this study have significantly reduced previously observed discrepancies in this minimum between diaphragm cell and capillary results.

The derivation of equations describing diffusion coefficients was improved using a limiting diffusion coefficient-- $D_0 = 10.226 \times 10^{-6}$ $\text{cm}^2\text{-sec}^{-1}$ --calculated with more accurate limiting equivalent conductivity data for the uranyl ion. The diffusion coefficient equation derived from capillary cell data using multiple linear regression is as follows:

$$D = 10.2068 \times 10^{-6} - 22.764 \times 10^{-6}c^{0.5} + 32.271 \times 10^{-6}c^{1.0} \\ - 23.234 \times 10^{-6}c^{2.0} + 6.658 \times 10^{-6}c^{3.0} \quad (32)$$

The above equation required no adjustment as did previous curve-fitting work when used in the solution of Fick's Second Law to predict experimental concentrations. In addition, the experimental concentrations were predicted more accurately than previous work.

New diaphragm cell data were experimentally determined and curve-fitted with concentration using the calculated limiting diffusion coefficient $D_0 = 10.226 \times 10^{-6} \text{ cm}^2\text{-sec}^{-1}$. The resulting diffusion coefficient equation is as follows:

$$D = 10.222 \times 10^{-6} - 11.914 \times 10^{-6} \bar{c}^{0.5} + 20.410 \times 10^{-6} \bar{c}^{1.0} - 12.941 \times 10^{-6} \bar{c}^{2.0} + 3.108 \times 10^{-6} \bar{c}^{3.0} \quad (25)$$

An equation was obtained using the calculated limiting diffusion coefficient $D_0 = 8.722 \times 10^{-6} \text{ cm}^2\text{-sec}^{-1}$. This equation yielded results comparable to those obtained with Equation (25) except at low concentrations where the effect of the value of the calculated limiting diffusion coefficient is realized. The above equation was selected as representing the diaphragm cell data on the basis of the improved results obtained with the capillary cell data, i.e., use of the improved limiting diffusion coefficient $D_0 = 10.226 \times 10^{-6} \text{ cm}^2\text{-sec}^{-1}$.

Analysis of previously obtained interferometer diffusion coefficients did not yield satisfactory equations describing these data due to the limited concentration range over which the diffusion coefficients were obtained. It was concluded that insufficient interferometer diffusion coefficient data were available to apply multiple linear regression. However, use of the limiting diffusion coefficient $D_0 = 10.226 \times 10^{-6} \text{ cm}^2\text{-sec}^{-1}$ was supported. Use of the limiting diffusion coefficient $D_0 = 8.722 \times 10^{-6} \text{ cm}^2\text{-sec}^{-1}$ yielded a positive limiting slope

and was rejected.

Selective curve-fit analysis yielded results which were widely varying and inconclusive. However, a minimum standard deviation and a minimum deviation from the experimental diffusion coefficient were obtained with the data from all three experimental methods when the inverse of the diffusion coefficient, $1/D$, was curve-fitted as a function of concentration.

Recommendations for future work in this area are listed and discussed below:

1. Additional diaphragm cell and capillary cell diffusion coefficient data should be obtained for additional analysis of these two methods. The discrepancy in the minimum diffusion coefficient at low concentration has been significantly reduced in this study but still exists. In addition, diaphragm cell experiments should be conducted with low concentration differences across the diaphragm.
2. Additional diffusion coefficient data should be obtained with the interferometer in the concentration range $\sqrt{c} = 0.5-1.0$. The additional data would allow improved analysis of the variation of the diffusion coefficient with concentration.
3. Additional multiple linear regression work should be performed to develop improved regression models. The selective curve-fit analysis used in this work could be used as a base. This study indicates a function of the inverse of the diffusion coefficient, $1/D$, with concentration could be used as a starting point for further study.

4. The measurement and determination of limiting equivalent conductivities and their effect on the overall determination of diffusion coefficients should be investigated for other electrolyte solutions.

A SELECTED BIBLIOGRAPHY

- (1) Bird, R. B., W. E. Stewart, and E. N. Lightfoot. Transport Phenomena. New York: John Wiley and Sons, 1960.
- (2) Burchard, J. K., and H. L. Toor. J. Phys. Chem., Vol. 60 (1962), 2016.
- (3) Cordfunke, E. H. P. The Chemistry of Uranium--Including Its Applications in Nuclear Technology. New York: Elsevier Publishing Company, 1969.
- (4) Dullien, F. A. L., and L. W. Shemilt. Can. J. Chem. Eng., Vol. 39 (1961), 242.
- (5) Ewell, R. H., and H. Eyring. J. Chem. Phys., Vol. 4 (1936), 283.
- (6) Fick, A., Pogg. Ann., Vol. 94 (1955), 59.
- (7) Finley, J. B. Ph.D. Thesis, Oklahoma State University (1964).
- (8) Gibbs, J. W. Collected Works. Vol. 1. New York: Longmans, Green, and Co., 1928.
- (9) Goldberg, N., and E. S. Amis. Z. Physik Chem., Vol. 22 (1959), 63.
- (10) Guggenheim, E. A. J. Phys. Chem., Vol. 33 (1929), 842.
- (11) Hale, C. F. Ph.D. Thesis, University of Colorado (1964).
- (12) Harned, H. S., and B. B. Owen. The Physical Chemistry of Electrolyte Solutions. New York: Reinhold Publishing Corp., 3rd. ed. (1958).
- (13) Hartley, G. S. Phil. Mag., Vol. 12 (1931), 473.
- (14) Hartley, G. S., and J. Crank. Trans. Faraday Soc., Vol. 45 (1949), 801.
- (15) Lewis, J. B. J. J. Appl. Chem., Vol. 5 (1955), 228.
- (16) Mills, R. J. J. Am. Chem. Soc., Vol. 77 (1955), 6116.
- (17) Olander, D. R. J. Phys. Chem., Vol. 67 (1963), 1011.

- (18) Ondrejcin, R. S. AEC Report No. DP-653. I. E. duPont de Nemours and Co., Explosives Department-Atomic Energy Division-Technical Division-Savannah River Laboratory (1961).
- (19) Onsager, L., and R. M. Fuoss. J. Phys. Chem., Vol. 26 (1934), 2689.
- (20) Robinson, R. A., and R. H. Stokes. Electrolyte Solutions. London: Buttersworth (1961).
- (21) Robinson, R. L. Ph.D. Thesis, Oklahoma State University (1964).
- (22) Shedlovsky, T. J. Amer. Chem. Soc., Vol. 54 (1932), 1411.
- (23) Skinner, R. D. M. S. Thesis, Oklahoma State University (1964).
- (24) Skinner, R. D. Ph.D. Thesis, Oklahoma State University (1967).
- (25) Steel, R. G. D., and J. H. Torrie. Principles and Procedures of Statistics. New York: McGraw-Hill Book Company, Inc. (1960).
- (26) Stokes, R. H. J. Amer. Chem. Soc., Vol. 72 (1950), 763.
- (27) Stokes, R. H. J. Amer. Chem. Soc., Vol. 72 (1950), 2243.
- (28) Tyrell, H. J. V. Diffusion and Heat Flow in Liquids. London: Buttersworth (1961).
- (29) West, J. B. Request for Continuation of Contract No. AT (11-1)-846. Oklahoma State University (1967).

APPENDIX A

CALCULATION OF INTEGRAL DIFFUSION COEFFICIENTS

FROM DIAPHRAGM CELL DATA (20)

Denoting the diaphragm cell compartment concentrations as c' and c'' , the rates of concentration change are related to the mass flux $J(t)$ as follows:

$$\frac{dc'}{dt} = -J(t)\frac{A}{V_B} \quad (A-1)$$

$$\frac{dc''}{dt} = +J(t)\frac{A}{V_T} \quad (A-2)$$

Adding equations (A-1) and (A-2):

$$\frac{d(c' - c'')}{dt} = -J(t)A\left(\frac{1}{V_B} + \frac{1}{V_T}\right) \quad (A-3)$$

The average value of D with respect to concentration over the concentration range c' to c'' is defined as follows:

$$\bar{D}(t) = \frac{1}{c_B - c_T} \int_{c_T}^{c_B} D dc = -\frac{1}{c_B - c_T} \int_{x=0}^{\lambda} D \left(\frac{\partial c}{\partial x}\right) dx = \frac{\lambda J(t)}{c_B - c_T} \quad (A-4)$$

Combining equations (A-3) and (A-4):

$$-\frac{d \ln(c_B - c_T)}{dt} = \frac{A}{\lambda} \left(\frac{1}{V_B} + \frac{1}{V_T}\right) \int_{t=0}^{t=t} \bar{D}(t) dt \quad (A-5)$$

Now denote the initial concentrations as c_{B_0} and c_{T_0} and the final concentrations as c_B and c_T , equation (A-5) is integrated to yield the following:

$$\ln \frac{c_{B_0} - c_{T_0}}{c_B - c_T} = \frac{A}{\lambda} \left(\frac{1}{V_B} + \frac{1}{V_T}\right) \int_{t=0}^{t=t} \bar{D}(t) dt \quad (A-6)$$

Now define an average value of $D(t)$ over time as follows:

$$\bar{D} = \frac{1}{t} \int_0^t \bar{D}(t) dt \quad (\text{A-7})$$

In addition, denote a cell constant β as follows:

$$\beta = \frac{A}{l} \left(\frac{1}{V_T} + \frac{1}{V_T} \right) \quad (\text{A-8})$$

Utilizing equations (A-6) and (A-7), the integral diffusion coefficient becomes:

$$\bar{D} = \frac{1}{\beta t} \ln \frac{c_{B_0} - c_{T_0}}{c_B - c_T} \quad (\text{A-9})$$

APPENDIX B

DERIVATION OF DIFFERENTIAL DIFFUSION

COEFFICIENTS FROM DIAPHRAGM CELL

INTEGRAL DIFFUSION

COEFFICIENTS (27)

The method of deriving differential diffusion coefficients from integral diffusion coefficients is outlined below:

1. The integral diffusion coefficients, \bar{D} , are regressed versus c_{B_0} .
2. The resulting correlation is used to make a first estimate of $\bar{D}_{c_m''}$.
3. The resulting values for $\bar{D}_{c_m''}$ are used to calculate $\bar{D}_{c_m'}$ according to the following equation:

$$\bar{D}_{c_m'} = \bar{D} - \left(\frac{c_m''}{c_m'}\right)(\bar{D} - \bar{D}_{c_m''}) \quad (B-1)$$

4. The calculated values of $\bar{D}_{c_m'}$ are regressed versus c_m' .
5. This second correlation is then used to estimate $\bar{D}_{c_m''}$ which are then used again in equation (B-1).
6. Steps (4) and (5) are repeated until $\bar{D}_{c_m'}$ does not change upon repeating the process.
7. The final values of $\bar{D}_{c_m'}$ are used to calculate differential diffusion coefficients according to the following equation:

$$D = \bar{D}_{c_m'} + c \frac{d\bar{D}_{c_m'}}{dc} \quad (B-2)$$

APPENDIX C

SELECTIVE CURVE-FIT REGRESSION

EQUATIONS

Listed below are the regression equations used to make a selective curve-fit on the diffusion coefficient data. The selective curve-fit will analyze a total of 36 different correlations. These correlations consist of 3 variations on the dependent variable D as shown below:

1. $x = D$
2. $x = 1/D$
3. $x = \log(D)$

The independent variable, a concentration variable, is transformed according to 12 variations as shown below:

1. $y = c$
2. $y = 1/c$
3. $y = \log(c)$
4. $y = e^c$
5. $y = c^2$
6. $y = 1/c^2$
7. $y = 1/e^{c^2}$
8. $y = e^{\log(c)}$
9. $y = 1/e^c$
10. $y = \log(c)/c$
11. $y = (1 - c)^2$
12. $y = c \log(c)$

The concentration variable \sqrt{c} was also used as the independent variable in this study.

APPENDIX D

DIAPHRAGM CELL COMPARTMENT VOLUME BUOYANCY

CORRECTION

A force balance analysis of a weighing balance yields the following equality:

actual weight of object - weight of air displaced by
 object = actual weight of weights - weight of air
 displaced by weights.

In equation form:

$$W_b^0 - W_b^0(\rho_a/\rho_b) = W_c^0 - W_c^0(\rho_a/\rho_c) \quad (D-1)$$

where W^0 = in-vacuo weight of object, gm

ρ = density, g/cc

a refers to air

b refers to object being weighed

c refers to the weights used on the balance.

The apparent weight in air, W_b , of the object is equal to the actual weight of the weights, W_c^0 , on the balance. Substituting W_b for W_c^0 in equation (D-1):

$$W_b^0(1 - \rho_a/\rho_b) = W_b(1 - \rho_a/\rho_b) \quad (D-2)$$

Dividing equation (D-2) by $(1 - \rho_a/\rho_b)$ and neglecting terms in ρ_a^2 and higher powers, equation (D-2) can be written as follows:

$$W_b^0 = W_b[1 + \rho_a(1/\rho_b - 1/\rho_c)]$$

For a weighing bottle containing a sample:

$$W_{b+s}^0 = W_{b+s} [1 + \rho_a (1/\rho_{b+s} - 1/\rho_c)] \quad (D-4)$$

A sample calculation for cell #1 upper compartment volume is illustrated below:

$$\text{density of glass} = 2.23 \text{ g/cc}$$

$$\text{density of brass weights} = 8.4 \text{ g/cc}$$

The ambient temperature during the tare weighing of the weighing bottle was 21.55°C.

$$\begin{aligned} \rho_a \text{ at } 21.55^\circ\text{C} &= (\rho_a \text{ at } 25.0^\circ\text{C}) \left(\frac{298.18^\circ\text{K}}{t+273.18^\circ\text{K}} \right) \\ &= (0.001185 \text{ g/cc}) \left(\frac{25.0+273.18}{21.55+273.18} \right) \\ &= 0.001199 \text{ g/cc} \end{aligned}$$

$$W_b = 77.3691 \text{ g}$$

$$\begin{aligned} W_b^0 &= 77.3691 \text{ g} [1 + 0.001199(1/2.23 - 1/8.4)] \\ &= 77.3393 \text{ g} \end{aligned}$$

$$W_{b+s} = 123.8675 \text{ g}$$

Calculate W_s as follows:

$$W_s = W_{b+s} - W_b^0 = 123.8675 \text{ g} - 77.3393 \text{ g} = 46.4682 \text{ g}$$

The ambient temperature during the gross weighing of the weighing bottle plus the water sample was 21.70°C.

$$\rho_s \text{ at } 21.70^\circ\text{C} = 0.997837 \text{ g/cc}$$

$$V_s = W_s / \rho_s = 46.4682 / 0.997837 = 46.5689 \text{ cc}$$

$$\begin{aligned}
 V_b &= W_b^0 / \rho_b = 77.3393 / 2.23 = 34.7082 \text{ cc} \\
 V_t &= V_s + V_b = 46.5689 + 34.7082 = 81.2771 \text{ cc} \\
 \text{apparent } \rho_{b+s} &= W_{b+s} / V_t = 123.8675 / 81.2771 \\
 &= 1.5240 \text{ g/cc} \\
 \rho_a \text{ at } 21.70^\circ\text{C} &= (0.001185 \text{ g/cc}) \left(\frac{25.0 + 273.18}{21.70 + 273.18} \right) \\
 &= 0.001198 \text{ g/cc} \\
 W_{b+s}^0 &= 123.8675 \text{ g} [1 + 0.001198(1/1.5240 - 1/8.4)] \\
 &= 123.9468 \text{ g} \\
 W_s^0 &= W_{b+s}^0 - W_b^0 = 123.9468 - 77.3993 = 46.5475 \text{ g}
 \end{aligned}$$

The ambient temperature during sampling of the diaphragm cell was 21.60°C.

$$\begin{aligned}
 \rho_s \text{ at } 21.60^\circ\text{C} &= 0.997860 \text{ g/cc} \\
 V_{\text{compartment}} &= W_s^0 / \rho_s = 46.5475 / 0.997860 = 46.6473 \text{ cc}
 \end{aligned}$$

As an iterative check on the procedure, use the calculated value of W_s^0 to determine V_s and the calculated value of W_{b+s}^0 to determine the apparent ρ_{b+s} .

$$\begin{aligned}
 V_s &= W_s^0 / \rho_s = 46.5475 / 0.997837 = 46.6484 \text{ cc} \\
 V_t &= V_s + V_b = 46.6484 + 34.7082 = 81.3556 \text{ cc} \\
 \text{apparent } \rho_{b+s} &= W_{b+s}^0 / V_t = 123.9468 / 81.3556 \\
 &= 1.5235 \text{ g/cc} \\
 W_{b+s}^0 &= 123.8675 \text{ g} [1 + 0.001198(1/1.5235 - 1/8.4)] \\
 &= 123.9468 \text{ g}
 \end{aligned}$$

This value checks with the previously calculated value. Now correct the compartment volume to 25°C.

$$V_{\text{compartment at } 25^{\circ}\text{C}} = V_{\text{compartment}} + \alpha(25 - t)$$

where α is the volume coefficient of expansion of glass

$$= 0.000025$$

$$V_{\text{compartment at } 25^{\circ}\text{C}} = 46.6473 + 0.000025(25 - 21.60)$$

$$V_{\text{compartment at } 25^{\circ}\text{C}} = 46.6513 \text{ cc}$$

APPENDIX E

DIAPHRAGM CELL COMPARTMENT VOLUME

CALIBRATION DATA

TABLE IX

DIAPHRAGM CELL COMPARTMENT VOLUME CALIBRATION DATA

Upper compartment	
volume, cc	cell #1
test #1	46.5513
test #2	46.5434
test #3	46.6162
average volume, cc	46.6036
average deviation, cc	0.0402
Lower compartment	
volume, cc*	cell #1
test #1	42.6180
test #3	42.6145
average volume, cc	42.6163
average deviation, cc	0.0022
Lower compartment	
volume, cc**	cell #1
test #1	42.8472
test #2	42.8494
average volume, cc	42.8483
average deviation, cc	0.0011
Upper compartment	
volume, cc	cell #2
test #1	50.1514
test #2	50.1607
average volume, cc	50.1560
average deviation, cc	0.0046
Lower compartment	
volume, cc	cell #2
test #1	48.0655
test #2	48.0503
average volume, cc	48.0579
average deviation, cc	0.0076

TABLE IX (CONTINUED)

Lower compartment	
volume, cc***	cell #5
test #1	45.6562
test #2	45.6831
average volume, cc	45.6696
average deviation, cc	0.0134

Lower compartment	
volume, cc****	cell #5
test #1	45.5419
test #2	45.5526
test #3	45.5010
test #4	45.6093
test #5	45.5317
test #6	45.5803
test #7	45.5775
average volume, cc	45.5563
average deviation, cc	0.0280

Upper compartment	
volume, cc	cell #6
test #1	48.4967
test #2	48.4850
test #3	48.4817
average volume, cc	48.4876
average deviation, cc	0.0059

Lower compartment	
volume, cc	cell #6
test #1	45.6965
test #2	45.6401
average volume, cc	45.6683
average deviation, cc	0.0282

TABLE IX (CONTINUED)

Upper compartment	
volume, cc	cell #3
test #1	45.5654
test #2	45.6062
average volume, cc	45.5858
average deviation, cc	0.0204
Lower compartment	
volume, cc	cell #3
test #1	44.8690
test #2	44.8932
average volume, cc	44.8811
average deviation, cc	0.0121
Upper compartment	
volume, cc	cell #4
test #1	47.5517
test #2	47.5462
average volume, cc	47.5490
average deviation, cc	0.0028
Lower compartment	
volume, cc	cell #4
test #1	50.4457
test #2	50.3941
average volume, cc	50.4199
average deviation, cc	0.0258
Upper compartment	
volume, cc	cell #5
test #1	44.1057
test #2	44.0749
average volume, cc	44.0903
average deviation, cc	0.0154

*Data taken prior to stirrer replacement in cell #1.

**Data taken after stirrer replacement in cell #1.

***Data taken prior to stirrer replacement in cell #5.

****Data taken after stirrer replacement in cell #5.

APPENDIX F

DIAPHRAGM CELL DIAPHRAGM VOLUME BUOYANCY

CORRECTION

The buoyancy correction used for calibration of the cell diaphragm is similar to that used for the cell compartment volumes, and a detailed listing of the equations used here would be redundant. A description on the procedure used is outlined below to illustrate the differences from the procedure used for the compartment volume calibrations.

(a) The in-vacuo weight and volume of the empty syringe were determined according to the procedure used to determine the in-vacuo weight and volume of the empty weighing bottle.

(b) Prior to water addition to a cell diaphragm, the volume of the water contained in the syringe was determined according to the procedure used to determine the volume of the compartment sample in the weighing bottle.

(c) After the addition of water to the diaphragm, the volume of the water remaining in the syringe was determined as in step (b).

(d) The volume of the diaphragm was then taken as the difference in the volumes determined in steps (b) and (c). This volume was then corrected to 25°C.

APPENDIX G

DIAPHRAGM CELL DIAPHRAGM VOLUME CALIBRATION

DATA

TABLE X
DIAPHRAGM CELL DIAPHRAGM VOLUME CALIBRATION DATA

Cell	Diaphragm Volume, cc			Average	Average Deviation, cc
	Test #1	Test #2	Test #3		
Cell #1	0.3447	0.3407	0.3400	0.3418	0.0019
Cell #2	0.3107	0.3125	0.3098	0.3110	0.0010
Cell #3	0.3358	0.3272	0.3271	0.3300	0.0038
Cell #4	0.3481	0.3529	0.3558	0.3523	0.0028
Cell #5	0.3492	0.3495	0.3512	0.3500	0.0008
Cell #6	0.4303	0.4239	0.4267	0.4270	0.0022

APPENDIX H

CELL CONSTANT COMPUTER PROGRAM

```

20  FORMAT(F10.6,F10.6,F10.6,F10.6,F10.6,F10.6)
21  FORMAT (F10.6,F10.6,F10.6,F10.6)
47  FORMAT(3X12HCELL NUMBER,,2X12,6X11HRUN NUMBER,,2X12)
48  FORMAT (3X30HCELL CONSTANT BETA, PER SQ CM,,F9.5)
1   READ20,CELNO,RUNNO,VU,VL,VD,PV
    READ21,SU,SL,DS,THETA
    DIMENSIONWBT(8),WBG(8),SBT(8),SBG(8),WR(8)
    NL=SL
    NU=SU
    NC=CELNO
    NR=RUNNO
    N=NU+NL
    DO2I=1,N
    READ21,WBT(I),WBG(I),SBT(I),SBG(I)
2   WR(I)=((WBG(I)-WBT(I))-((SBG(I)-SBT(I))*(WBT(I)/SBT(I))))
    SUM=0.0
    DO3I=1,NU
3   SUM=SUM+WR(I)
    WRAU=SUM/SU
    TUM=0.0
    J=1+NU
    DO6I=J,N
6   TUM=TUM+WR(I)
    WRAL=TUM/SL
    ROU2=10.0*WRAU*0.997044/(PV*DS)
    ROL2=10.0*WRAL*80.997044/(PV*DS)
    ROL1=(VI*ROL2+VU*ROU2+0.5*VD*(ROL2+ROU2))/(VL+0.5*VD)
    CLM=50.0*(ROL1+ROL2)
    CUM=50.0*ROU2
    A0=1.9632978
    A1=0.3816442
    A2=0.7358143
    A3=0.6834361
    A4=0.2210123
    DAM=A0-0.1*A1*CLM+0.01*A2*(CLM**2)-0.001*A3*(CLM**3)
    DBM=A4*0.0001*(CLM**4)
    DLM=DAM+DBM
    DCM=A0-0.1*CUM+0.01*A2*(CUM**2)-0.001*A3*(CUM**3)
    DDM=0.0001*A48(CUM**4)
    DUM=DCM+DDM
    RC=CUM/CLM
    DBAR=(DLM-RC*DUM)/(1.0-RC)
    DELR2=ROL2-ROU2
    ANTI=ROL1/DELR2
    TOP=LOG(ANTI)
    BETA=TOP/(DBAR*THETA)
    PRINT47,NCNR
    PRINT48,DELTA
    PAUSE
    GO TO 1
    END

```

APPENDIX I

CELL CONSTANT CALIBRATION DATA

TABLE XI
CELL CONSTANT CALIBRATION DATA

Cell	Cell Constant β , cm^{-2}			% deviation
	Test #1	Test #2	Average	
Cell #1 *	0.12597	0.12664	0.12630	0.27
Cell #1 **	0.12509	0.12323	0.12416	0.76
Cell #2	0.11848	0.11778	0.11813	0.30
Cell #3	0.12648	0.12626	0.12637	0.08
Cell #4	0.12680	0.12557	0.12618	0.49
Cell #5 *	0.12070	0.12027	0.12049	0.18
Cell #5 **	0.12124	0.12111	0.12118	0.05
Cell #6	0.12938	0.13001	0.12970	0.25

Cell	Cell Constant at End of Study	
	β , cm^{-2}	% Change
Cell #2	0.11827	+0.12
Cell #3	0.12681	+0.35
Cell #4	0.12680	+0.49
Cell #5	0.12971	+0.01

*Data taken prior to stirrer replacement in cells #1 and #5.
**Data taken after stirrer replacement in cells #1 and #5.

APPENDIX J

REFRACTOMETER CALIBRATION DATA

The refractometer calibration data are tabulated in Table XII.

The calibration equation is given below:

$$C = -14.49132 - 7.191073 (RI) + 13.553 (RI)^2 \quad (J-1)$$

$$\text{Standard error of estimate} = 0.00468 M$$

TABLE XII
REFRACTOMETER CALIBRATION DATA

Uranyl Nitrate Concentration, M	Refractive Index
0.0	1.33268
0.01995	1.33348
0.03995	1.33414
0.05613	1.33461
0.06054	1.33487
0.08000	1.33568
0.10106	1.33622
0.21221	1.34022
0.29921	1.34310
0.39811	1.34659
0.44899	1.34827
0.50013	1.35010
0.60381	1.35350
0.70169	1.35680
0.904736	1.36373
1.00207	1.36717
1.13623	1.37150
1.299678	1.37662
1.49998	1.38345
1.61202	1.38720
1.81182	1.39388
2.00678	1.39965

APPENDIX K

DIAPHRAGM CELL EXPERIMENTAL DATA

TABLE XIII
DIAPHRAGM CELL EXPERIMENTAL DATA

Run Set 1			
Run No.	RI _T	RI _B	Run Time, Sec.
111	1.35292	1.36481	1,407,085
112	1.33300	1.33395	597,615
113	1.34431	1.35710	918,905
114	1.33541	1.33727	1,207,332
115	1.34083	1.35074	892,665
121	1.33462	1.33770	803,940
122	1.33798	1.33469	918,942
123	1.33393	1.33499	1,207,696
124	1.35680	1.39836	892,662
131	1.35392	1.36514	1,406,485
132	1.33298	1.33393	597,408
133	1.34468	1.35864	918,403
134	1.33566	1.33804	1,207,973
135	1.34174	1.35182	892,442
141	1.33432	1.33790	605,735
142	1.33852	1.34524	918,610
143	1.33422	1.33516	1,209,369
144	1.35918	1.39275	892,475
151	1.35838	1.38094	1,037,295
152	1.33644	1.34048	919,197
153	1.33295	1.33319	1,208,672
161	1.35705	1.37869	1,036,583

TABLE XIII (CONTINUED)

Run No.	RI _T	RI _B	Run Time, Sec.
162	1.33632	1.34061	919,452
163	1.33295	1.33318	1,208,702
Run Set 2			
Run No.	RI _T	RI _B	Run Time, Sec.
211	1.33519	1.33722	1,135,284
212	1.33689	1.34306	729,081
213	1.33820	1.34329	1,040,438
221	1.33905	1.34859	788,301
222	1.33889	1.34845	788,485
223	1.34057	1.35488	698,427
231	1.34189	1.35998	604,968
232	1.34194	1.35971	604,961
233	1.34428	1.36765	606,248
241	1.34461	1.37138	522,148
242	1.34418	1.37234	522,135
243	1.34643	1.37816	528,176
251	1.34945	1.37782	713,781
252	1.35496	1.37654	1,040,465
253	1.34656	1.38918	460,422
261	1.34650	1.40727	370,914
262	1.34718	1.40780	370,909
263	1.34792	1.40929	372,333

APPENDIX L

ERROR ANALYSIS OF DIAPHRAGM CELL DATA

Equation (A-9) for calculation of integral diffusion coefficients from diaphragm cell data is shown below:

$$\bar{D} = \frac{1}{\beta t} \ln \frac{c_{B_0} - c_{T_0}}{c_B - c_T} \quad (\text{A-9})$$

Since the initial upper compartment concentration for all experimental runs, c_{T_0} , is zero, Equation (A-9) becomes:

$$\bar{D} = \frac{1}{\beta t} \ln \frac{c_{B_0}}{c_B - c_T} \quad (\text{L-1})$$

For analysis of experimental error by error propagation, differentiation of Equation (L-1) yields the following equation:

$$d\bar{D} = \left(-\frac{d\beta}{\beta^2 t} - \frac{dt}{\beta t^2} \right) \ln \left(\frac{c_{B_0}}{c_B - c_T} \right) + \frac{1}{\beta t} \frac{dc_{B_0}}{c_{B_0}} + \frac{dc_T - dc_B}{\beta t (c_B - c_T)} \quad (\text{L-2})$$

The error in the final concentration measurements is assumed to be the standard error of estimate in the curve-fitting of concentration versus refractive index measurements (see Appendix J). Since this value is the same for both dc_T and dc_B , Equation (L-2) becomes:

$$d\bar{D} = \left(-\frac{d\beta}{\beta^2 t} - \frac{dt}{\beta t^2} \right) \ln \left(\frac{c_{B_0}}{c_B - c_T} \right) + \frac{1}{\beta t} \frac{dc_{B_0}}{c_{B_0}} + \frac{dc_B - dc_B}{\beta t (c_B - c_T)} \quad (\text{L-3})$$

Equation (L-3) is used to evaluate the error in the experimental measurement and calculation of integral diffusion coefficients.

The error in the initial lower compartment concentration, dc_{B_0} , is calculated by differentiation of c_{B_0} . The term c_{B_0} is calculated by material balance of the diaphragm cell. The following assumptions are made in the material balance:

1. The initial diaphragm concentration is equal to the initial lower compartment concentration, c_{B_0} .

2. The final diaphragm concentration is equal to half the sum of the final upper and lower compartment concentrations. A material balance on the diaphragm cell yields the following equation:

$$c_{B_0}V_B + c_{B_0}V_D = c_TV_T + c_BV_B + \frac{1}{2}V_D(c_B + c_T) \quad (L-4)$$

Solution of Equation (L-4) for c_{B_0} yields the following equation:

$$c_{B_0} = \frac{c_TV_T + c_BV_B + \frac{1}{2}V_D(c_B + c_T)}{V_B + V_D} \quad (L-5)$$

Differentiation of equation (L-5) yields the following:

$$\begin{aligned} dc_{B_0} = & \frac{V_Tdc_T}{V_B + V_D} + \frac{\frac{1}{2}c_TdV_D}{V_B + V_D} - \frac{V_Tc_TdV_R}{(V_B + V_D)^2} - \frac{V_Tc_TdV_D}{(V_B + V_D)^2} \\ & + \frac{\frac{1}{2}V_Ddc_T}{V_B + V_D} + \frac{\frac{1}{2}c_TdV_D}{V_B + V_D} - \frac{\frac{1}{2}V_Dc_TdV_B}{(V_B + V_D)^2} - \frac{\frac{1}{2}V_Dc_TdV_D}{(V_B + V_D)^2} \\ & + \frac{V_Bdc_B}{V_B + V_D} + \frac{c_BdV_B}{V_B + V_D} - \frac{V_Bc_BdV_B}{(V_B + V_D)^2} - \frac{V_Bc_BdV_D}{(V_B + V_D)^2} \\ & + \frac{\frac{1}{2}V_Ddc_B}{V_B + V_D} + \frac{\frac{1}{2}c_BdV_D}{V_B + V_D} - \frac{\frac{1}{2}V_Dc_BdV_B}{(V_B + V_D)^2} - \frac{\frac{1}{2}V_Dc_BdV_D}{(V_B + V_D)^2} \end{aligned} \quad (L-6)$$

Summarizing terms:

$$\begin{aligned}
dc_{B_0} = & \left(\frac{V_T + \frac{1}{2}V_D}{V_B + V_D} \right) dc_T + \left(\frac{V_B + \frac{1}{2}V_D}{V_B + V_D} \right) dc_B + \left(\frac{C_T}{V_B + V_D} \right) dV_T \\
& + \left(\frac{C_B}{V_B + V_D} - \frac{V_T c_T + V_B c_B + \frac{1}{2}V_D c_T + \frac{1}{2}V_D c_B}{(V_B + V_D)^2} \right) dV_B \\
& + \left(\frac{\frac{1}{2}(c_T + c_B)}{V_B + V_D} - \frac{V_T c_T + V_B c_B + \frac{1}{2}V_D c_T + \frac{1}{2}V_D c_B}{(V_B + V_D)^2} \right) dV_D \quad (L-7)
\end{aligned}$$

As stated above, dc_T and dc_B are assumed as the standard error of estimate in the curve-fitting of concentration versus refractive index measurements, or $dc_T = dc_B = 0.00468$.

The errors in diaphragm cell volumes-- dV_T , dV_B , and dV_D --are assumed as the average deviation in the measurement of these quantities. These average deviations for the diaphragm cell compartments, dV_T and dV_B , are shown in Appendix E. The average deviations for the diaphragm volumes, dV_D , are shown in Appendix G.

The errors in the cell constants, d , are assumed as the average deviation in the cell constant measurements. These values are shown in Appendix I.

The error in experimental run time, dt , is assumed to be 10 seconds.

APPENDIX M

SELECTION OF DIAPHRAGM CELL DIFFUSION

COEFFICIENT REGRESSION MODEL

The initial step in deriving differential diffusion coefficients by the method of Stokes (27)--curve-fitting of \bar{D} as a function of c_{B_0} --was used to find the best multiple linear regression model for further work. The integral diffusion coefficients for all diaphragm cell experimental runs (excluding runs 112, 132, 153 and 163) are used as input data. (These values are shown in Table I). A data value for the limiting diffusion coefficient D_0 and limiting slope are not used for these regressions. The multiple linear regression models including the model used by Finley (cubic equation with square-root term) are shown below:

$$\bar{D} = D_0 + Pc_{B_0}^{0.5} + Qc_{B_0}^{1.0} + Rc_{B_0}^{2.0} + Sc_{B_0}^{3.0} \quad (M-1)$$

$$\bar{D} = D_0 + Pc_{B_0}^{0.5} + Qc_{B_0}^{1.0} + Rc_{B_0}^{2.0} \quad (M-2)$$

$$\bar{D} = D_0 + Pc_{B_0}^{1.0} + Qc_{B_0}^{2.0} + Rc_{B_0}^{3.0} \quad (M-3)$$

$$\bar{D} = D_0 + Pc_{B_0}^{1.0} + Qc_{B_0}^{2.0} \quad (M-4)$$

The multiple linear regression equations for (M-1) through (M-4) are shown in Figures 15-18, respectively. All regression equations indicate no correlation without utilization of data values for the limiting diffusion coefficient and slope. Equations (M-1) and (M-2) have a positive value for the square-root term concentration term. Equations (M-3) and (M-4) which exclude the square-root term have a positive slope in the first concentration term.

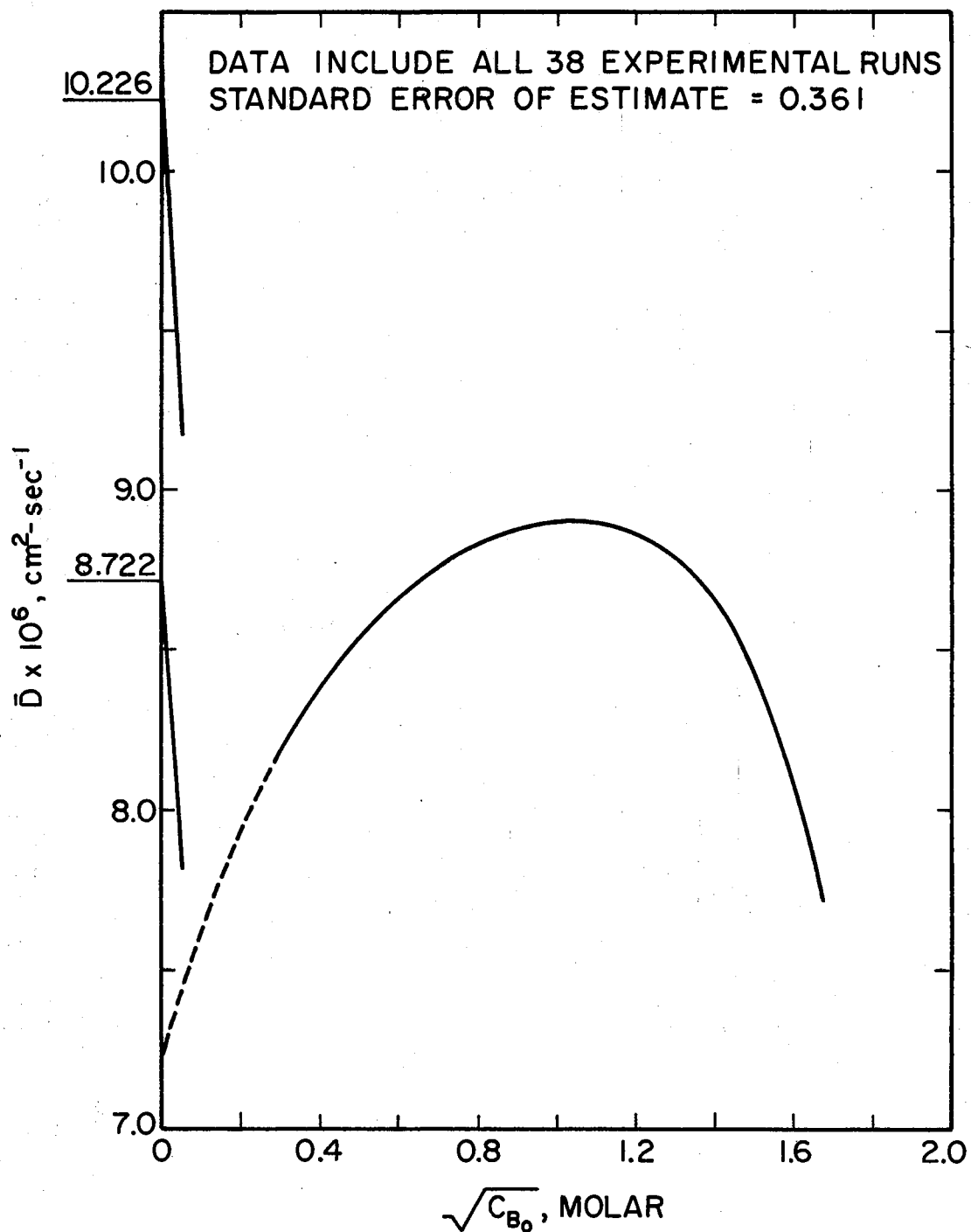


Figure 15. Multiple Linear Regression of Diaphragm Cell Integral Diffusion Coefficients According to the Model:

$$\bar{D} = D_0 + Pc_{B_0}^{0.5} + Qc_{B_0}^{1.0} + Rc_{B_0}^{2.0} + Sc_{B_0}^{3.0}$$

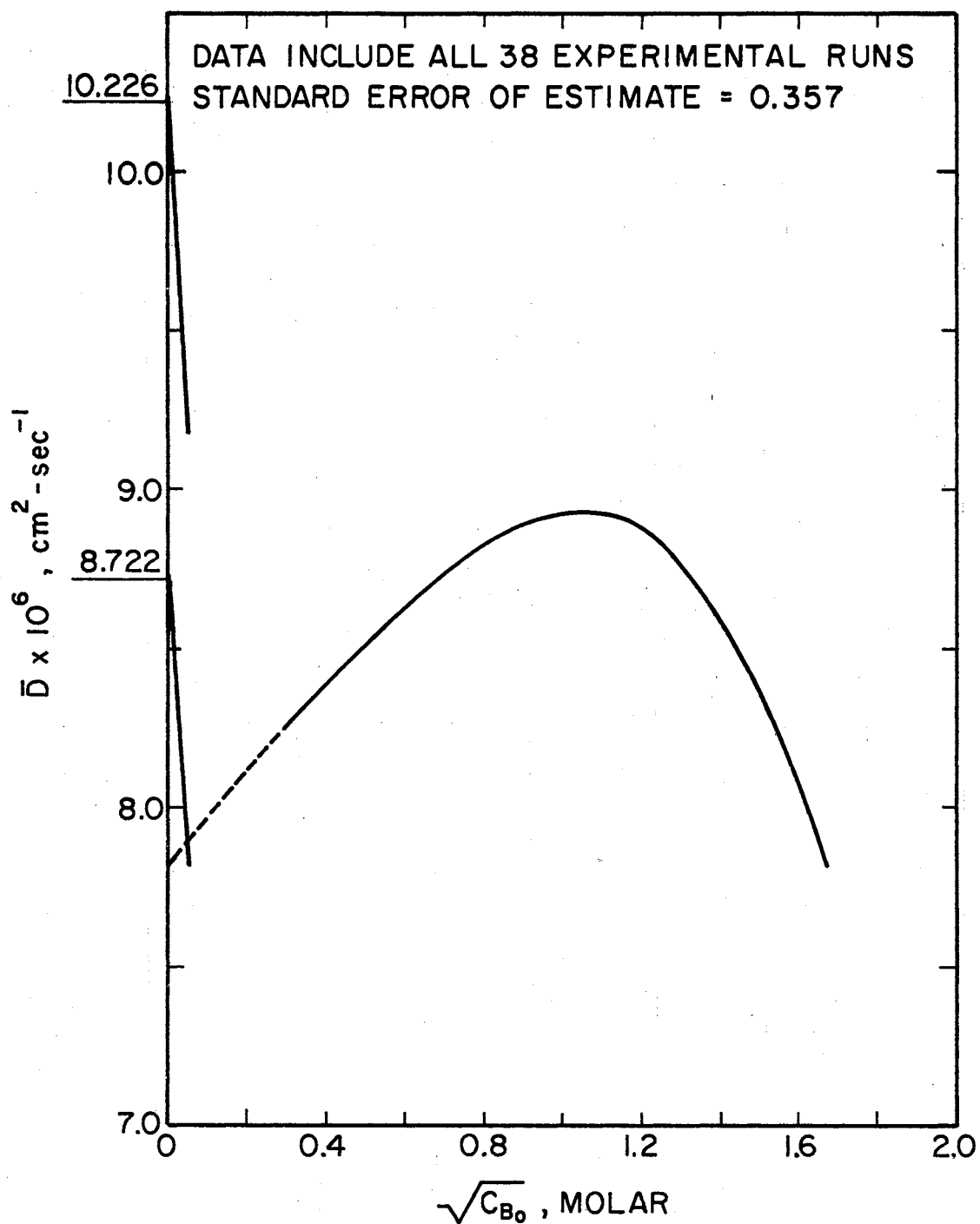


Figure 16. Multiple Linear Regression of Diaphragm Cell Integral Diffusion Coefficients According to the Model:

$$\bar{D} = D_0 + P c_{B_0}^{0.5} + Q c_{B_0}^{1.0} + R c_{B_0}^{2.0}$$

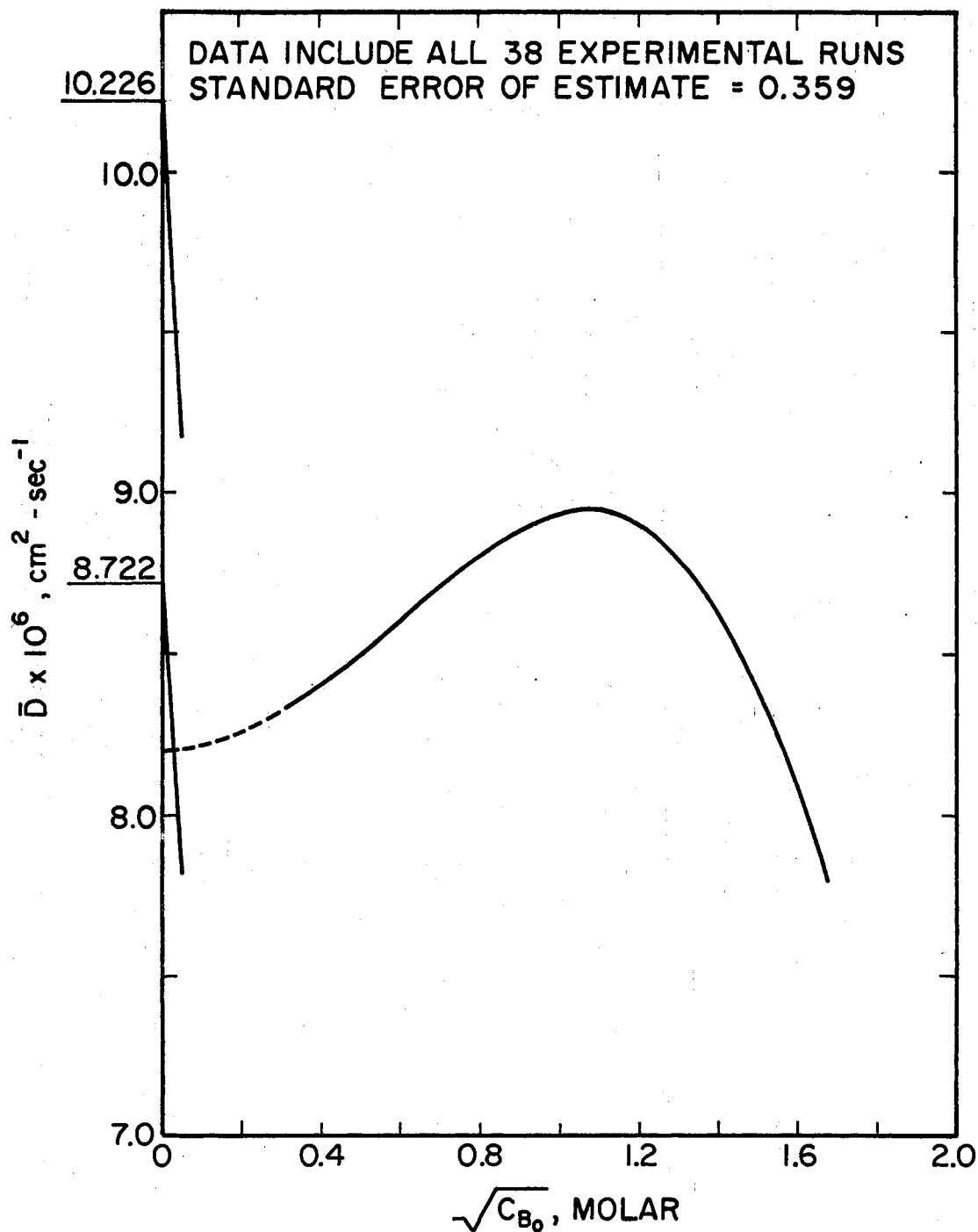


Figure 17. Multiple Linear Regression of Diaphragm Cell Integral Diffusion Coefficients According to the Model:

$$\bar{D} = D_0 + Pc_{B_0}^{1.0} + Qc_{B_0}^{2.0} + Rc_{B_0}^{3.0}$$

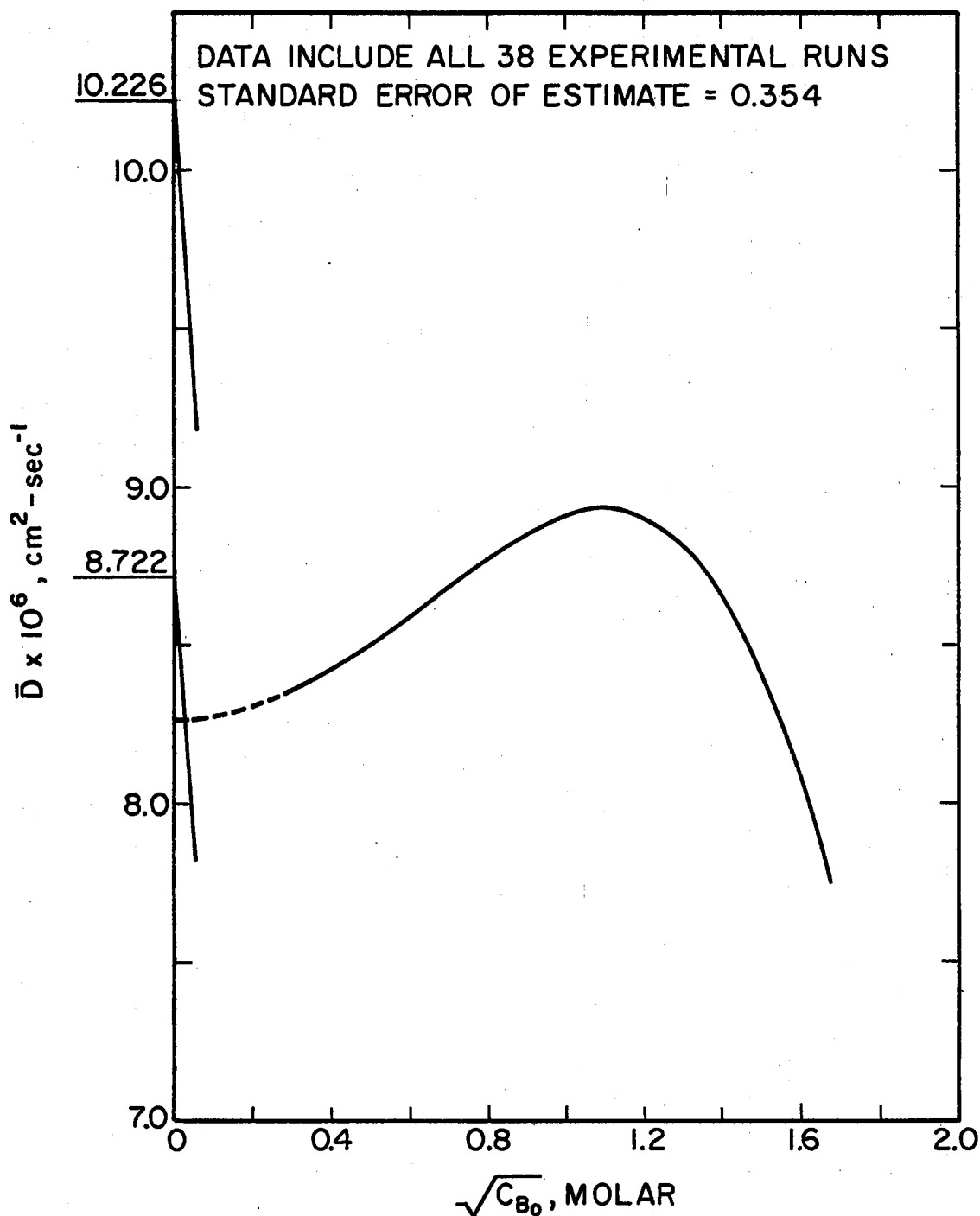


Figure 18. Multiple Linear Regression of Diaphragm Cell Integral Diffusion Coefficients According to the Model:

$$\bar{D} = D_0 + Pc_{B_0}^{1.0} + Qc_{B_0}^{2.0}$$

The average integral diffusion coefficients as shown in Table II were then curve-fitted according to the above multiple linear regression models. In addition, the curve-fitting was performed utilizing the two values for the limiting diffusion coefficient calculated using equations (5) through (7), $D_0 = 10.226 \times 10^{-6}$ and $D_0 = 8.722 \times 10^{-6}$, as input data. The limiting slope was not included in the curve-fitting at this time.

The multiple linear regression equations for (M-1) through (M-4) are shown in Figures 19-22, respectively. A summary of the limiting diffusion coefficients and slopes as generated by the multiple linear regression is shown in Table XIV. Again, when no value for the limiting diffusion coefficient is used in the curve-fitting, a positive limiting slope is generated. Therefore, all subsequent regression of diaphragm cell diffusion coefficients includes a value for the limiting diffusion coefficient.

All regression equations which exclude the square-root term have a positive slope except the cubic equation which used $D_0 = 10.226 \times 10^{-6}$ in the regression. However, this limiting slope, -1.660×10^{-6} , shows the greatest deviation from the calculated limiting slope, in this case -21.059×10^{-6} , than any of the other generated negative slopes. Therefore, regression models (M-3) and (M-4) are excluded from consideration. Subsequent multiple linear regression of any diffusion coefficient data includes a square-root term in the regression model.

The regression model to be used then narrows down to a choice between equations (M-1) and (M-2) using a value for the limiting

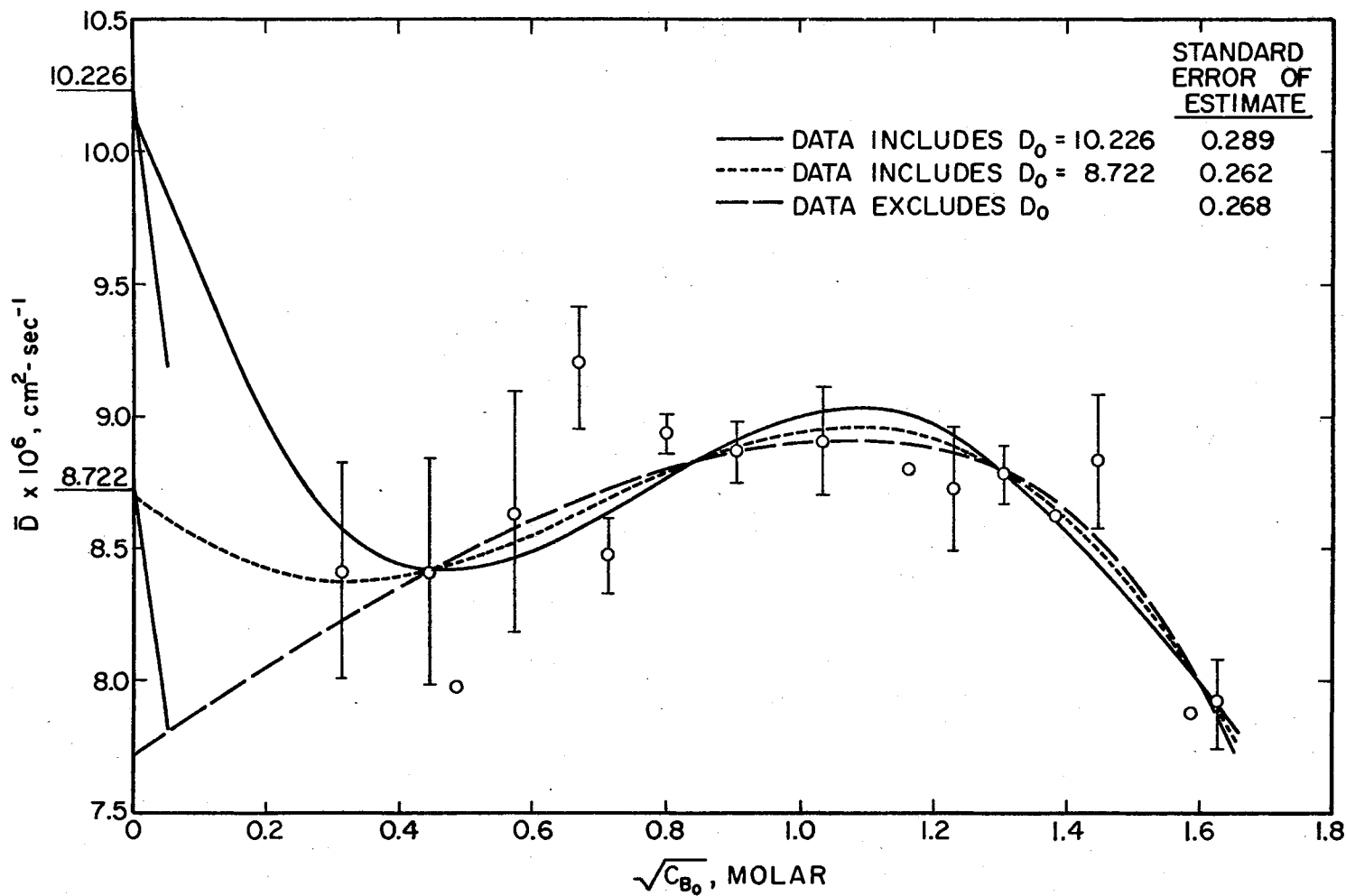


Figure 19. Multiple Linear Regression of Diaphragm Cell Average Integral Diffusion Coefficients According to the Model: $\bar{D} = D_0 + Pc_{B_0}^{0.5} + Qc_{B_0}^{1.0} + Rc_{B_0}^{2.0} + Sc_{B_0}^{3.0}$

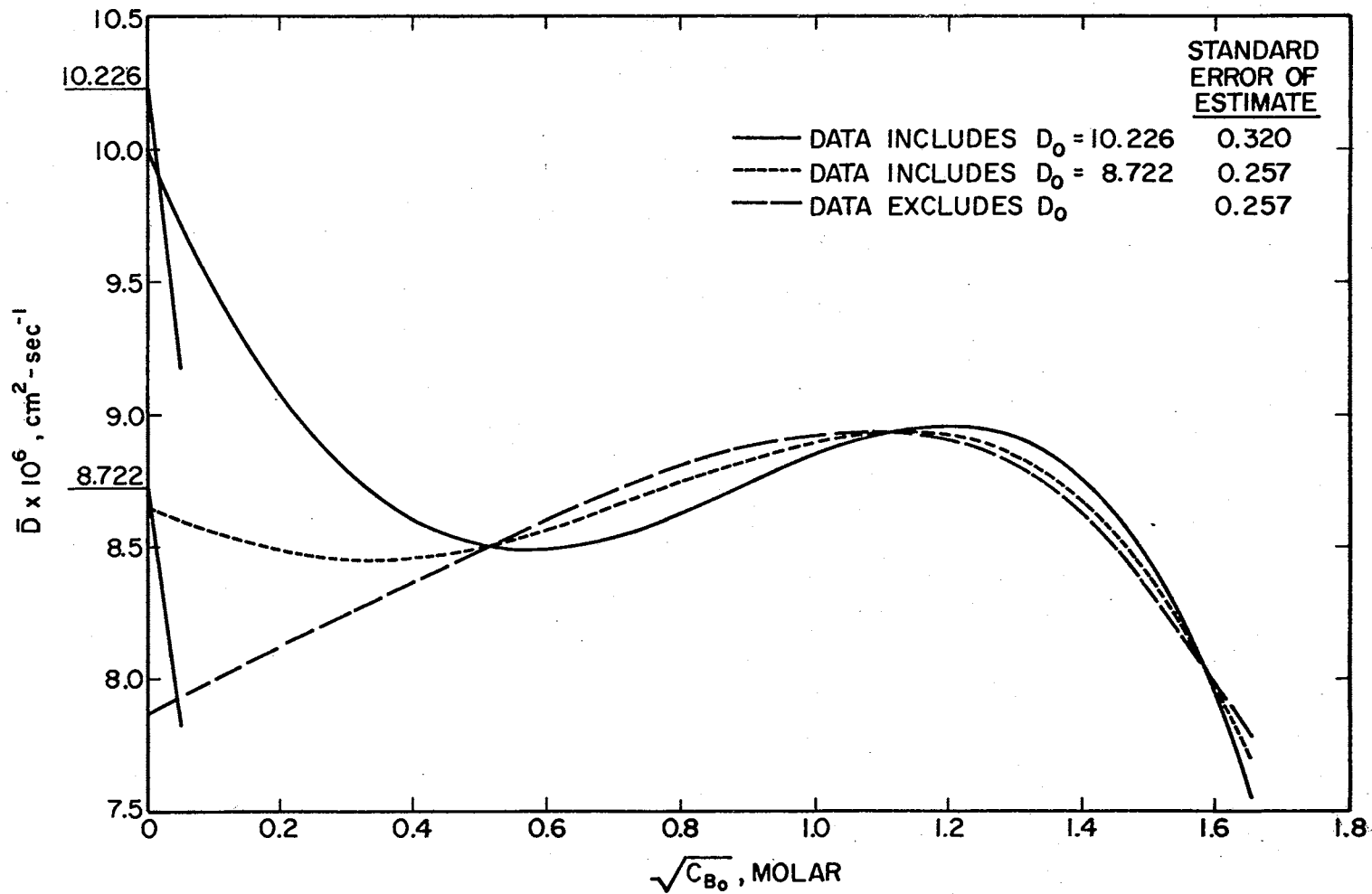


Figure 20. Multiple Linear Regression of Diaphragm Cell Average Integral Diffusion Coefficients According to the Model: $\bar{D} = D_0 + P\bar{C}_{B_0}^{0.5} + Q\bar{C}_{B_0}^{1.0} + R\bar{C}_{B_0}^{2.0}$

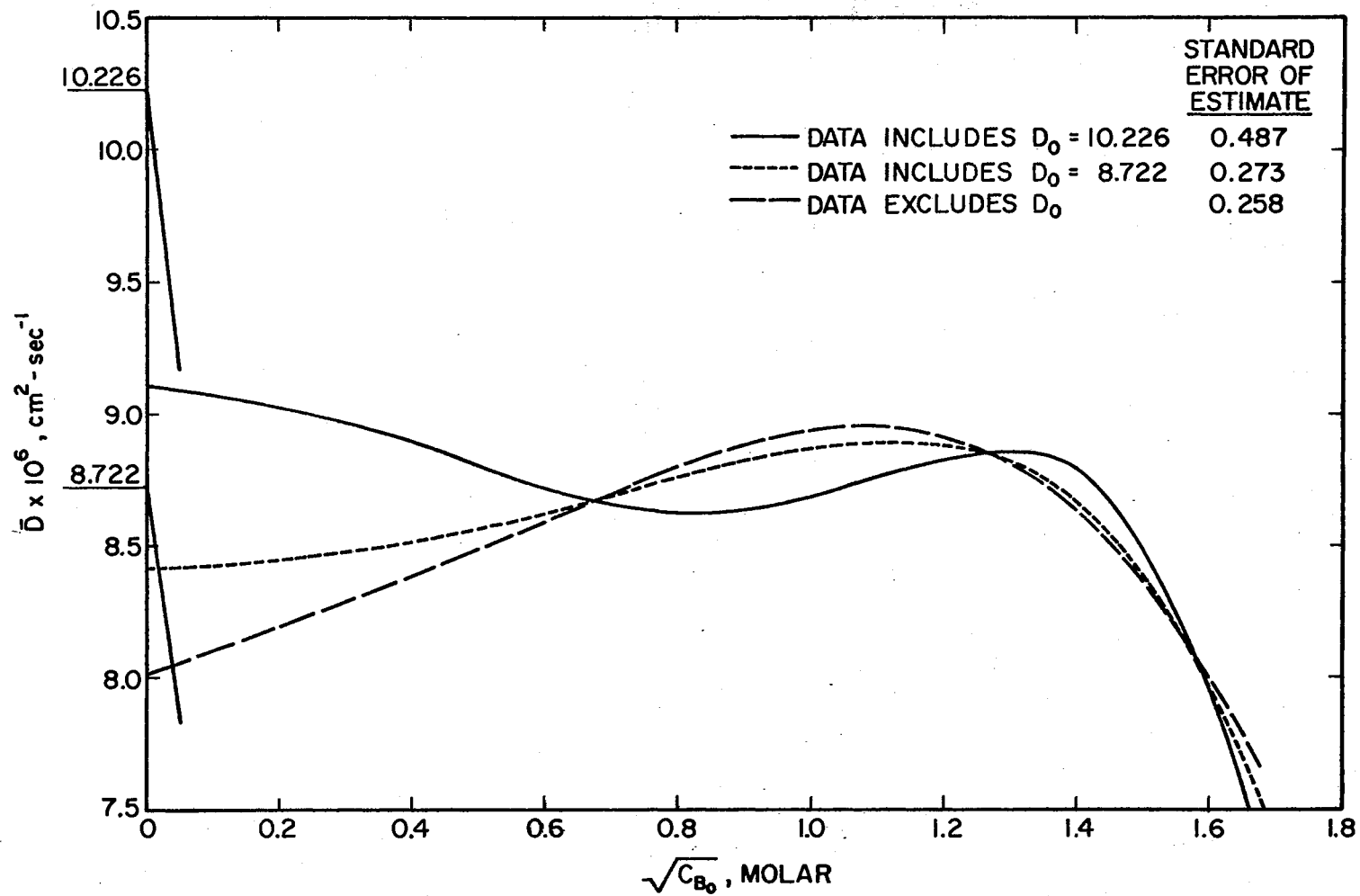


Figure 21. Multiple Linear Regression of Diaphragm Cell Average Integral Diffusion Coefficients According to the Model: $\bar{D} = D_0 + P\bar{C}_{B_0}^{1.0} + Q\bar{C}_{B_0}^{2.0} + R\bar{C}_{B_0}^{3.0}$

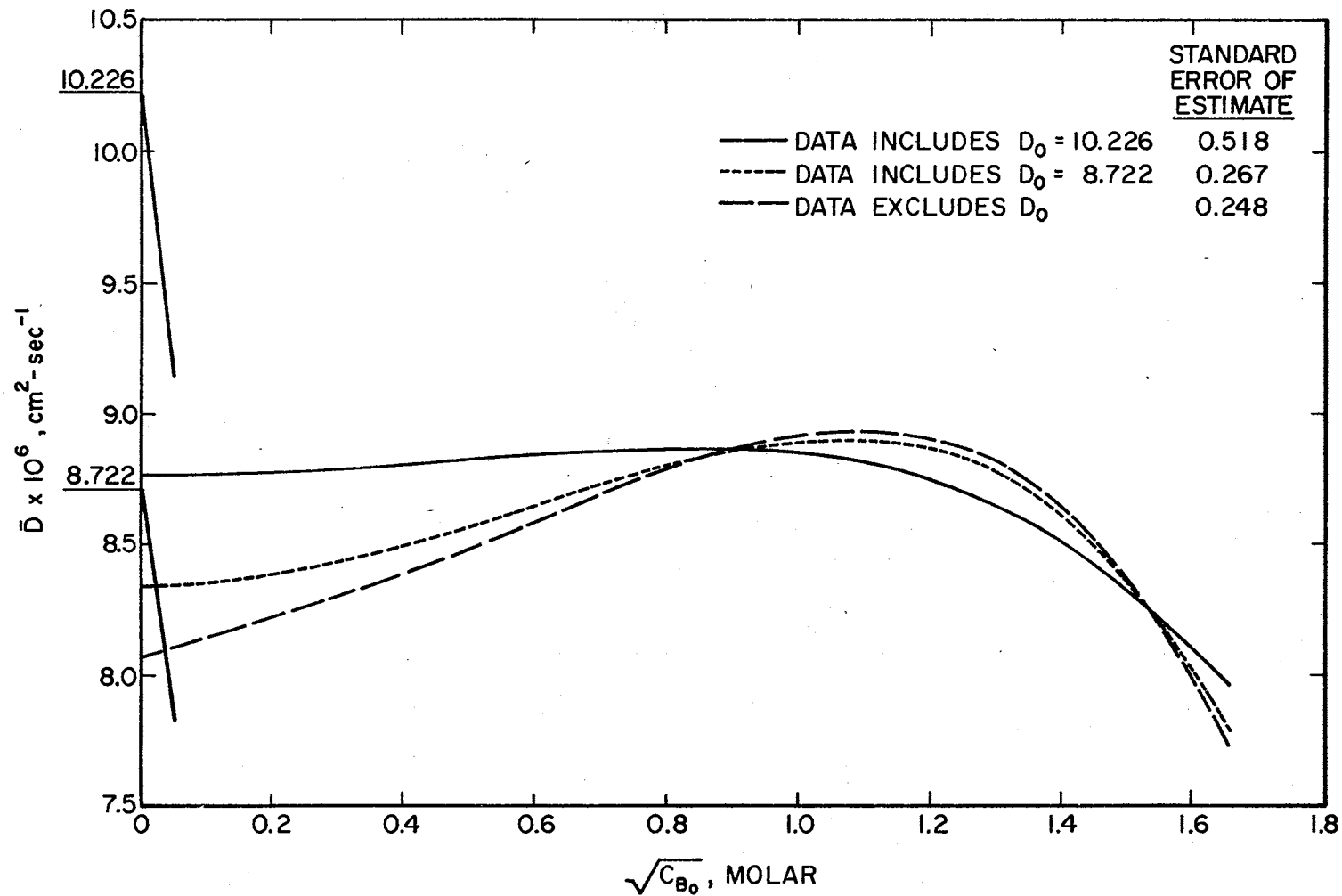


Figure 22. Multiple Linear Regression of Diaphragm Cell Average Integral Diffusion Coefficients According to the Model: $\bar{D} = D_0 + PC_{B_0}^{-1.0} + Qc_{B_0}^{-2.0}$

diffusion coefficient in the curve-fitting. As seen in Table XIV, equation (m-1) yields limiting values which have the lowest deviation from the calculated limiting values. Regression model (M-1) was selected for all subsequent multiple linear regression of diaphragm cell data.

Therefore, the regression equations of \bar{D} as a function of c_{B_0} which are used to derive differential diffusion coefficients appear below. Using $D_0 = 10.226 \times 10^{-6}$:

$$\begin{aligned} \bar{D} = & 10.143 \times 10^{-6} - 8.001 \times 10^{-6} c_{B_0}^{0.5} + 9.947 \times 10^{-6} c_{B_0}^{1.0} \\ & - 3.590 \times 10^{-6} c_{B_0}^{2.0} + 0.519 \times 10^{-6} c_{B_0}^{3.0} \end{aligned} \quad (M-5)$$

Using $D_0 = 8.722 \times 10^{-6}$:

$$\begin{aligned} \bar{D} = & 8.687 \times 10^{-6} - 2.081 \times 10^{-6} c_{B_0}^{0.5} + 3.597 \times 10^{-6} c_{B_0}^{1.0} \\ & - 1.407 \times 10^{-6} c_{B_0}^{2.0} + 0.158 \times 10^{-6} c_{B_0}^{3.0} \end{aligned} \quad (M-6)$$

TABLE XIV

LIMITING DIFFUSION COEFFICIENTS AND SLOPES GENERATED IN MULTIPLE LINEAR REGRESSION OF INTEGRAL DIFFUSION COEFFICIENTS

Regression Model	Data Includes $D_0 = 10.226 \times 10^{-6}$			Data Includes $D_0 = 8.722 \times 10^{-6}$		
	Limiting Diffusion Coefficient $\times 10^6$	Limiting Slope $\times 10^6$	Standard Error of Estimate	Limiting Diffusion Coefficient $\times 10^6$	Limiting Slope $\times 10^6$	Standard Error of Estimate
$\bar{D} = D_0 + P c_{B_0}^{0.5} + P c_{T_0}^{1.0} + R c_{B_0}^{2.0} + S c_{B_0}^{3.0}$	10.143	-8.002	0.289	8.687	-2.081	0.262
$\bar{D} = D_0 + P c_{B_0}^{0.5} + Q c_{B_0}^{1.0} + R c_{B_0}^{2.0}$	9.992	-5.594	0.320	8.642	-1.350	0.257
$\bar{D} = D_0 + P c_{B_0}^{1.0} + Q c_{B_0}^{2.0} + R c_{B_0}^{3.0}$	9.117	-1.660	0.487	8.421	+0.579	0.273
$\bar{D} = D_0 + P c_{B_0}^{1.0} + Q c_{B_0}^{2.0}$	8.765	+0.299	0.518	8.345	+0.997	0.267

TABLE XIV (CONTINUED)

Regression Model	No Data Value for D_o Used in Regression		
	Limiting Diffusion Coefficient x 10^6	Limiting Slope x 10^6	Standard Error of Estimate
$\bar{D}=D_o+Pc_{B_o}^{0.5}+Pc_{T_o}^{1.0}+Rc_{B_o}^{2.0}+Sc_{B_o}^{3.0}$	7.663	+2.087	0.268
$\bar{D}=D_o+Pc_{B_o}^{0.5}+Qc_{B_o}^{1.0}+Rc_{B_o}^{2.0}$	7.937	+0.864	0.257
$\bar{D}=D_o+Pc_{B_o}^{1.0}+Qc_{B_o}^{2.0}+Rc_{B_o}^{3.0}$	8.161	+1.414	0.258
$\bar{D}=D_o+Pc_{B_o}^{1.0}+Qc_{B_o}^{2.0}$	8.200	+1.239	0.248

APPENDIX N

INTERFEROMETER DATA

TABLE XV
INTERFEROMETER DATA

\bar{c}	$\sqrt{\bar{c}}$	$D \times 10^6$ $\text{cm}^2\text{-sec}^{-1}$
0.00456	0.0675	10.40
0.100	0.1000	8.62
0.0254	0.1594	8.33
0.0489	0.2211	8.33
0.0794	0.2818	7.74
0.103	0.3209	8.43
0.246	0.4960	8.07

SOURCE: (29)

APPENDIX O

CAPILLARY CELL DATA

TABLE XVI
CAPILLARY CELL DATA

\bar{c}	$\sqrt{\bar{c}}$	$\bar{D} \times 10^6$ $\text{cm}^2\text{-sec}^{-1}$
0.036	0.190	7.10
0.182	0.427	6.84
0.364	0.603	6.90
0.430	0.656	7.37
0.501	0.708	7.90
0.5285	0.727	8.04
0.603	0.777	8.05
0.7045	0.839	8.19
1.060	1.030	8.03
1.4065	1.186	8.21

SOURCE: (7)

APPENDIX P

SELECTIVE CURVE-FIT ANALYSIS

Using selective curve-fitting, an attempt was made to determine the statistical consistency of a regression model to curve-fit diffusion coefficients as a function of concentration. The diaphragm cell differential diffusion coefficients, interferometer diffusion coefficients, and capillary cell integral diffusion coefficients were curve-fitted as a function of \bar{c} and $\sqrt{\bar{c}}$ using the regression models shown in Appendix C. The diaphragm cell data were curve-fitted using $D_0 = 10.226 \times 10^{-6}$ $\text{cm}^2\text{-sec}^{-1}$ and $D_0 = 8.722 \times 10^{-6}$ $\text{cm}^2\text{-sec}^{-1}$ as input data values. The capillary cell and interferometer data also used these two limiting diffusion coefficient values as input data in the curve-fitting. In addition, these diffusion coefficients were also curve-fitted without use of a data value for D_0 .

Statistical variables calculated for each curve-fit included the standard deviation, maximum deviation of diffusion coefficient and value of concentration at which the deviation occurs, residual squared, and F-ratio. For each statistical variable, the three regression models yielding the most favorable statistics are shown in the following tables. The diaphragm cell results, interferometer results, and capillary cell results are shown in Tables XVII through XX, Tables XXI through XXVI, and Tables XXVII through XXXII, respectively.

Results vary widely and are inconclusive. However, it was noted that regression models describing the diffusion coefficient function $1/D$ yielded a minimum standard deviation and least maximum deviation for all cases. The work contained in this analysis should provide a basis for further model testing.

TABLE XVII

STATISTICAL ANALYSIS OF D VS \bar{c} CORRELATION FOR DIAPHRAGM CELL DATA,
DATA SET INCLUDES $D_o = 10.226$

Statistical Standard	Correlation	Intercept	Slope	Value of Statistic
Minimum Standard Deviation	$1/D=1/\bar{c}$	0.115	-0.171×10^{-9}	0.0045
	$1/D=1/\bar{c}^2$	0.115	-0.171×10^{-17}	0.0045
	$1/D=\log(\bar{c})/\bar{c}$	0.115	0.930×10^{-11}	0.0045
Least Minimum Deviation	$1/D=\log(\bar{c})$	0.116	0.855×10^{-3}	0.0075 at $\bar{c} = 1.306$
	$1/D=1/\bar{c}$	0.115	-0.171×10^{-9}	0.0084 at $\bar{c} = 1.306$
	$1/D=1/\bar{c}^2$	0.115	-0.171×10^{-17}	0.0084 at $\bar{c} = 1.306$
	$1/D=\log(\bar{c})/\bar{c}$	0.115	0.930×10^{-11}	0.0084 at $\bar{c} = 1.306$
Minimum Residual Squared	$\log(d)=(1-\bar{c})^2$	2.174	-0.531×10^{-3}	0.1×10^{-4}
	$D=(1-\bar{c})^2$	8.800	0.022	0.002
	$1/D=(1-\bar{c})^2$	0.114	0.365×10^{-3}	0.0004
Maximum F-Ratio	$D=1/\bar{c}$	8.716	0.151×10^{-7}	15.981
	$D=1/\bar{c}^2$	8.716	0.151×10^{-15}	15.981
	$D=\log(\bar{c})/\bar{c}$	8.716	0.022	15.981

TABLE XVIII

STATISTICAL ANALYSIS OF D VS \sqrt{c} CORRELATION FOR DIAPHRAGM CELL DATA,
DATA SET INCLUDES $D_0 = 10.226$

Statistical Standard	Correlation	Intercept	Slope	Value of Statistic
Minimum Standard Deviation	$1/D=1/\sqrt{c}$	0.115	-0.171×10^{-9}	0.0045
	$1/D=1/(\sqrt{c})^2=1/\bar{c}$	0.115	-0.171×10^{-17}	0.0045
	$1/D=\log(\sqrt{c})/\sqrt{c}$	0.115	0.930×10^{-11}	0.0045
Least Maximum Deviation	$1/D=\log(\sqrt{c})$	0.115	0.905×10^{-3}	0.0080 at $\sqrt{c}=1.143$
	$1/D=1/\sqrt{c}$	0.115	-0.171×10^{-9}	0.0084 at $\sqrt{c}=1.143$
	$1/D=1/(\sqrt{c})^2=1/\bar{c}$	0.115	-0.171×10^{-17}	0.0084 at $\sqrt{c}=1.143$
	$1/D=\log(\sqrt{c})/\sqrt{c}$	0.115	0.930×10^{-11}	0.0084 at $\sqrt{c}=1.143$
Minimum Residual Squared	$1/D=1/e(\sqrt{c})^2=1/e\bar{c}$	0.116	-0.258×10^{-2}	0.010
	$\log(D)=1/e(\sqrt{c})^2=1/e\bar{c}$	2.158	0.025	0.012
	$D=1/e(\sqrt{c})^2=1/e\bar{c}$	8.645	0.251	0.015
Maximum F-Ratio	$D=1/\sqrt{c}$	8.716	0.151×10^{-7}	15.981
	$D=1/(\sqrt{c})^2=1/\bar{c}$	8.716	0.151×10^{-15}	15.981
	$D=\log(\sqrt{c})/\sqrt{c}$	8.716	-0.819×10^{-9}	15.981

TABLE XIX

STATISTICAL ANALYSIS OF D VS \bar{c} CORRELATION FOR DIAPHRAGM CELL DATA,
DATA SET INCLUDES $D_0 = 8.722$

Statistical Standard	Correlation	Intercept	Slope	Value of Statistic
Minimum Standard Deviation	$1/D=(1-\bar{c})^2$	0.113	0.483×10^{-2}	0.0032
	$1/D=\bar{c} \log(\bar{c})$	0.116	0.763×10^{-2}	0.0032
	$1/D=1/e^{\bar{c}}$	0.112	0.369×10^{-2}	0.0035
Least Maximum Deviation	$1/D=\bar{c} \log(\bar{c})$	0.116	0.763×10^{-2}	0.0050 at $\bar{c} = 0.051$
	$1/D=\bar{c}^2$	0.114	0.773×10^{-3}	0.0053 at $\bar{c} = 0.051$
	$1/D=e^{\bar{c}}$	0.114	0.166×10^{-3}	0.0058 at $\bar{c} = 1.306$
Minimum Residual Squared	$D=1/\bar{c}$	8.722	0.312×10^{-11}	0.7×10^{-7}
	$D=1/\bar{c}^2$	8.722	0.312×10^{-19}	0.7×10^{-7}
	$D=\log(\bar{c})/\bar{c}$	8.722	-0.170×10^{-12}	0.7×10^{-7}
Maximum F-Ratio	$D=(1-\bar{c})^2$	8.870	-0.372	4.257
	$\log(D)=(1-\bar{c})^2$	2.182	-0.042	4.162
	$1/D=(1-\bar{c})^2$	0.113	0.483×10^{-2}	4.066

TABLE XX

STATISTICAL ANALYSIS OF D VS \sqrt{c} CORRELATION FOR DIAPHRAGM CELL DATA,
DATA SET INCLUDES $D_0 = 8.722$

Statistical Standard	Correlation	Intercept	Slope	Value of Statistic
Minimum Standard Deviation	$1/D = (1 - \sqrt{c})^2$	0.114	0.524×10^{-2}	0.0033
	$1/D = 1/e^{\sqrt{c}}$	0.112	0.559×10^{-2}	0.0035
	$1/D = 1/e^{(\sqrt{c})^2}$ $= 1/e^c$	0.112	0.371×10^{-2}	0.0035
Least Maximum Deviation	$1/D = 1/\sqrt{c}$	0.115	-0.124×10^{-11}	0.0061 at $\sqrt{c} = 1.143$
	$1/D = 1/(\sqrt{c})^2$ $= 1/c$	0.115	-0.124×10^{-19}	0.0061 at $\sqrt{c} = 1.143$
	$1/D = \log(\sqrt{c})/\sqrt{c}$	0.115	0.674×10^{-13}	0.0061 at $\sqrt{c} = 1.143$
Minimum Residual Squared	$D = 1/\sqrt{c}$	8.722	0.312×10^{-11}	0.7×10^{-7}
	$D = 1/(\sqrt{c})^2 = 1/c$	8.722	00.312×10^{-19}	0.7×10^{-7}
	$D = \log(\sqrt{c})/\sqrt{c}$	8.722	-0.170×10^{-12}	0.7×10^{-7}
Maximum F-Ratio	$D = (1 - \sqrt{c})^2$	8.814	-0.405	2.797
	$\log(D) = (1 - \sqrt{c})^2$	2.176	-0.046	2.730
	$1/D = (1 - \sqrt{c})^2$	0.114	0.524×10^{-2}	2.662

TABLE XXI

STATISTICAL ANALYSIS OF D VS \bar{c} CORRELATION FOR INTERFEROMETER DATA,
DATA SET INCLUDES $D_0 = 10.226$

Statistical Standard	Correlation	Intercept	Slope	Value of Statistic
Minimum Standard Deviation	$1/D = \log(\bar{c})$	0.126	0.232×10^{-2}	0.0072
	$1/D = \bar{c} \log(\bar{c})$	0.105	-0.074	0.0075
	$1/D = \log(\bar{c})/\bar{c}$	0.118	0.144×10^{-8}	0.0090
Least Maximum Deviation	$1/D = \bar{c} \log(\bar{c})$	0.105	-0.074	0.011 at $\bar{c} = 0.0046$
	$1/D = (1 - \bar{c})^2$	0.158	-0.049	0.014 at $\bar{c} = 0.0046$
	$1/D = 1/e^{\bar{c}}$	0.205	-0.096	0.014 at $\bar{c} = 0.0046$
Minimum Residual Squared	$D = \bar{c}^2$	8.948	-0.178×10^{-2}	0.140
	$D = 1/e^{\bar{c}^2}$	-9.541	18.491	0.141
	$\log(d) = \bar{c}^2$	2.186	-1.979	0.144
Maximum F-Ratio	$\log(d) = \log(\bar{c})$	2.069	-0.021	8.617
	$D = \log(\bar{c})$	7.884	-0.193	8.617
	$1/D = \log(\bar{c})$	0.126	0.232×10^{-2}	8.534

TABLE XXII

STATISTICAL ANALYSIS OF D VS \bar{c} CORRELATION FOR INTERFEROMETER DATA,
DATA SET INCLUDES $D_0 = 10.226$

Statistical Standard	Correlation	Intercept	Slope	Value of Statistic
Minimum Standard Deviation	$1/D = \sqrt{\bar{c}} \log \sqrt{\bar{c}}$	0.096	-0.077	0.0032
	$1/D = (1 - \sqrt{\bar{c}})^2$	0.141	-0.039	0.0060
	$1/D = 1/e^{\sqrt{\bar{c}}}$	0.176	-0.073	0.0062
Least Maximum Deviation	$1/D = \sqrt{\bar{c}} \log \sqrt{\bar{c}}$	0.096	-0.077	0.0059 at $\sqrt{\bar{c}} = 0.321$
	$1/D = (1 - \sqrt{\bar{c}})^2$	0.141	-0.039	0.0081 at $\sqrt{\bar{c}} = 0.281$
	$1/D = 1/e^{\sqrt{\bar{c}}}$	0.176	-0.073	0.0084 at $\sqrt{\bar{c}} = 0.281$
Minimum Residual Squared	$D = (\sqrt{\bar{c}})^2 = \bar{c}$	9.201	-0.068	0.318
	$\log(D) = (\sqrt{\bar{c}})^2 = \bar{c}$	2.214	-0.747	0.324
	$1/D = (\sqrt{\bar{c}})^2 = \bar{c}$	0.110	-0.083	0.330
Maximum F-Ratio	$D = \sqrt{\bar{c}} \log(\sqrt{\bar{c}})$	10.354	6.474	8.243
	$\log(D) = \frac{1}{\sqrt{\bar{c}}} \log(\sqrt{\bar{c}})$	2.339	0.706	7.555
	$1/D = \sqrt{\bar{c}} \log(\sqrt{\bar{c}})$	0.096	-0.077	6.690

TABLE XXIII

STATISTICAL ANALYSIS OF D VS. \bar{c} CORRELATION FOR INTERFEROMETER DATA,
DATA SET INCLUDES $D_0 = 8.722$

Statistical Standard	Correlation	Intercept	Slope	Value of Statistic
Minimum Standard Deviation	$1/D = \bar{c} \log(\bar{c})$	0.110	-0.051	0.0071
	$1/D = 1/e^{\bar{c}}$	0.182	-0.069	0.0078
	$1/D = (1-\bar{c})^2$	0.148	-0.035	0.0078
Least Maximum Deviation	$1/D = \bar{c} \log(\bar{c})$	0.110	-0.051	0.015 at $\bar{c} = 0.0046$
	$1/D = 1/e^{\bar{c}}$	0.182	-0.069	0.017 at $\bar{c} = 0.0046$
	$1/D = (1-\bar{c})^2$	0.148	-0.035	0.017 at $\bar{c} = 0.0046$
Minimum Residual Squared	$D = 1/\bar{c}$	8.560	0.162×10^{-6}	0.0052
	$D = 1/\bar{c}^2$	8.560	0.162×10^{-12}	0.0052
	$D = \log(\bar{c})/\bar{c}$	8.560	-0.117×10^{-7}	0.0052
Maximum F-Ratio	$1/D = \bar{c} \log(\bar{c})$	0.110	-0.051	3.852
	$\log(D) = \bar{c} \log(\bar{c})$	2.207	0.451	3.572
	$D = \bar{c} \log(\bar{c})$	9.126	0.400	3.291

TABLE XXIV

STATISTICAL ANALYSIS OF D VS \sqrt{c} CORRELATION FOR INTERFEROMETER DATA,
DATA SET INCLUDES $D_0 = 8.722$

Statistical Standard	Correlation	Intercept	Slope	Value of Statistic
Minimum Standard Deviation	$1/D = \sqrt{c} \log(\sqrt{c})$	0.105	-0.050	0.0058
	$1/D = (1 - \sqrt{c})^2$	0.135	-0.027	0.0063
	$1/D = 1/e^{\sqrt{c}}$	0.160	-0.051	0.0064
Least Maximum Deviation	$1/D = \sqrt{c} \log(\sqrt{c})$	0.105	-0.050	0.011 at $\sqrt{c} = 0.0068$
	$1/D = (1 - \sqrt{c})^2$	0.135	-0.027	0.013 at $\sqrt{c} = 0.0068$
	$1/D = 1/e^{\sqrt{c}}$	0.160	-0.051	0.013 at $\sqrt{c} = 0.0068$
Minimum Residual Squared	$D = 1/(\sqrt{c})^2 = 1/c$	8.560	0.162×10^{-12}	0.0052
	$D = \log(\sqrt{c})/\sqrt{c}$	8.560	-0.117×10^{-7}	0.0052
	$D = 1/\sqrt{c}$	8.560	0.162×10^{-6}	0.0052
Maximum F-Ratio	$1/D = \sqrt{c} \log(\sqrt{c})$	0.105	-0.050	8.564
	$\log(D) = \sqrt{c} \log(\sqrt{c})$	2.256	0.451	8.200
	$D = \sqrt{c} \log \sqrt{c}$	9.574	4.056	7.762

TABLE XXV

STATISTICAL ANALYSIS OF D VS \bar{c} CORRELATION FOR INTERFEROMETER DATA,
DATA SET EXCLUDES D_0

Statistical Standard	Correlation	Intercept	Slope	Value of Statistic
Minimum Standard Deviation	$1/D=1/\bar{c}^2$	0.122	-0.553×10^{-6}	0.0032
	$1/D=\log(\bar{c})/\bar{c}$	0.124	0.227×10^{-4}	0.0032
	$1/D=1/\bar{c}$	0.125	-0.124×10^{-3}	0.0034
Least Maximum Deviation	$1/D=1/\bar{c}$	0.125	-0.124×10^{-3}	0.0058 at $\bar{c} = 0.079$
	$1/D=\log(\bar{c})/\bar{c}$	0.124	0.227×10^{-4}	0.0060 at $\bar{c} = 0.079$
	$1/D=1/\bar{c}^2$	0.122	-0.553×10^{-6}	0.0068 at $\bar{c} = 0.079$
Minimum Residual Squared	$D=\bar{c}^2$	8.707	-12.740	0.106
	$D=1/e\bar{c}^2$	-4.509	13.217	0.107
	$\log(d)=\bar{c}^2$	2.160	-1.425	0.110
Maximum F-Ratio	$D=1/\bar{c}^2$	8.158	0.467×10^{-4}	7.033
	$\log(d)=1/\bar{c}^2$	2.099	0.506×10^{-5}	5.338
	$D=\log(\bar{c})/\bar{c}$	8.041	-0.190×10^{-2}	5.297

TABLE XXVI

STATISTICAL ANALYSIS OF D VS \sqrt{c} CORRELATION FOR INTERFEROMETER DATA,
DATA SET EXCLUDES D₀

Statistical Standard	Correlation	Intercept	Slope	Value of Statistic
Minimum Standard Deviation	$1/D = \sqrt{c} \log(\sqrt{c})$	0.095	-0.083	0.0033
	$1/D = \log(\sqrt{c})$	0.131	0.682×10^{-2}	0.0033
	$1/D = 1/\sqrt{c}$	0.122	-0.178×10^{-3}	0.0037
Least Maximum Deviation	$1/D = \sqrt{c} \log(\sqrt{c})$	0.095	-0.083	0.0061 at $\sqrt{c} = 0.321$
	$1/D = \log(\sqrt{c})$	0.131	0.682×10^{-2}	0.0067 at $\sqrt{c} = 0.281$
	$1/D = 1/\sqrt{c}$	0.122	-0.178×10^{-3}	0.0076 at $\sqrt{c} = 0.281$
Minimum Residual Squared	$D = (\sqrt{c})^2 = c$	8.927	-0.050	0.244
	$\log(D) = (\sqrt{c})^2 = c$	2.184	-0.558	0.252
	$1/D = (\sqrt{c})^2 = c$	0.113	0.062	0.258
Maximum F-Ratio	$D = 1/\sqrt{c}$	8.176	0.015	50.582
	$D = \log(\sqrt{c})$	7.437	-0.572	49.835
	$D = \log \sqrt{c} / \sqrt{c}$	8.227	-0.295×10^{-2}	46.358

TABLE XXVII

STATISTICAL ANALYSIS OF D VS \bar{c} CORRELATION FOR CAPILLARY CELL DATA,
DATA SET INCLUDES $D_0 = 10.226$

Statistical Standard	Correlation	Intercept	Slope	Value of Statistic
Minimum Standard Deviation	$1/D=1/\bar{c}$	0.131	-0.333×10^{-7}	0.0088
	$1/D=1/\bar{c}^2$	0.131	-0.333×10^{-13}	0.0088
	$1/D=\log(\bar{c})/\bar{c}$	0.131	0.241×10^{-8}	0.0088
Least Maximum Deviation	$1/D=1/\bar{c}$	0.131	-0.333×10^{-7}	0.015 at $\bar{c} = 0.182$
	$1/D=1/\bar{c}^2$	0.131	-0.333×10^{-13}	0.015 at $\bar{c} = 0.182$
	$1/D=\log(\bar{c})/\bar{c}^2$	0.131	0.241×10^{-8}	0.015 at $\bar{c} = 0.182$
Minimum Residual Squared	$1/D=(1-\bar{c})^2$	0.128	-0.409×10^{-3}	0.0001
	$\log(d)=1/e^{\bar{c}}$	2.068	-0.011	0.0005
	$D=\bar{c}$	7.850	0.086	0.0015
	$D=e^{\log(\bar{c})}$	7.850	0.086	0.0015
Maximum F-Ratio	$D=1/\bar{c}$	7.663	0.256×10^{-5}	19.743
	$D=1/\bar{c}^2$	7.663	0.256×10^{-11}	19.743
	$D=\log(\bar{c})/\bar{c}$	7.663	-0.186×10^{-6}	19.743

TABLE XXVIII

STATISTICAL ANALYSIS OF D VS \sqrt{c} CORRELATION FOR CAPILLARY CELL DATA,
DATA SET INCLUDES $D_0 = 10.226$

Statistical Standard	Correlation	Intercept	Slope	Value of Statistic
Minimum Standard Deviation	$1/D=1/\sqrt{c}$	0.131	-0.333×10^{-7}	0.0088
	$1/D=1/(\sqrt{c})^2=1/\bar{c}$	0.131	-0.333×10^{-13}	0.0088
	$1/D=\log(\sqrt{c})/\sqrt{c}$	0.131	0.241×10^{-8}	0.0088
Least Maximum Deviation	$1/D=1/\sqrt{c}$	0.131	-0.333×10^{-7}	0.015 at \sqrt{c} =0.427
	$1/D=1/(\sqrt{c})^2=1/\bar{c}$	0.131	-0.333×10^{-13}	0.015 at \sqrt{c} =0.427
	$1/D=\log(\sqrt{c})/\bar{c}$	0.131	0.241×10^{-8}	0.015 at \sqrt{c} =0.427
Minimum Residual Squared	$\log(D)=e^{\sqrt{c}}$	2.060	0.243×10^{-3}	0.2×10^{-5}
	$\log(D)=1/e^{(\sqrt{c})^2}=1/e^{\bar{c}}$	2.067	-0.011	0.0005
	$D=(\sqrt{c})^2=\bar{c}$	7.850	0.086	0.0015
Maximum F-Ratio	$D=1/\sqrt{c}$	7.663	0.256×10^{-5}	19.744
	$D=1/(\sqrt{c})^2=1/\bar{c}$	7.663	0.256×10^{-11}	19.744
	$D=\log(\sqrt{c})/\sqrt{c}$	7.663	-0.186×10^{-6}	19.744

TABLE XXIX

STATISTICAL ANALYSIS OF D VS \bar{c} CORRELATION FOR CAPILLARY CELL DATA,
DATA SET INCLUDES $D_0 = 8.722$

Statistical Standard	Correlation	Intercept	Slope	Value of Statistic
Minimum Standard Deviation	$1/D=1/\bar{c}$	0.131	-0.165×10^{-7}	0.0088
	$1/D=1/\bar{c}^2$	0.131	-0.165×10^{-13}	0.0088
	$1/D=\log(\bar{c})/\bar{c}$	0.131	0.119×10^{-8}	0.0088
Least Maximum Deviation	$1/D=\bar{c}\log(\bar{c})$	0.127	-0.018	0.014 at $\bar{c} = 0.182$
	$1/D=1/\bar{c}$	0.131	-0.165×10^{-7}	0.015 at $\bar{c} = 0.182$
	$1/D=1/\bar{c}^2$	0.131	-0.165×10^{-13}	0.015 at $\bar{c} = 0.182$
	$1/D=\log(\bar{c})/\bar{c}$	0.131	0.119×10^{-8}	0.015 at $\bar{c} = 0.182$
Minimum Residual Squared	$D-(1-\bar{c})^2$	7.922	-0.424	0.055
	$\log D=(1-\bar{c})^2$	2.069	-0.061	0.067
	$1/D=(1-\bar{c})^2$	0.126	0.873×10^{-2}	0.079
Maximum F-Ratio	$D=1/\bar{c}$	7.663	0.106×10^{-5}	3.371
	$D=1/\bar{c}^2$	7.663	0.106×10^{-11}	3.371
	$D=\log(\bar{c})/\bar{c}$	7.663	-0.767×10^{-7}	3.371

TABLE XXX

STATISTICAL ANALYSIS OF D VS \sqrt{c} CORRELATION FOR CAPILLARY CELL DATA,
DATA SET INCLUDES $D_0 = 8.722$

Statistical Standard	Correlation	Intercept	Slope	Value of Statistic
Minimum Standard Deviation	$1/D = \sqrt{c} \log(\sqrt{c})$	0.122	-0.044	0.0068
	$1/D = 1/\sqrt{c}$	0.131	-0.165×10^{-7}	0.0088
	$1/D = (1/\sqrt{c})^2 = 1/c$	0.131	-0.165×10^{-13}	0.0088
	$1/D = \log(\sqrt{c})/\sqrt{c}$	0.131	-0.119×10^{-8}	0.0088
Least Maximum Deviation	$1/D = \sqrt{c} \log(\sqrt{c})$	0.122	-0.044	0.0093 at $\sqrt{c} = 0.603$
	$1/D = 1/\sqrt{c}$	0.131	-0.165×10^{-7}	0.015 at $\sqrt{c} = 0.427$
	$1/D = 1/(\sqrt{c})^2 = 1/c$	0.131	-0.165×10^{-13}	0.015 at $\sqrt{c} = 0.427$
	$1/D = \log(\sqrt{c})/\sqrt{c}$	0.131	-0.119×10^{-8}	0.015 at $\sqrt{c} = 0.427$
Minimum Residual Squared	$1/D = (1 - \sqrt{c})^2$	0.130	-0.437×10^{-3}	0.0002
	$\log(D) - (1 - \sqrt{c})^2$	2.044	-0.929×10^{-2}	0.0014
	$D = (1 - \sqrt{c})^2$	7.732	0.120	0.0039
Maximum F-Ratio	$D = \sqrt{c} \log(\sqrt{c})$	8.193	2.583	10.836
	$\log(D) - \sqrt{c} \log(\sqrt{c})$	2.102	0.337	10.701
	$1/D = \sqrt{c} \log(\sqrt{c})$	0.122	-0.044	10.513

TABLE XXXI

STATISTICAL ANALYSIS OF D VS \bar{c} CORRELATION FOR CAPILLARY CELL DATA,
DATA SET EXCLUDES D_0

Statistical Standard	Correlation	Intercept	Slope	Value of Statistic
Minimum Standard Deviation	$1/D=(1-\bar{c})^2$	0.122	-0.028	0.0054
	$1/D=1/e^{\bar{c}}$	0.109	0.037	0.0055
	$1/D=\bar{c}$	0.142	-0.018	0.0062
	$1/D=e^{\log(\bar{c})}$	0.142	-0.018	0.0062
Least Maximum Deviation	$1/D=1/e^{\bar{c}^2}$	0.113	0.026	0.0091 at $\bar{c}=0.364$
	$1/D=\bar{c}$	0.142	-0.018	0.0099 at $\bar{c}=0.364$
	$1/D=e^{\log(\bar{c})}$	0.142	-0.018	0.0099 at $\bar{c}=0.364$
Minimum Residual Squared	$1/D=1/\bar{c}^2$	0.130	0.151×10^{-4}	0.141
	$\log(D)=1/\bar{c}^2$	2.044	-0.115×10^{-3}	0.145
	$D=1/\bar{c}^2$	7.735	-0.875×10^{-3}	0.148
Maximum F-Ratio	$D=(1-\bar{c})^2$	8.170	-1.579	15.472
	$D=1/e^{\bar{c}}$	8.922	-2.109	15.458
	$\log(D)=(1-\bar{c})^2$	2.101	-0.210	15.330

TABLE XXXII

STATISTICAL ANALYSIS OF D VS \sqrt{c} CORRELATION FOR CAPILLARY CELL DATA,
DATA SET EXCLUDES D_0

Statistical Standard	Correlation	Intercept	Slope	Value of Statistic
Minimum Standard Deviation	$1/D = 1/e^{(\sqrt{c})^2} = 1/e^{\bar{c}}$	0.109	0.037	0.0055
	$1/D = \sqrt{\bar{c}}$	0.150	-0.027	0.0058
	$1/D = e^{\log(\sqrt{\bar{c}})}$	0.150	-0.027	0.0058
Least Maximum Deviation	$1/D = \bar{c} \log \sqrt{\bar{c}}$	0.124	-0.039	0.0091 at $\sqrt{\bar{c}} = 0.603$
	$1/D = (\sqrt{\bar{c}})^2 = \bar{c}$	0.142	-0.018	0.0099 at $\sqrt{\bar{c}} = 0.603$
	$1/D = 1/e^{(\sqrt{\bar{c}})^2} = 1/e^{\bar{c}}$	0.109	0.037	0.010 at $\sqrt{\bar{c}} = 0.603$
Minimum Residual Squared	$1/D = 1/(\sqrt{\bar{c}})^2 = 1/\bar{c}$	0.127	0.565×10^{-3}	0.225
	$\log(D) = 1/(\sqrt{\bar{c}})^2 = 1/\bar{c}$	2.054	-0.427×10^{-2}	0.229
	$D = 1/(\sqrt{\bar{c}})^2 = 1/\bar{c}$	7.815	-0.032	0.233
Maximum F-Ratio	$D = 1/e^{(\sqrt{\bar{c}})^2} = 1/e^{\bar{c}}$	8.922	-2.109	15.465
	$\log(d) = 1/e^{(\sqrt{\bar{c}})^2} = 1/e^{\bar{c}}$	2.201	-0.279	15.012
	$1/D = 1/e^{(\sqrt{\bar{c}})^2} = 1/e^{\bar{c}}$	0.109	0.037	14.551

APPENDIX Q

NOMENCLATURE

- A - total effective cross-sectional area of diaphragm pores
 c - solute concentration, molar
 \bar{c} - average solute concentration, molar
 D - differential diffusion coefficient, $\text{cm}^2\text{-sec}^{-1}$
 \bar{D} - integral diffusion coefficient, $\text{cm}^2\text{-sec}^{-1}$
 D_* - solution dielectric constant
 $\bar{D}(t)$ - time-dependent diffusion coefficient, $\text{cm}^2\text{-sec}^{-1}$
 D_0 - Nernst limiting diffusion coefficient, $\text{cm}^2\text{-sec}^{-1}$
 J - mass flux, $\text{gm}/\text{cm}^2\text{-sec}$
 $J(t)$ - time-dependent mass flux, gm/cm^2
 l - length of diffusion path, cm
 P, Q, R, S - coefficients of diffusion coefficient correlation models
 t - diffusion time, sec
 T - temperature, $^{\circ}\text{C}$.
 V - diaphragm cell compartment volume, cm^3
 V_i - number of cations, anions produced by dissociation of one mole of electrolyte
 x - length of diffusion path, cm
 y - mean molar activity coefficient
 z - ionic valence

Greek Symbols

- β - diaphragm cell constant, cm^{-2}
 λ° - limiting ionic equivalent conductivity
 Λ° - limiting electrolyte equivalent conductivity
 $\delta_{(0)}$ - limiting slope in Nernst's equation
 ζ_0 - solvent viscosity

Subscripts

- 1 - diaphragm cell lower compartment concentration, molar
- 2 - diaphragm cell upper compartment concentration, molar
- B - final diaphragm cell lower compartment concentration, molar
- B_0 - initial diaphragm cell lower compartment concentration, molar
- T - final diaphragm cell upper compartment concentration, molar
- T_0 - initial diaphragm cell upper compartment concentration, molar
- c_m' - average of c_B and c_{B0}
- c_m'' - average of c_T and c_{T0}

Superscripts

- o - limiting value at infinite dilution
- ' - diaphragm cell lower compartment
- '' - diaphragm cell upper compartment

VITA

James LeRoy Snyder

Candidate for Degree of

Doctor of Philosophy

Thesis: CORRELATION OF URANYL NITRATE DIFFUSION COEFFICIENTS DERIVED FROM DIAPHRAGM CELL, INTERFEROMETER, AND CAPILLARY CELL METHODS

Major Field: Chemical Engineering

Biographical:

Personal Data: Born in Centralia, Illinois, February 9, 1937, the son of Arthur L. and Blanche M. Snyder.

Education: Attended grade school in Centralia, Illinois; attended high school in Centralia, Illinois; graduated from high school in May, 1953; attended University of Illinois, Urbana, Illinois, 1953 to 1958; received the degree of Bachelor of Science in Chemical Engineering, February, 1958; attended Oklahoma State University, Stillwater, Oklahoma, 1962 to 1967; received the degree of Master of Science in Chemical Engineering, May, 1965; completed the requirements for the Doctor of Philosophy degree in May, 1972.

Professional Experience: Employed as a process engineer for three months with Shell Oil Company, 1957. Served six months in the U. S. Army, 1958. Employed for four years in the Experimental Laboratory, Catalytic Cracking Department, and Technological Department of Shell Oil Company, 1958 to 1962. Employed as a Senior Process Engineer, Group Leader--Acetyl Group, Group Leader--Long Range Development Group, and Unit Supervisor--Acetyls/Vinyl Acetate Units with Celanese Chemical Company, 1967 to 1972.